The Paton WELDING JOURNAL

December 2000 # 12

English translation of the monthly «Avtomaticheskaya Svarka» journal published in Russian since 1948

«The Paton Welding Journal» monthly is published by the E.O. Paton Electric Welding Institute of the National Academy of Sciences of Ukraine with the support rendered by the International Association «Welding».

Promotion group:
V.N.Lipodaev, V.I.Lokteva
A.T.Zelnichenko (Exec. director)
Translators:
S.A.Fomina, I.N.Kutianova, T.K.Vasilenko

Editorial and advertising offices are located at PWI, Dept. 51, 11, Bozhenko str., 03680, Kyiv, Ukraine.
Tel.: (38044) 227 67 57
Fax: (38044) 268 04 86
E-mail: paton@i.kiev.ua

Subscriptions:
$460, 12 issues

«The Paton Welding Journal» Website:
http://www.nas.gov.ua/pwj

CONTENTS

PLASMA TECHNOLOGIES

PLASMA TECHNOLOGIES AT THE TRANSITION OF THE CENTURIES

At the transition to the XXI century we try to summarize results and define prospects for further development of the advanced areas of welding science and technology of interest for a wide circle of readers of our Journal. This issue of the Journal is dedicated to one of such advanced areas — the plasma technology in welding and related industries.

Plasma, i.e. an ionized gas generated by plasmatrons, finds wide practical application in various fields of modern science and technology, in particular in new technologies for high-efficiency production of chemical products (plasmachemistry), as well as aerodynamic and space research.

The use of plasmatrons in welding engineering (cutting, welding, surfacing and spraying) and related industries (melting, remelting of metals and spheroidization of fine particles) gained an intensive development in the second half of the XX century. In its power density, a plasma heat source holds the intermediate but most advantageous place between electric-arc and beam (electron beam and laser) heat sources. It allows achieving an increased temperature and density of the heat flow on a workpiece, as compared with the arc sources. And even if inferior to the beam sources in power concentration, it is much less expensive and more open for technical implementation.

In fact, the plasma equipment is comparable with the electric-arc one in cost and complexity of fabrication. Like the electric-arc equipment, it can be used under shop conditions, in manual and mechanized processes, in open sites, under any climatic conditions, as well as under water and in space.

In volumes of industrial application the plasma welding technology is inferior to the oxygen and electric-arc ones, but the rates of its progression are growing and fields of its application are increasingly widening.

If in electric-arc welding processes the major heat is transferred from the arc to a workpiece through the near-electrode regions, in plasma processes heating of the metal treated is done primarily by the convective mechanism of heat transfer from the arc column. In this sense the term «plasma arc» is correct.

In comparison with the electric-arc technologies, the plasma technologies are characterized by wider capabilities in terms of regulation of parameters of the plasma arcs. Formation of the plasma arc depends to a large degree upon the geometry of the plasmatron arc chamber, flow rate and direction of the plasma gas, its chemical composition, length of the exposed portion of the arc column (or jet), composition and direction of the secondary gas (if used), point of introduction of a filler material to the arc, etc.

Volt-ampere characteristics of the plasma arcs are of great variety, which is associated with the regulated parameters indicated above and properties of the plasmatron power supplies.

In general, characteristic features of the plasma arcs include power, heat flow density, mean-mass temperature, gas-dynamic pressure and chemical-metallurgical effect on a workpiece. Each of the technological processes is characterized by certain prevailing parameters of formation of the plasma arc:

• plasma cutting is characterized by an intensive constriction of the arc column by the gas flow, which determines its high heat flow density, gas-dynamic pressure and, hence, cutting properties;

• microplasma welding is characterized by constriction of the anode region of the arc column by a heat-conducting hydrogen-containing secondary gas flow, which provides the «jewelry»-like process of welding metals of small thickness, the so-called «needle-shaped» plasma;

• as compared with electric-arc surfacing, plasma surfacing offers the possibility of introducing the metal to be deposited (wire or powder) into the anode region of the plasma arc column and, therefore, separately regulating heat input into the filler and base metals, which provides shallow penetration of the base metal and desirable chemical composition of the deposited layer;

• in plasma spraying the introduction of powder or wire into the high-velocity extended plasma jet provides an intensive heating of fine particles, their acceleration to high velocities and, therefore, high adhesion properties of coatings of the most refractory materials;

• plasma arc remelting offers a unique possibility of refining the metal treated through its interaction with high-power extended plasma arcs at almost any chemical composition of the plasma gas within a wide range of high temperatures.

Owing to characteristic configurations and parameters of the plasma arcs used, all the above technologies have found high-efficiency commercial application and have been intensively upgraded for many years since their emergence by the E.O. Paton Electric Welding Institute. Particularly wide are the volumes of manufacture and application of microplasma welding units (over 7,000) and air-plasma cutting units (over 5,000) built by the PWI.

We hope that the plasma technology — a creation of the XX century — will fully demonstrate its advancement and maturity in the XXI century. Not getting ahead into the distant future, we can outline the following prospects for its development in the next decade:

• under conditions of the market economy, first of all it is the use of inexpensive plasma gases: air, water vapours, commercial-purity nitrogen, natural hydrocarbon and carbon dioxide gases;

• application fields of the plasma technologies will be further extended, e.g. in medicine — the surgery instruments such as scalpels and coagulators. Of high promise are the works on development of methods and equipment for robotized plasma cutting under water and under conditions of increased radiation;

• the key-hole penetration effect on the weld edges in plasma welding of metals of medium thickness is similar to that obtained in electron beam and argon-arc welding using activating flux;

• scopes of application of the plasma technologies for surface heating intended for flame scarfing or thermal hardening of pieces, accompanying preheating methods and heat treatment of the welds produced by traditional arc and resistance welding methods will further increase;

• the search will go on for further extension of life of heat-loaded components of the plasmatrons (cathodes, nozzles and anodes) and development of more efficient cooling systems based on the latest achievements of heat engineering;

• in view of high power of the plasmatrons, building of small-sized and cost-effective electric current sources based on the inverter-type converters is more pressing for the plasma technology than for electric-arc welding.

The hottest challenge for the immediate period of transition to the market economy is to attract young specialists to R&D activity in the field of plasma technology, as well as to other priority areas of science and technology. It is the task of the young specialists to take the baton from the older generation of scientists and practical engineers.

Wide popularization of advances in the plasma technology in welding periodicals will undoubtedly help overcome the old-fashioned stereotypes concerning the seeming difficulties associated with utilization of the plasma processes and equipment. We do hope that reading the articles contained in this issue of the Journal, written by leading specialists involved in the plasma technologies, will also be helpful in this respect.

Prof. B.E. Paton

AIR-PLASMA CUTTING: STATE-OF-THE-ART AND PROSPECTS

E.M. ESIBYAN
The E.O. Paton Electric Welding Institute, NASU, Kyiv, Ukraine

ABSTRACT

Analysis of the current status of air-plasma cutting, its technological capabilities and cost-effectiveness is given and the prospects for development of this method of processing metals and their alloys are shown. Thermal and electrophysical properties of air-plasma arc, various design solutions and schematics, used in development of plasmatrons and power sources are described. The technical characteristics of the currently available locally made and foreign air-plasma units are given.

Key words: *plasmatron, air-plasma cutting unit, thermochemical cathode, active insert, energy-heat balance of the arc, plasmatron power source, arc column concentration*

Background. Thirty-five years ago the E.O. Paton Electric Welding Institute developed the first in the world unit for air-plasma cutting (APC) which passed production trials in the Leninskaya Kuznitsa Ship-building Yard. The small team of the laboratory led by the author of this paper, which was part of academician K.K. Khrenov's department, in a short period developed a number of units (AVPR-1, AVPR-2, AVPR-3) and organised their batch production. Several years later, in co-operation with the Institute of Electrodynamics we developed and put into batch production the widely known Kiev-4 unit, whose modifications are still used with success in the enterprises of the CIS countries and are in demand. PWI priority in development and improvement of APC is confirmed by a number of publications, author's certificates and foreign patents [1 – 11].

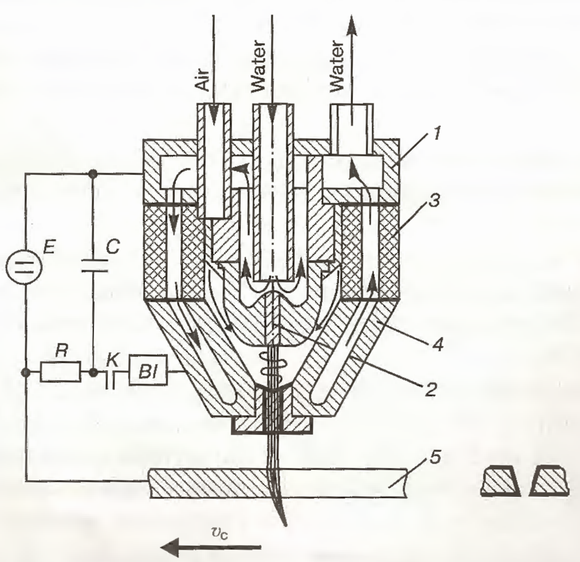

Figure 1. Schematic of APC process: *1* — cathode unit of the plasmatron; *2* — cathode with a captive nut swirler; *3* — insulation casing of the plasmatron; *4* — nozzle unit; *5* — item being cut up; *E* — current source; *BI* — block of spark ignition of the pilot arc; *R* — resistance; *K* — contactor; *C* — capacitor

Later on, at the start of 1970s, APC units developed in VNIIESO, TsNIITS (Leningrad), VNIIavtogenmash (Moscow) were accepted by industry. In 1980s APC began to be widely used in all the developed countries of the world, while the earlier applied plasma cutting with special gases (argon-hydrogen, nitrogen-hydrogen mixtures) became rare.

NPMGP «Plasmatron» Science-Production Small State Business of the PWI Science-Technology Complex set up on the base of the laboratory, where the first local APC units were created, carries on their development and has established its own production of new models and provides their technological support to meet the demands of the new times. As to their scientific-technical level Duplex-1, Duplex-2, Kiev-5 and Kiev-8U units currently manufactured by NPMGP «Plasmatron», are not inferior to the best analogs available in the CIS countries and abroad, and are even superior to them by some parameters.

This paper is an attempt at generalising the gained experience of research and development work on creation of APC units and technologies.

Thermal and electrophysical features of the process. APC is characterised by complex phenomena of conversion of the electric energy of the power source into the thermal energy of the plasma arc, intensive constriction of its column in the forming chamber of the plasmatron and through penetration of the cut metal by the plasma arc with the melt blowing out of the cut gap (Figure 1).

Air as the cutting gas is the natural mixture of molecular gases (78 % nitrogen and 21 % oxygen)

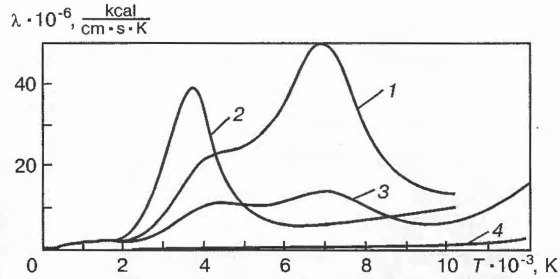

Figure 2. Dependencies of gas heat conductivity on temperature: *1* — air; *2* — hydrogen; *3* — nitrogen; *4* — argon

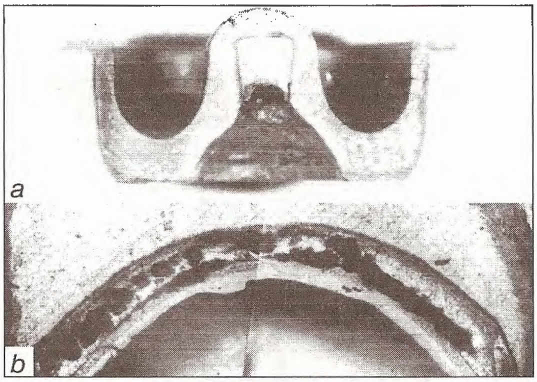

Figure 3. Microsections of a worn thermochemical cathode (*a*) (×10) (reduced by 2/3) and its emitting protective film (*b*) (×100) (reduced by 1/2)

and, in addition to the obvious cost advantages, when compared to the earlier used special gases, it has the highest thermophysical parameters. When thermodynamic functions of the gases are considered [12], the high (comparable to that of hydrogen) heat content of the air in the arc column plasma should be noted, which is associated with absorption of a considerable amount of electric power applied to the arc at the expense of dissociation of oxygen and nitrogen molecules. On the other hand, the column of the air-plasma arc provides a higher intensity of convective heat transfer into the metal being cut due to a higher temperature (about 7000 K) of the heat conductivity maximum λ_{max} of air, while in hydrogen λ_{max} is observed at the temperature of about 4000 K, and λ_{max} level of nitrogen is three times lower than that of the air (Figure 2). Oxygen presence in the air plasma in cutting of steels provides an additional heat effect due to the exothermal reaction of iron oxidation. Oxygen additions to air, as shown by studies [13], even though they result in a certain increase in the cutting speed, do not, however, make it so significant as to be cost-effective.

The ability to create the APC process was predetermined by development of a special kind of *thermochemical (film) cathodes* resistant to an aggressive oxidising medium. Their designs were protected by a number of inventions — foreign patents or author's certificates [8, 9] which formed the basis of further developments of APC units and technologies. The mechanism of operation of thermochemical cathodes is due to formation, in zirconium interaction with air during arcing, of a refractory film (Figure 3) of zirconium nitride (ZrN) and its dioxide (ZrO_2) at the edge of the cylindrical zirconium insert pressed into the copper yoke. Hafnium insert is also used instead of the zirconium, which forms hafnium nitride (HfN) and its dioxide (HfO_2) in interaction with air.

Compared to tungsten used as the arc cathode in the inert and neutral atmosphere, zirconium and hafnium proper, have lower melting temperature and heat conductivity and are more active adsorbents of oxygen and nitrogen. Therefore, application of these materials as electrodes (in the form of rods similar to those of tungsten) leads to their fast failure. The cathode design shown in Figure 3, *a* is exactly the one that provides the conditions for a long-term operation of the cathode.

The arc is initially excited between the copper yoke of the cathode and the nozzle, and then is moved to the yoke edge by the eddy air flow and heats the nitride-dioxide film formed there above its melting temperature. The film which was not electrically conducting in the cold state, acquires high emission properties and, due to that, as well as the high values of melting and boiling temperature, provides a long-time and stable running of the air-plasma arc in the cathode spot.

As shown by metallographic, chemical and X-ray investigations of transverse microsections of a copper-zirconium cathode (Figure 3, *b*), the thickness of the protective film is 180 – 200 μm at the working current of 150 – 200 A, its intermediate layer adjacent to zirconium consisting mainly of zirconium nitride (150 μm thickness), while the thin surface layer (30 μm) is zirconium dioxide.

Such a structure of the film is quite justified by the fact that in zirconium dioxide the boiling temperature (5025 K) is higher, while the electron work function (3.1 eV) is lower than those of zirconium nitride (3700 K and 3.9 eV, respectively). This to some extent suggests the presence of the mechanism of thermoelectronic emission from the molten and partially evaporating film surface [4].

V.I. Lakomsky is his work [14] devoted to detailed investigations of the oxide powdered cathodes developed by him, and containing zirconium with activating additives, showed that the film under consideration, consists of a non-stoichiometric zirconium oxide.

In case of the arc extinction, this film quickly solidifies, shrinks and cracks, and with the arc restriking is comes off partially or completely because of thermal shock. As a result, the service life of the thermochemical cathode essentially depends on

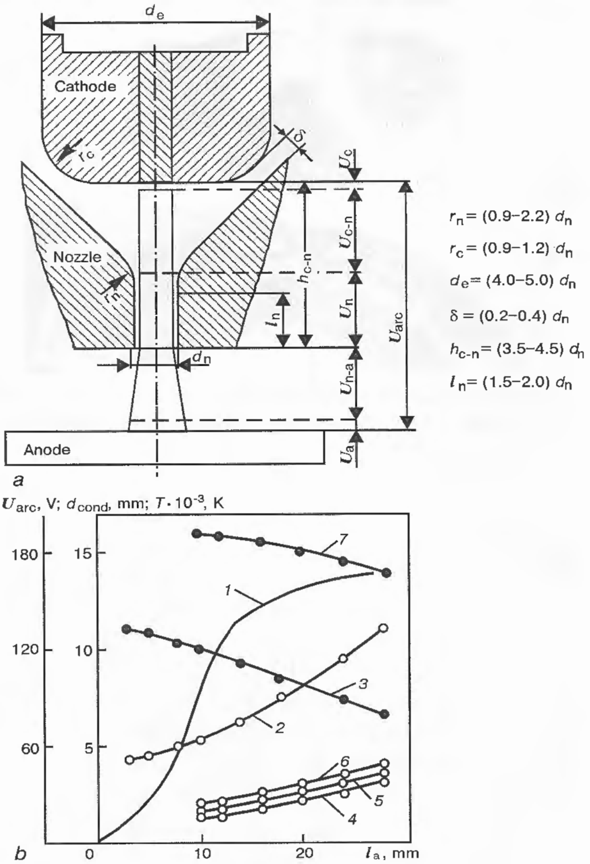

Figure 4. Parameters of the cutting air-plasma arc in the forming chamber (*a*) and depending on l_a (*b*): U_{arc} (*1*), d_{cond} at I_a = 300 A (*2*), T at I_a = 300 A, d_n = 3 mm (*3*) for freely expanding arc and d_{cond} at I_a = 100 (*4*), 200 (*5*), 300 A (*6*), T at I_a = 300 A, d_n = 3 mm (*7*) for a constricted arc

the number of the arc excitations, as well as on a variety of other factors. Among them are: insert material (zirconium or hafnium), purity of the yoke copper, quality of contact between them, cathode design, arc current I_a and its density on the cathode j_c, air purity and its flow rate, temperature and flow rate of the water or air for cooling the cathode. The results of experimental investigations of the service life of the cathodes can be represented in the form of dependencies of the depth of the erosion crater on the number of arc ignitions and duration of arcing at its cyclic striking, characteristic for plasma cutting. Many of these studies served as the basis for development of the commercial cathode designs for certain types of APC plasmatrons, while the technological details of their manufacturing constitute our khow.

The optimal density of current on the cathode j_c, equal to 90 – 100 A/mm^2, was established experimentally by varying the ratio of the values of the arc current and diameter of the active insert. This was done proceeding from minimal erosion of the cathode, higher emmissivity and melting temperature of the cathode film compared to the copper yoke, as well as the assumption that the cathode spot is limited by the area of the cathode insert. For cathodes of the plasmatrons designed for arc current of 100, 200 and 300 A, active inserts of 1.2, 1.6 and 2 mm diameter are recommended, respectively.

The cutting properties of APC plasmatrons essentially depend on the configuration of their *forming system* (cathode-nozzle chamber and swirler). Its optimal design parameters [10] shown in Figure 4, *a*, provide the maximal concentration of the cutting section of the arc column with a long service life of the cathode and the nozzle.

The initial dimensional parameter of the plasmatron chamber is nozzle diameter d_n which is selected proceeding from the optimal current density in the nozzle channel $j_n = 4\,I_a/\pi d_n^2$. The latter is equal to 40 – 70 A/mm^2 for I_a = 300 – 100 A in plasmatrons with water cooling and 40 – 45 A/mm^2 for $I_a \leq 150$ A in plasmatrons with air cooling.

The concentration of the air-plasma arc column was determined by measurement of its electrically conducting diameter d_{cond} and potential U_{arc} when the open part of the arc column was crossed by cathode-connected probes. Their distance from the cathode was determined by distance l_a [6]. U_{arc} distribution, shown in Figure 4, *a*, can be expressed in the form of a sum of voltage drop in the characteristic sections of the arc column:

$$U_{arc} = U_c + U_{c\text{-}n} + U_n + U_{n\text{-}a} + U_a. \quad (1)$$

Graphoanalytical processing of $U_{arc} = f(l_a)$ and $d_{cond} = f(l_a)$ functions for the open part of arc column (Figure 4, *b*) allowed calculation of the dependence of j, E and σ parameters on l_a from the following formulas:

$$j = \frac{4\,I_a}{\pi d_{cond}^2}, \quad E = \frac{\Delta U}{\Delta l_a}, \quad \sigma = jE, \quad (2)$$

where j is the current density, A/mm^2; E is the electrical intensity, V/mm^2; σ is the electrical conductivity, Ohm^{-1}·mm^{-1}.

Thermodynamic functions $T_{air} = f(\sigma)$ known for air [12], were used to calculate the temperature averaged over the electrically conducting section of the arc column: $T = f(l_a)$. The results of these calculations are given in Figure 4, *b*.

Coefficients ε and μ expressing the degree of the arc column constriction and exspansion were proposed [6] for evaluation of the effectiveness of the arc column formation by the results of probe measurements:

$$\varepsilon = \frac{d_{exp}}{d_{con}}, \quad \mu = \frac{\Delta l_a}{\Delta d_{con}} = \text{ctg}\,\alpha, \qquad (3)$$

where d_{exp} and d_{con} are the electrically conducting diameters of the freely expanding and constricted arcs at the same values of l_a and I_a, respectively; α is the angle of divergence of the electrically conducting channel of the constricted arc column.

The high degree of constriction and the low angle of divergence of the arc column are indicative of the high effectiveness of the forming system and the cutting ability of the plasmatron.

Solving the problem of *heat transfer by the plasma arc into the metal being cut* by calculation methods involves a number of assumptions which make the exact quantitative evaluation of the results impossible. In general terms it can be noted that the vector of the cutting heat flow of the arc coincides with the vector of cutting speed, while an intensive melting out of the metal is due to heat transfer from the leading front of the arc column immersed into the almost entire thickness of the metal. At the expense of the effect of the arc column shunting, the anode spot moves abruptly from the upper plane of the cut to the lower plane, which is indicated by the high-frequency oscillations of the cutting arc voltage recorded in the oscillograms [15]. A certain lack of parallelism of the cut edges with their widening upwards is found because of the drop in the concentration and temperature of the arc column with its immersion into the thickness of the metal being cut (Figure 1).

The thermal effectiveness of APC process was evaluated proceeding from the energy-heat balance of the arc (Figure 5, *a*), calculated by the results of calorimetric measurements of power losses in the cathode (P_c) and nozzle (P_n) units of a plasmatron, moved along the water-cooled copper anode. The power loss in the open section of the arc column P_{col} was found proceeding from it being equal to P_n (per a unit of the column length). In order to eliminate the impact of convective flows of plasma on the anode [6], power P_a evolved by the electronic current on the arc anode, was determined by calorimetric measurements of the anode with local matching of the anode spot to it and aiming the plasma jet upwards (from the plasmatron turned upside down). The data of calorimetric studies in the form of dependencies of power losses P_n, P_c and P_a on the arc current, are given in Figure 5, *b*. A small percentage of scatter in the balance components is related to the increase of P_c due to power losses arising in the arc column with its lowering into the crater hollow formed during the cathode erosion. Power $P_{col.\text{-}i}$ was calculated by detracting from the arc power all the measured consumption items of the balance.

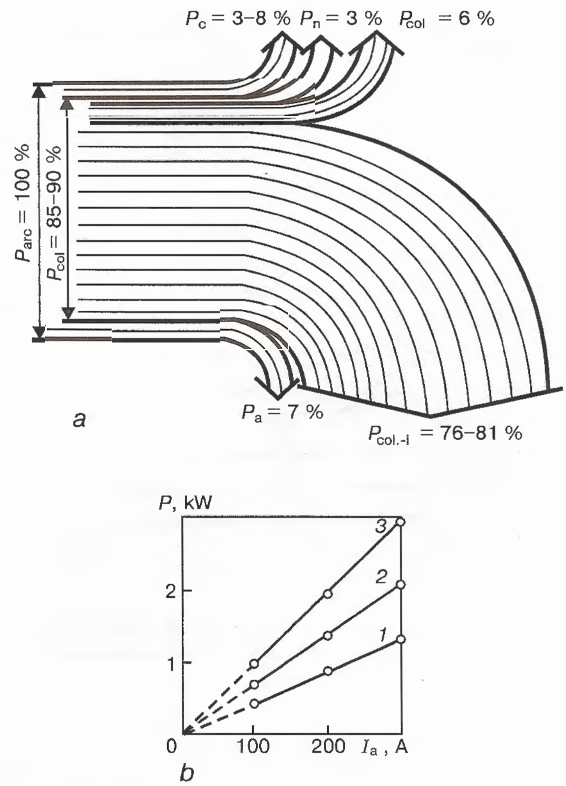

Figure 5. Energy-heat balance of the air-plasma arc (*a*) and dependencies of thermal power losses on I_a (*b*) in the nozzle P_n (*1*), in the cathode P_c (*2*) and by electronic current in the anode P_a (*3*)

Analysis of the energy-heat balance shows that the thermal power evolved in the item being processed, $P_i = P_a + P_{col.\text{-}i} = 83 - 88$ %. Part of it is properly used for melting out the metal from the cut cavity (P_{cut}), while the remaining part (P_m) is transferred to the cut edge.

By the estimate of K.V. Vasiliev [13] in high-speed APC, thermal efficiency of the process $\eta = P_{cut}/P_i$ can be up to 0.80 – 0.85. Therefore, P_{cut} is equal to (66 – 75) % P_{arc}, P_m — (13 – 17) % P_{arc}.

Thus, the process of APC is characterised by a high thermal efficiency, which is to a greater extent due to the plasma flow of an extended column of the constricted arc. In this case the terms «plasma cutting» and «plasma arc» can be regarded as justified — unlike the regular electric arc processes in which the main part of the heat evolved in the item being processed is found in the near-electrode areas.

The vector of heat removal into the cut edges, normal to the vector of cutting speed, can be calculated by N.N. Rykalin's theory proceeding from the model of the limiting state of heat propagation from a linear powerful quickly-moving source in a plate (without heat removal). Using the results of

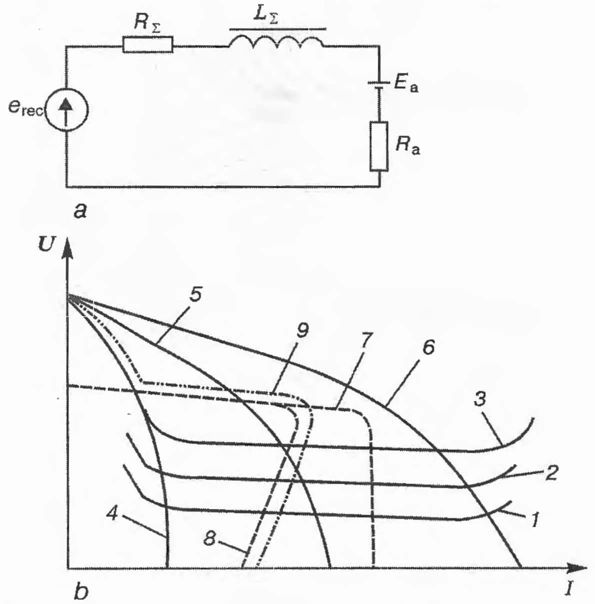

Figure 6. Equivalent circuit of the electric circuit of the source–arc system (*a*) and a family of static volt-ampere characteristics (*b*): VAC_a (*1* – *3*) and VAC_s (*4* – *9*)

such calculations and investigating the transverse microsections of the cut edges, K.V. Vasiliev [13], generalised extensive data on the surface structure of the cut edges, consisting of a partially-melted layer (cast area measured by fractions of a millimeter) and a region of the HAZ, whose depth at the high speeds characteristic of APC, does not exceed 1 mm.

The *electrical parameters of the current source–arc system* have an essential influence on the processes proceeding at APC. The equivalent circuit of the source–arc circuit is given in Figure 6, *a*, while the static volt-ampere characteristics of the arc (VAC_a) and the source (VAC_s) — in Figure 6, *b*. The family of VAC_a (curves *1* – *3*) can be conditionally divided into three characteristic sections: sloping ($I_a \leq 50$ A), independent ($I_a = 50$ – 400 A) and rising ($I_a \geq 400$ A).

The equation of electric equilibrium of the source–arc system can be represented as

$$e_{rec} = iR_\Sigma + L_\Sigma \frac{di}{dt} + E_a + iR_a, \qquad (4)$$

where e_{rec}, i are the instantaneous values of the rectifier open-circuit voltage and current in the source–arc circuit, respectively; E_a is the arc voltage in an independent section of VAC_a, represented in the equivalent circuit as anti-emf; R_a is the non-linear ohmic resistance of the arc (positive in the rising section of VAC_a and negative in the drooping section); R_Σ, L_Σ are the reduced to the rectified current circuit total ohmic resistance and inductance of the source.

For a three-phase full-wave rectifier

$$e_{rec} = \frac{\pi}{3} U_{op.-c} \sin\left(\omega t + \frac{\pi}{6}\right), \qquad (5)$$

where $U_{op.-c}$ is the effective value of the rectifier open-circuit voltage.

The VAC_a slope depends on the degree of constriction of arc column ε, while E_a value is determined by the dimensions of the plasmatron chamber and parameters of its operational mode (length of the open and cutting sections of the arc column, plasma gas flow rate, cutting speed).

Depending on the circuit designs of an uncontrolled rectifier, the natural VAC_s (Figure 6, *b*) can be steep-falling (curve *4*) or drooping (curves *5*, *6*), while with the addition of feedbacks to the controllable rectifier, it is represented by curves *7* – *9*.

The key problem of the source–arc system is the issue of its stability. Within the limited scope of this paper, we will try to describe some of its aspects just in general terms.

When the arc stability is considered, let us assume as its disturbing parameter, the deviation of arc voltage ΔU_{arc} arising with the change of the values determining it: arc length, gas flow rate, etc. The reaction to this disturbance is the change of current Δi which is determined by the arc transition to another VAC_a. The speed of the transition process is determined by the speed of change of U_{arc} and inertia of the source–arc system characterised by its electromagnetic time constant $\tau_e = L_\Sigma / (R_\Sigma + + R_a)$.

In addition to the generally known condition of *static stability of arcing* (VAC_s should be steeper than VAC_a), the *dynamic stability of the system* is determined from equation (4) and is dictated by the following conditions:

• continuity of arc current at pulsed voltage at the rectifier output, provided by the optimal value of inductance of the power transformer and the smoothing throttle. Design should take into account that the thermal inertia of the air-plasma arc column defined by us in [5] as the duration of existence of the plasma without energy supply from the outside, at I_a = 200 A is equal to $4 \cdot 10^{-4}$ s. Therefore, the thermal constant of arcing time τ_a is incommensurably small compared to τ_e, and it can be neglected in calculations;

• absence of self-excited oscillations of arc current arising under certain conditions in resonance (inductive-capacitive) sources or in sources with feedbacks. In case of appearance of self-excited oscillations, the arc is not always extinguished, so that this condition can also be called *dynamic stability of current of the source–arc system*. It is due to a greater τ_e, compared to the time constant of the control circuit of the source τ_{contr}, and is calculated with application of the criteria of stability of the theory of automatic regulation.

The critical conditions of static and dynamic stability of the system are especially important in the sloping region of VAC_a, for instance, in ignition of the pilot arc, where the current is limited by admissible load on the nozzle, while the possibilities of increasing $U_{op.-c}$ are limited by electrical safety conditions.

With a higher density of current in the channel of the plasmatron nozzle, there is the risk of disturbance of the *spatial stability of the arc*, i.e. development of a breakdown of the gas interlayer that insulates the nozzle channel inner surface from the arc column, and, as a result — division of the cutting arc into two parts, namely cathode–nozzle and nozzle–item being cut. In this case the condition of spatial stability of the arc is expressed as

$$E_n l_n < U_{br}, \quad (6)$$

where E_n is the intensity in the nozzle channel, V/mm; l_n is the length of the nozzle channel, mm; U_{br} is the breakdown voltage of the above gas interlayer.

With optimal current density j_n and l_n/d_n ratio, the spatial stability is provided by a smooth or stepwise rise of I_a at the start of the cutting process. This is especially necessary at working currents which exceed 100 A, as alternatively the stepwise surge of current causes a peak of E_n and interlayer breakdown. The procedure of determination of the optimal curve of the working current rise is protected by an author's certificate for invention [11].

Finally, introduction of the notion of *technological stability of the source–arc system* by us in APC is dictated by an essential deterioration of its cutting properties in the case of an extremely low slope of VAC_s (curve *6* in Figure 6, *b*). Then:

- in manual cutting extreme variations of I_a leading to a marked deterioration of the quality of the cut edge surface (formation of scratches) are found as a result of variation of the values of l_a and respective U_{arc};
- manual and machine cutting of thick metals with the arc immersion into the depth of the metal is characterised by a drop of I_a and of its cutting ability, respectively.

In uncontrollable rectifiers with $U_{op.-c}$ limitation by not more that 300 V (as required by GOST 12221–79 for plasma cutting equipment), in the region of currents above 150 A the VAC_s slope becomes too low and by the above reasons, the technological stability of the arc becomes a critical value. In controlled thyristor rectifiers, introduction of a negative current feedback (deviation feedback) provides a VAC_s shown in Figure 6, *b*, by curve *7*, i.e. stability of the arc current is provided with variation of its length, working gas flow rate and mains voltage. Still higher performance of the cutting arc is observed with introduction of an additional positive feedback by U_{arc} (disturbance feedback). In this case, VAC_s (curve *8*) differs in I_a rising with the greater length of the cutting section of the arc column, thus providing a high quality of the cut edges and improvement of the cutting ability of the arc.

Curve *9* shown in Figure 6, *b* is an ideal VAC_s, allowing for the requirements of all the factors of the system stability and high efficiency of the source. Such a characteristic is provided by a combination of two rectifiers — one with the VAC_s working section described by curve *8* and low-power volt-adding one with VAC_s section corresponding to curve *4*.

The electrical and thermophysical regularities of APC process presented in a concise form, were the basis for development of various production designs of air-plasma cutters and power sources.

Circuit and structural principles of designing the plasmatrons and power sources for APC. The requirements to *designs of plasmatrons* for APC are determined by their applications and operational conditions. Plasmatrons for machine and manual cutting, operating in a shop or in open sites under different climatic conditions, have their special design features. The general requirements are as follows:

- high quality of formation of the plasma arc which is provided by the geometry of the cathode-nozzle chamber of the plasmatron;
- maximal operational life of plasmatron elements exposed to high temperatures (cathode and nozzle), ability to quickly replace them, low cost;
- small weight, reliability in operation, air-tightness of the plasmatron and its cable-hose lines;
- manoeuvrability of manual cutters, ability to perform the cutting in difficult-of-access places with different configuration of the items.

Figure 7 shows the most commonly used in production cathode designs and block diagrams of the plasmatrons. Cathode with a conical fastening to the cathode unit and hafnium insert (Figure 7, *a*) is characterised by a high metal content and complexity of its replacement. Cathodes with captive nut fastening and heat-removing tail part (Figure 7, *b*) and with threaded fastening to the cathode unit (Figure 7, *c*) feature a much smaller metal content and rather long operational life even provided the hafnium insert is replaced by a less expensive zirconium insert. Application of a hafnium insert in the design (Figure 7, *c*) provides a

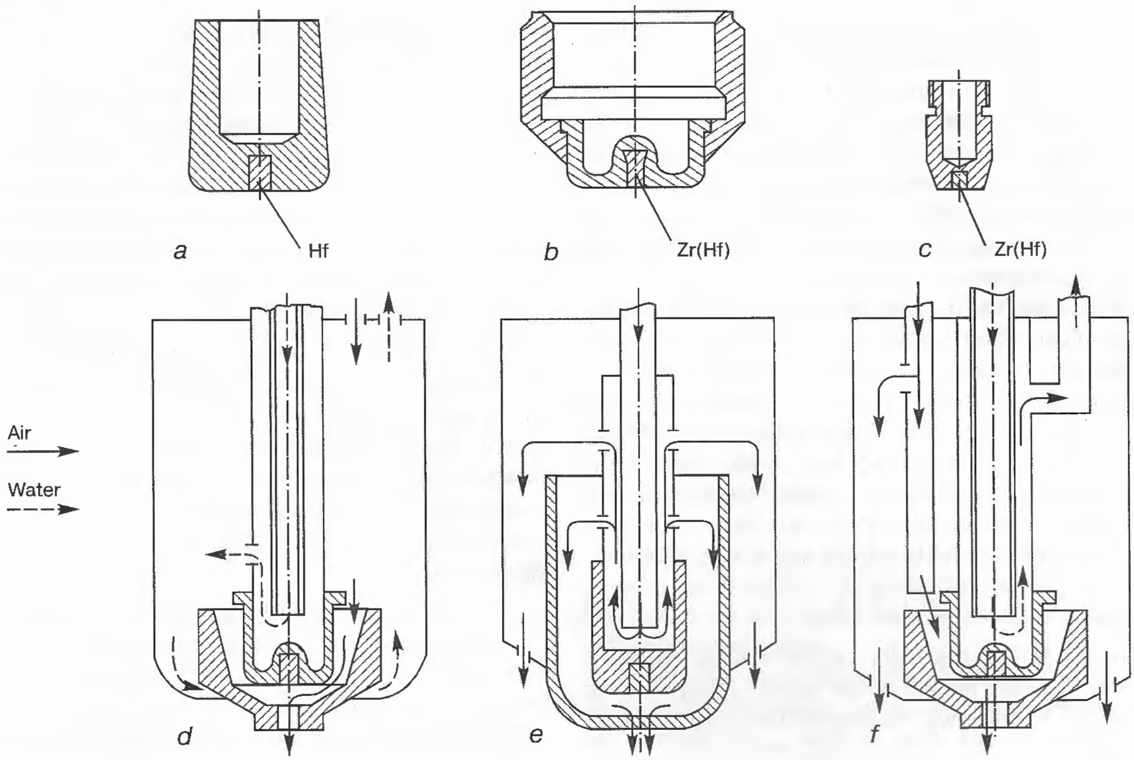

Figure 7. Block diagrams of the cathodes and plasmatrons (for nomenclature see the text)

long operational life of the water-cooled cathode at the arc current of 140 – 160 A.

Plasmatron cooling circuits are the main design factor that determines their purpose. So, the plasmatrons with water cooling of the cathode and the nozzle units (Figure 7, *d*) are designed for machine cutting in shop conditions in the range of currents of 50 to 300 A. Their starting is only possible with a pilot (auxiliary) arc excited by a spark breakdown of the cathode–nozzle gap.

Plasmatrons (Figure 7, *e*) with air cooling of the cathode-nozzle pair (with re-routing part of the air for plasmaforming), are used, as a rule, for manual cutting. In the case of low requirements to air-tightness, they can be designed to be simpler without sealing rubber gaskets and with a mobile nozzle which provides a simpler contact ignition of the arc without limiting the length of the cable-hose lines. In small-sized water-cooled manual cutters designed for up to 80 A current, and cutting of thin metal (up to 15 mm), there is no need for current supply to the nozzle. The positive potential applied from the power source to the item being cut is transferred to the nozzle when it contacts the item. An intermediate arc, automatically transferred to the main arc, is ignited by lightly pressing the nozzle. Operation with the nozzle resting against the item being cut, is rather convenient for the cutting operator.

In manual cutting of medium-thick metals at the current of 80 – 160 A it is rational to apply the pilot arc with its contact or spark ignition in the cutters with air cooling (Figure 7, *e*), while at higher currents (up to 200 – 250 A) — in those with water-air cooling (Figure 7, *f*).

Circuit solutions of the *plasmatron power sources* evolved from simple (using batch-produced welding transformers and rectifiers) up to sophisticated thyristor-controlled rectifiers with feedbacks and a smooth adjustment of current or inductive-capacitive rectifiers with stepwise regulation of current [1, 7]. The high weight and dimensions limited their application.

At present new possibilities are opened up when inverted converters are used as the sources. Inversion of rectified mains voltage of 20 to 50 kHz frequency using powerful transistors allows a many times reduction of the weight and dimensional characteristics and material content of rectifiers in a wide power range, and providing in them any VAC, a smooth current regulation and a high efficiency. A somewhat high cost of the high-frequency power transistors and diodes still limits wide application of inverted converters in welding equipment. In the units for plasma cutting and for other kinds of plasma processing, however, their application can already be considered to be justified.

The sources for machine APC are designed to have a remote control panel incorporating pneumatic and water service lines, a block for spark ignition of the pilot arc, instruments for monitoring and adjustment of the plasmatron parameters. Such a remote panel is usually combined with the control panel of the plasma-cutting machines. The sources for manual APC are, as a rule, made as one module.

Technological capabilities of APC. This process is indispensable in thermal cutting of stainless steels and non-ferrous metals. Considering, however, that today the actual APC capabilities are limited by metal thickness of up to 80 mm, an intensive search for the methods to increase the cut metal thickness should be carried on for the above materials.

An alternative to APC of carbon and low-alloyed steels still remains to be gas-oxygen cutting (GOC), which, as can be seen from Figure 8, *b*, is markedly inferior to APC as to achievable speeds for small and medium thicknesses, while at steel thickness above 60 mm, the speeds of both welding processes become practically the same.

In the existing complicated economic situation, the main share of APC unit users is made up by enterprises which apply them for *scrapping obsolete equipment*. With the absence of any requirements to the quality of the cut edges, the main requirements to such units are simplicity, reliability and air cooling of the cutter with its minimal weight and convenience of manoeuvring. All these requirements are met by Kiev-5 and Kiev-8U units produced by NPMGP «Plasmatron», which can cut metals up to 50 and 70 mm, respectively, and also provide comparatively high cutting speeds at a relatively low cost and minimal power consumption. Kiev-8U unit, in addition to the air-cooled cutter, is also fitted with a water-cooled one, which under the shop conditions, in combination with the tracers or other mechanisation means, provides *high-quality cutting in blanking production.*

The quality of thermal cutting of metals (APC and GOC) is evaluated by a common system developed by VNIIavtogenmash (GOST 14792–80). The system is based on four groups of indices characterised by quality classes.

The first group of quality indices, namely the accuracy of the dimensions of the cut out blanks, is determined, in addition to the precision of the mechanism of the cutter displacement, also by the absence of the processed sheet displacement under the impact of thermal deformations and the constant axially symmetric position of the cutting arc column relative to the plasmatron — the so-called jet accuracy of the cutting arc. The dimensional accuracy is largely dependent also on the degree of concentration of the cutting arc column, i.e. on ε and μ coefficients.

The second group of characteristics includes the allowances for the cut edge macrogeometry, i.e. angle of its bevel, which is largely determined by the cutting speed (it becomes greater with the increase of the latter).

The third group is made up by the allowable values of microgeometry of the cut surface (scratch depth, surface roughness), and the fourth one — by the allowable width of the HAZ and its cast region.

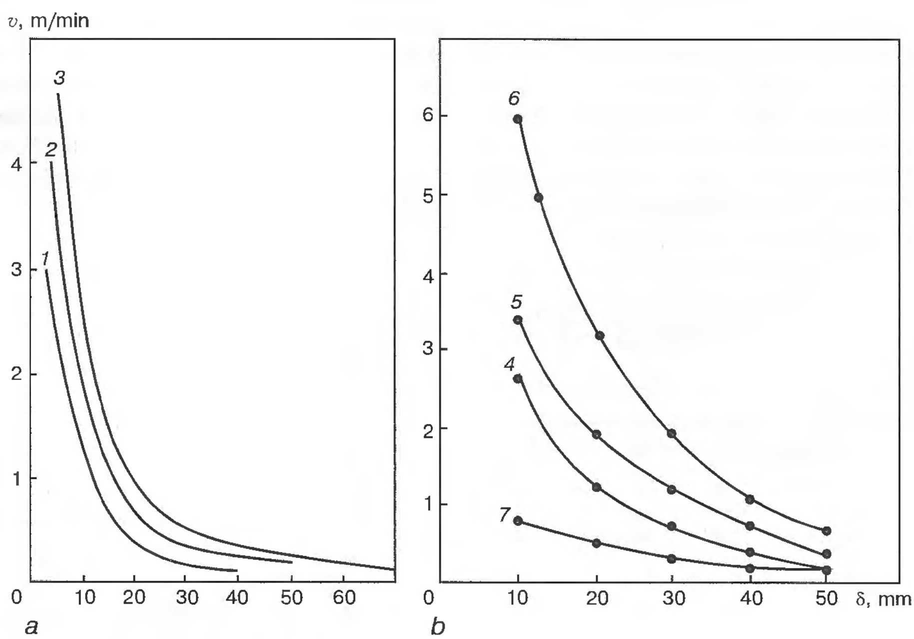

Figure 8. Speed characteristics of APC by air-cooled plasmatrons (*a*) using Kiev-5 units with d_n = 2.2 mm at I_a = 100 – 120 (*1*), 120 – 140 A (*2*) and Kiev-8U units with d_n = 2.2 mm at I_a = 140 – 160 A (*3*) and by water-cooled plasmatrons (*b*): sound cutting at I_a = 200 A, d_n = 2 mm (*4*) and I_a = 300 A, d_n = 3 mm (*5*); high-speed severing at I_a = 400 A, d_n = 4 mm (*6*); GOC is shown for comparison (*7*)

According to GOST 14792–80, 1st class corresponds to the highest requirements to the characteristics, 2nd — to those really achievable in production, 3rd — to minimal requirements to the limit values of the characteristics.

In machine APC in the thickness range of 5 – 50 mm, the 2nd class can be achieved for all the quality characteristics. In manual APC, with application of tracers, additional machining of the edges is required (most often with a grinder), in order to provide the required quality of the edges during production of parts and blanks for subsequent welding. In this case a 0.1 – 0.2 mm layer of the cast region, is removed, which is saturated with nitrogen detrimental for welding steels.

There are methods to improve the quality of the edge surface by adding oxygen to the plasma air, or introducing thin turbulent water jets into the arc column in the nozzle area [16]. All these techniques, however, significantly complicate APC and increase its cost, and, therefore, in practice they are used in special cases, for instance, in ship-building when cutting out sheet structures of hull steels 6 – 14 mm thick, which are to be further welded by automatic submerged-arc process (in order to avoid the formation of pores, caused by edge nitriding).

The distance from the nozzle edge to the item being treated, has an essential influence on the quality and effectiveness of APC. In manual cutting the optimal distance is maintained by fastening support rollers, pins or ceramic extensions to the nozzle unit of the cutter, and in machine cutting — with capacitive sensors.

Correction of the cutting speed (its lowering in the case of small rounding-off radii) is required in high-quality machine cutting of complex-shaped parts around a curvilinear contour. Therefore, precise cutting out of parts around a complex contour, is performed in two-axis machines with numerical programmed control and automatic regulation of the cutting speed, height and angle of rotation of the plasmatron axis relative to the item being processed. In the technology developed by us, together with Kyiv Politechnical Institute «KPI» [17], precise APC of the cutting edges (blades of fodder choppers, harrow teeth, etc.) is performed with their simultaneous quenching by the same plasma arc, thus eliminating the operations of stamping, milling or heat treatment earlier used in manufacture of these parts.

Table 1. Operating costs per 1 lin. m of the cut on low-carbon steels, hrvn. (as of 01.04.99)

Processing method	*Thickness of the steel being cut, mm*					
	10	*20*	*40*	*60*	*100*	*200*
GOC	1.00	1.30	1.60	1.80	2.80	4.50
APC when the following units are used:						
Kiev-5	0.10	0.20	0.56	1.30	–	–
Kiev-8U	0.07	0.17	0.48	1.20	–	–

The urgency of application of APC for *repair purposes*, gave rise to the idea of creating all-purpose Duplex-1, Duplex-2 units, which have no analogs by their technological capabilities. They perform both plasma cutting, and electric arc welding with consumable stick electrodes and nonconsumable tungsten-electrode argon-arc welding at straight and reverse polarity direct current, without any change of connections or complicated switching. The low weight and the high efficiency of the inverter power sources allow these units to be used in case of time deficit in mobile emergency means with self-sufficient power supply, in particular, in repair of heating and water-supply systems of the city public utilities. Cutting can be performed with success in the flooded and water-filled pipelines, which is impossible with GOC.

Economic effectiveness of APC. As applied to alloyed steels and non-ferrous metals, APC is a no-alternative cutting process, which is everywhere and effectively used both in metal scrapping and for high-quality cutting in all the modern industries.

Evaluation of the effectiveness of APC of widely used carbon and low-alloyed steels, is usually performed in comparison with GOC. Important in this case are the specific conditions of the particular productions, including the scope of cutting, range of thickness of the metals being severed, terms of work performance (APC has considerable advantages as to the achievable speeds), requirements to surface finish and geometry of edge preparation for welding, etc.

Common characteristics for evaluation in all the cases are operational costs per 1 lin. m of the cut: in APC — for consumable parts of the plasma cutter and power, in GOC — for consumable parts of the gas cutter, combustible gases and their feeding.

These costs, calculated by us in [18], are shown in Table. 1.

In general terms evaluation of effectiveness is performed allowing for all the above factors by the period of return-on-investment into the equipment for one and the other process.

As shown by production experience, in scrapping metal 5 to 40 mm thick, allowing for the cutting operator salary and operating costs, the return-on-investment for one Kiev-5 unit with its continuous two-shift operation is not more than 3 months, and further on the profit from GOC replacement by APC is calculated proceeding only from the operating costs (see Table 1). When these cutting processes are compared, it is also necessary to take into account such difficult-to-evaluate factors as an almost complete absence of deformations in APC, versatility of this process in relation to various kinds of metals, almost instantaneous start (in GOC a lot of time and combustible materials are consumed in the metal preheating at the start of cutting), ability of the cutter immersion into the water in APC (gas flame dies out in the water), as well as performance of welding operations with the Duplex units using one and the same power source.

Safety measures in operation of APC units. According to GOST 12221–79, admissible voltage $U_{op.-c}$ of the power source for semi-automatic plasma cutting should not exceed 300 V, while that for machine cutting — 500 V. To meet these requirements our units were designed to additionally incorporate automatic switching off of rectifier voltage in the case of the arc extinction, as well as protective insulation of the outer surface of the metal body and the nozzle unit.

APC processes generate gas and dust evolutions, noise and light radiation of the arc to varying degrees. In manual cutting of up to 15 mm metal at small currents with the nozzle resting against the item being cut, the arc does not blind the eyes, and the gas and dust evolution and noise are almost not noticeable. Nonetheless, under these conditions, individual protective means used by gas cutting operator (special clothes and goggles with light filters) can be recommended.

In cutting at the currents of 150 A and higher of more than 20 mm thick metals, the noise and gas and dust evolution are increased. In order to protect the plasma cutter in cutting 20 – 40 mm metal, protective means for electric arc welding operator (special clothes, and helmet with light filters) and above 40 mm — also noise-protecting earphones should be used. When working under the shop conditions, use of effective local exhaust and general shop ventilation by dilution, is mandatory. A detailed evaluation of the hazardous factors and the norms for protection from them is given in [1].

With the increase of the arc current and thicknesses of the metals being cut, the arc column concentration is decreased and the cut becomes wider, in addition to the hazardous factors becoming more pronounced. Here, the efficiency of the cutting process drops, accordingly, and the operational life of the cathode and the nozzle is reduced. Therefore, it is necessary to try to achieve the maximal cutting ability of the air-plasma arc at up to 150 A currents in manual cutting with air cooling of the cutter and at up to 200 A currents in machine and manual cutting with its water cooling.

Comparative analysis of the modern units for APC. Parameters of the currently available locally-made and foreign APC units are given in Tables 2 and 3.

Analysing the parameters of the units shown in Table 2, it should be noted that in the majority of them the main characteristic — the maximal thickness of the metals being cut — is achieved at increased currents and a short operational period (35 – 40 % duty cycle at 10 min working cycle), this practically not allowing an effective use of these units for cutting metals of the indicated maximal thicknesses.

The locally-produced Duplex-1 and Duplex-2 units at 60 % duty cycle, in addition to rather

Table 2. Parameters of the units with air cooling of the cutters for APC of metals up to 30 mm thick

Parameter	*UPVR-0401*	*UPVR-0901*	*Karat-60*	*Karat-100M*	*Airjet-60*	*Airjet-100*	*LPE-50*	*LPE-100*	*Duplex-1*	*Duplex-2*
	OAO «Firm SELMA» (Simferopol)		*Enagro-Torets Company (Konstantinovka, Donetsk distr.)*		*Castolin Company (Switzerland)*		*ESAB Company (Sweden)*		*NPMGP «Plasmatron» of PWI STC (Kyiv)*	
Consumed power, kW	9	16	8	32	9	16	10	30	2 – 5	3 – 10
Rated current, A	40	90	60	100	60	100	50	100	30	90
Duty cycle, %	40	40	35	100	35	35	35	60	60	60
Maximal thickness of cut steel and aluminium, mm	5	30	10	25	15	30	15	30	10	30
Weight, kg	40	125	80	200	18	28	90	185	25	110
Air flow rate at the pressure of 0.4 – 0.6 MPa, l/min	120	150	200	210	180	180	130	180	40	50

Table 3. Parameters of the units for APC of up to 60 mm thick metal.

Parameter	*Karat-200-802*	*PPR-200*	*Kiev-5*	*Kiev-8U*
	Enagro-Torets Company (Konstantinovka, Donetsk distr.)	*PWI Pilot Plant of Welding Equipment (Kyiv)*	*NPMGP «Plasmatron» of PWI STC (Kyiv)*	
Consumed power, kW	45	45	23	30
Rated current, A	200	200	120	140
Duty cycle, %	100	60	100	100
Maximal thickness of cut steel and aluminium, mm	50	60	50	70
Weight, kg	300	300	190	250
Air flow rate at the pressure of 0.4 – 0.6 MPa, l/min	100	50	200	200
Cutter cooling	Water	Water	Air	Air

effective severing of the thicknesses indicated in Table 2, are also superior to all the local and foreign analogs by being versatile (the same unit can perform both cutting and electric arc welding).

The advantages of the local Kiev-5 and Kiev-8U units are obvious among APC units of medium power (Table 3). At smaller consumed power, up to 150 A current, 100 % duty cycle and air cooling of the cutters, they provide the same maximal thickness of metal cutting, as their analogs with water cooling of the cutters.

Higher power APC units with water cooling of the plasmatrons (Kiev-4M, Kiev-6, APR-404), the fabrication of which is not cost-effective under the present conditions, in view of the high consumption of reactive materials and weight and dimensional characteristics, are still used in many enterprises where their service life is not yet over.

Prospects for development of APC and allied technologies with application of inexpensive oxygen-containing plasma-forming media. Further development of APC as a highly efficient and cost-effective cutting process is anticipated in the following areas:

- cutting thick metal (up to 200 mm and more). Progress in this area is based on a number of original ideas that require further investigations for their implementation;
- underwater APC, the practicability of which at down to 30 m depth, was confirmed by our experimental work as far back as in 1980s;
- robotic cutting at increased radiation level that we believe will be required in the near future;
- high-quality automatic cutting of thin and medium-thick metals, based on developments of plasmatrons with a high concentration of the arc column at minimal power consumption.

As demonstrated by our studies, plasmatrons with thermochemical cathode have a satisfactory operating life with application of inexpensive materials as plasma-forming media (carbon dioxide gas, water and commercial purity nitrogen).

Encouraging experimental work has been performed on CO_2 plasma welding of low-carbon and low-alloyed steels, also in a tandem with submerged-arc welding.

We can see good prospects for application of commercial purity nitrogen for plasma welding of copper and plasma surfacing in a number of processes where nitriding of the deposited layer provides its higher wear resistance.

Application of water vapours as a plasma-forming medium, tried out by us, showed that use of vapour-plasma cutting and welding under special conditions, is promising.

In our opinion, application of surface treatment of the welds to remove their reinforcement and thermal stresses, can be of interest.

Effectiveness of application of air with a small addition of propane-butane for plasma spraying, confirmed by our joint work with VNIIavtogenmash and the Institute of Gas of the NAS of Ukraine [19], resulted in development of Kiev-7 production unit, which was put into batch production in Barnaul Mechanical Engineering Plant in co-operation with PWI Pilot Plant of Welding Equipment. Kiev-7 units are being used with success in many enterprises of the CIS countries, they still attract a lot of interest and we hope that their manufacture will be resumed at a new quality level.

The described prospects make us feel confident that plasma technologies with application of inexpensive working gases will become advanced and competitive exported products in the near future.

REFERENCES

1. Esibyan, E.M. (1971) *Plasma arc equipment*. Kyiv: Tekhnika.
2. Esibyan, E.M., Gvozdetsky, V.S. (1981) Plasma welding and cutting. In: *Welding in the USSR*. Moscow: Nauka.

3. Esibyan, E.M., Gladky, P.V., Nikiforov, N.I. *et al.* (1999) *Equipment for plasma welding, surfacing and cutting*. Encyclopedia. Moscow: Mashinostroyeniye.
4. Danchenko, M.E. (1974) *Development and investigation of plasmatrons with a zirconium cathode*. Synops. of thesis of Cand. of Sci. (Eng.). Kyiv.
5. Esibyan, E.M., Malkin, V.B., Ionin, V.E. (1969) On inertia of the electric arc. *Avtomaticheskaya Svarka*, **7**, 32 – 34.
6. Esibyan, E.M., Danchenko, M.E. (1970) Energy properties of an arc with zirconium cathode. *Ibid.*, **1**, 5 – 8.
7. Esibyan, E.M., Dotsenko, V.D. (1970) Some features of calculation of a thyristor rectifier that powers the arc. *Ibid.*, **2**, 25 – 29.
8. Esibyan, E.M., Danchenko, M.E. *Non-consumable electrode for arc processes*. Pat. **2.044.232** (B) France, Int. Cl. B 23 K 35/00, 27/00. Publ. 26.11.71. Same: Pat. **3.676.639** USA. Same: Pat. **85904** GDR. Publ. 28.05.70.
9. Esibyan, E.M., Danchenko, M.E. *Non-consumable electrode for arc processes*. USSR author's certificate **420222**, Int. Cl. B 23 K 35/00, 9/16. Publ. 5.08.76.
10. Esibyan, E.M. Dudko, D.A., Danchenko, M.E. *et al.* *Plasma cutter*. USSR author's certificate **493097**, Int. Cl. B 23 K 31/00. Publ. 25.06.78. Same: Pat. **4.055.741** USA.
11. Esibyan, E.M., Dotsenko, V.D., Malkin, V.B. *et al.* *Method of plasma cutting*. USSR author's certificate **562397**, Int. Cl. B 23 K 31/00. Publ. 25.06.77.
12. Vagraftik, N.B. (1963) *Reference book on thermophysical properties of gases and liquids*. Moscow: Fizmatgiz.
13. Vasiliev, K.V. (1973) State-of-the-art and problems in plasma arc cutting of metals. In: *Plasma processes in metallurgy and technology of inorganic materials*. Moscow: Nauka.
14. Lakomsky, V.I. (1997) *Oxide cathodes of the electric arc*. Zaporozhje: Internal.
15. Bykhovsky, D.G. (1972) *Plasma cutting*. Leningrad: Mashinostroyeniye.
16. Shirshov, I.G., Kotikov, V.N. (1987) *Plasma cutting*. Leningrad: Mashinostroyeniye.
17. Khilchevsky, V.V., Esibyan, E.M. (1991) Formation of the cutting edges of a blade tool by air-plasma cutting. *Tekhnol. i Organiz. Proizvodstva*, **32**, 29 – 31.
18. Esibyan, E.M. (1999) Selection of the means and equipment for thermal cutting of metals. *Svarshchik*, **3**, 4 – 6.
19. Esibyan, E.M., Saakov, A.G. (1989) Energy and technological features of air-gas plasma spraying. *Avtomaticheskaya Svarka*, **10**, 28 – 32.

ACTIVITY OF THE RUSSIAN INSTITUTE OF WELDING IN THE FIELD OF PLASMA EQUIPMENT AND TECHNOLOGY (REVIEW)

V.V. SMIRNOV, M.D. ROGOVOJ and **V.I. POVSTYAN**
Russian Institute of Welding, St.-Petersburg, Russia

ABSTRACT

Developments of the Russian Institute of Welding in the field of plasma treatment of materials: spraying, surfacing and welding, as well as air-plasma cutting and plasma recycling of wastes, are described. They include technologies for air-plasma cutting of ferrous metals and stainless steels up to 40 mm thick, aluminium and copper up to 50 and 20 mm thick, respectively, lines for automatic welding of super thin-walled (0.17 – 0.50 mm) small-diameter (4 – 8 mm) tubes and ecological plasma arc reactor which can be installed into any gas line.

Key words: *plasma surfacing and welding, air-plasma unit, tube welding line, plasmatron, recycling of wastes*

The Russian Institute of Welding pays special consideration to development of technologies and equipment for various types of plasma treatment of materials.

Manufacture of parts by plasma spraying. The Institute has developed the technology for the manufacture of parts by the method of plasma spraying involving deposition of materials on the mandrel (master pattern).

Owing to its high productivity, relatively low running costs (cheap and readily available air is used as the working gas), this method can find application in the manufacture of pressing dies for plastic materials. With this method the time needed to make a pressing die is shorter by a factor of more than a hundred, as compared with other known electrochemical methods. The normal practice in this case is to deposit first a layer 0.5 – 1.0 mm thick using powders of self-fluxing alloys, which provide hardness of more than *HRC* 45, and then a filling layer of a material that has good mechanical workability.

Roughness of the working surface of a part made by this method depends upon roughness of the surface of the master pattern and size of particles of the spraying powder, and normally it is not higher than $R_a = 0.63$ μm. It can be improved by using a combined method which involves deposition of a thin layer (0.05 – 0.10 mm thick) by electrochemical methods or by condensation of a nickel coating after dissociation of nickel tetracarbonyl.

Another application of this method is for manufacture of ceramic parts of the type of tubes, crucibles, etc. The resulting parts are thin-walled, having very precise geometrical dimensions.

In the next years the progress in plasma spraying should be targeted on development of the plasma technology and package of equipment with a superior quality and productivity, as compared to those currently applied.

Air-plasma cutting. Today this is the most efficient method for cutting low-alloy and alloyed steels, non-ferrous metals and alloys. Plasma cutting is much superior to oxygen cutting in the process speed on metals up to 30 mm thick, while in combination with the CNC high-speed machines it becomes the basic method for cropping metal in ship and machine building. Semi-automatic (manual) plasma severing has also gained a wide acceptance.

The Institute has developed and manufactures plasma cutting machines operating at currents of 50, 100, 200 and 400 A, which provide high-quality cutting of metals with thickness ranging from 2 to 100 mm.

The use of power supplies equipped with the microprocessor-based control systems leads to a substantial improvement of the quality of cutting and decrease of not less than 2 times in consumption of fast wearing components of the plasmatrons.

Analysis of the market of plasma equipment shows that foreign companies widely practice replacement of thyristorized power supplies by the inverter-type ones.

The Institute has also developed and makes self-contained units for air-plasma cutting and electric arc welding of metals under field conditions, i.e. where no power lines are available. In this case a unit is located on the MAZ-522 trailer chassis in a body encased for warmth-keeping (KUNG-P10). The body also houses a power-generating unit with a capacity of 100 kW, one heating-ventilation and two compressor units, two storage batteries, a converter and a kit of spares. The body with a load carrying capacity of 10.5 t can be transported by any vehicle (car, tractor or prime mover). The power-generating unit consists of a diesel engine and generator connected via a board flange into one unit.

The air-plasma machine with a rated current of 200 A is intended for cutting ferrous metals and stainless steels up to 40, aluminium — up to 50 and copper — up to 20 mm thick. It can be employed for cropping of ships, aircraft and other large-sized structures under any climatic conditions, i.e. from the Extreme North to the south of the country. Availability of a separate room makes it possible to provide suitable conditions of life for the attending personnel. As an option, an electric welding equipment can be located in the KUNG-P10 body, which enables the machine to be used as a base for arrangement of a repair shop.

In the next years development of the plasma cutting process will be towards building of a package of equipment for cutting ferrous and non-ferrous metals 100 – 300 mm thick.

Plasma surfacing. Surfacing can be used to make the most diverse items with the desirable surface properties, i.e. corrosion-, heat-, wear-resistant, antifriction, etc., as well as to repair worn-out pieces.

Plasma surfacing can be performed at a direct current of reverse or straight polarity, using wire or powder consumables.

Owing to minimum penetration of the base metal and its minimum dilution with the deposited metal, the process of plasma surfacing at a DCRP provides the preset properties of the metal even in the first of the deposited layers, as compared with the third or fourth layer in the case of arc surfacing. This leads to metal saving and raises labour productivity.

Powder materials, such as Co-based alloys of the type of stellites, and Ni-based alloys of the type of Calmolloys, Fe-based powders, stainless steel and bronze wire, can be used as the coating materials.

Plasma surfacing gains wide acceptance in manufacture and repair of valves of various-application internal combustion engines, rolling mill shafts and other parts.

Developments of the Institute include also plasma surfacing machines operating at currents of 300, 500 and 800 A.

In the next years developments in the field of plasma surfacing will be targeted on the following:

- devising of the integrated process control systems to ensure continuous correction of the surfacing parameters to provide desirable properties of the deposited layer;
- using combined plasma and arc surfacing methods.

Plasma welding. Plasma welding provides the highest effect when used for joining metals with a high thermal conductivity, such as copper, aluminium and their alloys. This method allows avoidance of preheating and performance of single-pass welding on a wide range of thicknesses of materials. Thus, the straight-polarity plasma arc can weld copper up to 50 mm thick in a single pass without groove preparation. Plasma welding of aluminium and its alloys at a DCRP provides a high quality of welded structures up to 20 mm thick. Strength characteristics of the weld metal containing no tungsten inclusions and no oxide films are at a level of 95 % of those of the base metal.

The Institute has developed a range of the plasma welding machines. Available are machines operating at currents of 50, 100, 300, 500 and 800 A. The technology and optimal layout of the microplasma equipment have been devised for all types of welding of parts of thin-sheet metals (bellows, casings of instruments, magnetic cores, transformers, components of thermoelectric transducers and many others).

An important property of microplasma welding is a high degree of constriction of the arc and low sensitivity of sizes of the weld being formed (its width and depth) to variations in the arc length.

The use of this welding method instead of argon-arc welding leads to a substantial increase in productivity and quality of welding of thin metals (0.1 – 2.0 mm) and improves vendibility of products.

Modern electronics allows a contactless ignition of the arc, regulation of the current drop at the end of welding and fast and precise setting of the process parameters.

Microplasma welding units (Alfa-T, UPS-0401, UPS-0401M and UMS-0801) manufactured by the Institute passed industrial validation and are in operation at enterprises of the north-western region of the country, the Urals and Siberia.

In the next years developments in the field of plasma welding will be done in the following areas:

• optimization of the technology of welding using a penetrating plasma arc;

• development and mastering of production of new power sources equipped with the microprocessor-based control systems.

Plasma recycling of wastes. This area is one of the most promising, as the environment control becomes an increasingly pressing and global problem that affects all spheres of the human activity.

Specialists of the Joint-Stock Company «Plasma-Trust» (Moscow) and the Russian Institute of Welding have developed, manufactured and tested an installation for recycling of medical, industrial and other wastes. Recycling of these wastes is done in an electric-arc plasma furnace at a temperature of 2000 – 5000 °C without prior separation and disinfection. This provides sterility of the products of recycling and protection of the personnel and equipment from contamination and the environment from harmful components of gases ejected into the atmosphere during operation of the installation. The products of recycling are slag and metal suitable for further use.

Experimental-technological works conducted using the pilot installation proved feasibility of utilizing such facilities at enterprises of chemical, metallurgical, fuel-energy and pharmaceutical industries, as well as at enterprises of the Ministry of Defence for the following purposes:

• neutralization of chemical and biological weapons;

• recycling of galvanic slime and other toxic wastes, including wastes of power generating objects (power and heating plants, nuclear power stations, etc.);

• disposal at customs points of hazardous, infected, substandard products and products banned for import;

• sanitary decontamination of territories after accidents, epidemics, etc.

Current environmental condition of the air basin of many industrialized cities is coming to a catastrophe. The situation with pollution of the atmosphere with toxic products of gas ejected from industrial enterprises, large heat-power and boiler stations grows progressively worse. Benzopyrene is the most carcinogenic of such products.

This gave rise to development of the experimental sample of the ecological plasma arc reactor which can be built-in into any industrial gas line. Decomposition of benzopyrene occurs under the effect of an intensive ultraviolet radiation of the high-current plasma arc of the plasmatron.

The prototype of the ecological plasma arc reactor was tested to advantage at the Research Centre for Engineering Ecology of the Donetsk Branch of the All-Russian Research Institute for Ferrous Metals and Energy Treatment.

This ecological reactor can be used at metallurgical and power generation plants, at chemical factories, heat and power stations and at large city boiler stations.

Production of tubes. Production of welded tubes with super thin walls, which are not inferior in their quality to cold-drawn tubes is more cost effective.

To manufacture the super thin-walled (0.17 – 0.50 mm) welded tubes of a small diameter (4 – 8 mm) from corrosion-resistant steels, the Institute has developed the LDG-43 tube welding line. It provides automatic high-speed welding of the formed tubes and their coiling into bundles, the total length of a tube being 1000 m.

The tube welding line consists of a decoiling device, unit for forming a tubular billet, welding unit (shielding chamber, arc torch with a precision displacement mechanism, power supply and control panel), drawing and coiling devices. Productivity of the LDG-43 line is up to 9 – 12 m/min. The

LDG-43 tube welding lines are now in operation at nine factories of Russian Federation.

Plasma machining. One of the advanced processes that leads to a dramatic rise in labour productivity of the forming process is machining using plasma preheating. In this case the metal to be removed by a cutter is heated by the arc stabilized by vortex and walls of the plasmatron nozzle. Good controllability of the process, high specific power of the arc, long life of the cathode and nozzle of the plasmatron make this process advantageous over other processes of metal working with preheating, e.g. electric-resistance, electric-arc, high-frequency, etc.

This process is especially efficient in rough machining of large parts, e.g. in removal of casting edges, etc. The promising future of this process is proved by the fact that it has already found commercial application at a number of leading enterprises of Russian Federation.

Application of this process for treatment of manganese steels of the type of 110G13L (C – 1.1; Mn – 13.0 wt.%) provides an increase of 8 – 10 times in labour productivity, as compared with those traditionally used, and a decrease by half in consumption of hard-alloy cutting tools.

This method is applied for treatment of liners of cone crushers at the Joint-Stock Company «Uralmash». More than a dozen of units for plasma machining of such parts are in operation at the mining plants and granite quarries. Productivity of the process increases 3 times.

In the next years development of the plasma machining process will be done in the following areas:

• development of the technology for half-finish and finish machining;

• widening of its application in mining and metallurgical industries.

Associates of the Institute continue working in all of the above areas.

FEATURES OF PLASMA ARC CUTTING IN NITROGEN-OXYGEN MIXTURES (REVIEW)

K.V. VASILIEV
VNIIavtogenmash, Moscow, Russia

ABSTRACT

Published data on the influence of nitrogen and oxygen in the plasma on cutting speed have been analyzed. Influence of the composition of the plasma and cutting modes on the composition of the combustion products has been investigated. New concepts of the mechanism of iron burning in steel cutting in the nitrogen-oxygen plasma are substantiated. Development of a combined autogenous-plasma machine is described.

Key words: *plasma arc cutting, carbon steels, nitrogen-oxygen plasma, cathode, cutting speed*

In the second half of XX century the technology for preparatory operations in metal structure fabrication was augmented by introduction of a new advanced process, namely plasma arc cutting [1, 2]. Our Institute carried out the basic research, technology and equipment development [3] that ensured a fast introduction of the technology in processing of aluminium, copper, and alloys based on these and other metals, as well as stainless and other alloyed steels. By the end of 1960s the scope of its application had reached 5 % of the total volume of application of thermal cutting in the country. Considering the relative scope of processing the above metals, this was an acceptable level.

Carbon steels, however, became the most widely accepted in metal structure fabrication, the blanks from them being produced by a simple and inexpensive method of oxygen cutting. Nonetheless, the research forecasts made at that time [4] and the experience of plasma arc cutting of alloyed steels indicated that the new technology can offer a significant advantage of high cutting speeds in the range of small and medium thicknesses, providing a higher cost-effectiveness and minimal thermal deformations, especially in the oxygen plasma at the expense of the possible exoergic reactions. The low wear resistance of tungsten in such a plasma was improved by its gas shielding [5, 6].

By varying the ratio of oxygen and the cathode-shielding inexpensive nitrogen, Browning established the dependence of the cutting speed on oxygen content in the plasma (Figure 1) which demonstrated that even its small additives to nitrogen, increase the cutting speed. Compared to nitrogen plasma, at 25 % oxygen, the cutting speed is increased by 50 % or more. According to his data, further increase of oxygen content (up to 100 %), is accompanied by just a 10 – 15 % increase of speed. This allowed considering air plasma to be a rational working medium for steel cutting, and provided an impetus for searching for a wear-resistant cathode material for working in it. Studies performed by PWI [7], TsNII TS [8], Linde Company, USA [9], etc. promoted creation of zirconium and later on also hafnium (VNIIESO) cathodes.

O'Brien also checked the influence of oxygen concentration and derived a similar dependence. However, the nature of increase (significant with a small oxygen content and negligible at more than 30 % oxygen) of the cutting speed defies theory and practical experience of oxygen (autogenous) cutting. They demonstrate the absence of exoergic reaction, if the cutting medium has more than 75 % nitrogen [10], ability to cut with an oxygen jet, starting from 85 % and quick increase of cutting speed at its higher purity. Air-plasma cutting became widely accepted, but with the rise in the cost of power and equipment, its application began to shrink.

The above contradictions made us more thoroughly study the dependence of the steel cutting speed on the content of oxygen and nitrogen in the plasma. As in the US publications the cutting speed in working media with 30 to 100 % oxygen was demonstrated to rise slowly, we paid special attention to studying the change of speed in this range [11], and have revealed a peculiar nature of this dependence, not described earlier, namely first rising up to concentrations of 65 – 70 %, and then dropping by 10 to 12 %. The maximal speed was by 35 to 40 % higher than with air plasma. Such a nature indicated that in terms of cost it is optimal

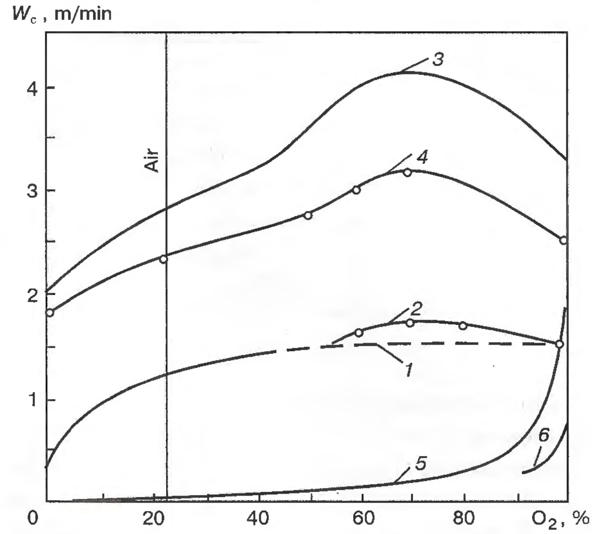

Figure 1. Speed of steel cutting with oxygen depending on nitrogen content by the data of Browning (*1*); Vasiliev, Isachenko (*2*); Severens, Anderson (*3*); calculated-experimental values (in the plasma) (*4*); Wells calculated values (*5*); practical data of Guzov (oxygen jet) (*6*)

to cut steels in the medium with 70 % O_2 and 30 % N, but this was not clear. Our additional verification, and then repeating these experiments at VNIIESO [12], and by foreign researchers [13, 14], confirmed the nature of the dependence earlier established by us.

Chemical analysis of the cutting products under various conditions has also been performed (Table 1). In air-plasma cutting they contained up to 40 % of oxides. With the increase of current, cutting speed and reduction of the cut thickness, their amount decreases. The oxides were recorded in oxygen-depleted mixtures (10 %), while their traces were found even in cutting in nitrogen plasma. With increase (up to 70 %) of oxygen concentration in the plasma, the amount of the oxides in the cutting products increases and then does not grow any more, and F_3O_4 content is even decreased. In-

Table 1

Plasma composition	*Steel thickness, mm*	*Working current, A*	*Cutting speed, m/min*	*Composition of cutting products, %*			
				Fe	*FeO*	*$Fe_3O_4 + Fe_2O_3$*	*Oxides (sum)*
Nitrogen	20	300	1.00	99.9	Traces		0.1
N_2 + 10 % O_2	20	300	1.00	87.0	11.0	1.0	12.0
Air	20	210	3.00	88.0	8.0	4.0	12.0
Same	20	300	2.10	87.0	8.0	5.0	13.0
»	35	220	0.30	59.0	35.0	6.0	41.0
N_2 + 30 % O_2	20	280	2.75	86.0	13.5	0.5	14.0
N_2 + 40 % O_2	20	280	3.00	83.0	15.0	2.0	17.0
N_2 + 50 % O_2	20	300	2.75	83.0	16.0	2.0	18.0
N_2 + 70 % O_2	20	300	3.00	80.0	18.0	2.0	20.0
Oxygen	20	300	3.00	80.0	19.9	0.1	20.0

Table 2

Steel thickness, cm	Cutting speed, cm/s	Current, A	Arc power		Reaction power		Total power, ×4.186, W
			×4.186, W	%	×4.186, W	%	
1.0	1.67	205	6888	82.6	1447	17.4	8335
1.0	5.00	220	7234	78.5	1979	21.5	9213
2.0	1.33	210	6048	78.2	1683	21.8	7731
2.0	1.67	200	5760	75.6	1858	24.4	7618
3.5	0.45	220	8448	81.8	1876	18.2	10324

dividual digressions from this tendency are due to the possibility of further oxidation of the cutting products in the flash on the cut lower edges, in the two-phase flame of the arc and in the slag collectors. Therefore, an attempt was made to evaluate their composition at different concentrations of oxygen by X-ray diffraction analysis. Study of air-plasma cutting slags demonstrated that they consist of α-Fe with the initial steel parameters and of oxides. The increase of oxygen in the plasma increases the share of oxides and oxygen in wustite from 23.21 up to 24.28 %. Flowing out of the cut cavity, the melt is enriched in oxygen and nitrogen, thus forming γ-phase. It then decomposes into Fe_3C and α-Fe, oxidized by the plasma flame and the oxygen from the air. At the temperature below 570 °C FeO decomposes into α-Fe and Fe_3O_4. Thus, α-Fe, oxides and carbides are found in the slag composition. The oxygen, with its high content in the plasma, greatly enriches the melt. A lot of oxides of all the three types precipitate from it, while the γ-phase is almost absent.

The flash differs in its composition from the slag, by the presence of a much larger amount of FeO and Fe_3O_4, as well as the absence of Fe_2O_3 and γ-phase, i.e. oxidation proceeds at $T > 570$ °C. A lot of manganese and carbon are lost in the flash.

The layer of scale on the cut surface can consist of oxides of all the three types and of α-Fe. With the increase of oxygen content in the plasma, the amount of FeO and of the dissolved oxygen is increased in the scale layer, while the fraction of α-Fe decreases. With feeding 100 % nitrogen into the plasma, scale forms in small amounts, obviously, at the expense of air in-take from the atmosphere. Fe_3O_4 prevails in it.

Both analyses indicate that in our case the cut steel, unlike other oxygen processes, reacts with the nitrogen-oxygen plasma of different composition in the cut cavity, thus contributing to the arc energy the appropriate amount of heat of the exoergic reaction of iron oxidation. The causes for its specific nature in the nitrogen-oxygen plasma lie in the features of the cutting process, which consist in the simultaneous melting action of the arc, particularly high temperature and speed of the cutting jet, presence of charged particles connected to the arc, electric field and plasma composition.

Calorimetric investigations showed (Table 2), that the cutting arc is the main factor in metal penetration and cut formation. Washing the melt off, reveals the steel surface prepared for exoergic oxidation by plasma. The experts give different opinions on the influence of the high temperature of oxygen. Some of them believe that oxidation proceeds faster with the increase of temperature. I. Boshnakov [15], contrarily, assesses its influence as negative, noting that at oxygen heating up to 200 – 300 °C, the cutting speed drops by 20 – 40 %, while at the temperatures of 500 – 1200 °C — by 40 – 60 %. In his opinion, the process speed is increased in cutting with the cold or even liquid oxygen. Probably, the high plasma temperatures proper do not increase the cutting speed, as in keeping with the temperature fields of the condition of iron and oxides, the equilibrium of equation $Fe + 0.5O_2 \rightleftarrows FeO$ shifts to the left, and oxygen density is also decreased.

The thickness of the swept-off melt film in cutting, which influences its speed, depends on the plasma speed W_e

$$\Delta_\delta = \sqrt{\frac{2\delta W_c\, \mu C_e}{\alpha_e W_e}},$$

where δ is the thickness; μ is the dynamic viscosity of the melt; W_c is the cutting speed; α_e is the coefficient of heat removal from the cutting arc; C_e is the plasma heat content. The difference in the speeds of the plasma flow and the oxygen jet, however, is not so great and cannot account for the specific dependence of the cutting speed on oxygen concentration in the plasma.

The Vagner oxidation theory [16] is based on electrolytic dissolution of metals. The cutting arc creates an electric field that affects particle migration through a layer of oxides, which can speed up, slow down or even change the polarity and value of external potential during the reaction. However, test cutting at straight and reverse polarity did not reveal any great differences between them, or any significant influence of the external field.

Under the impact of high temperatures and the electric field of the arc, however, clusters of charged particles in the form of ozone can appear in oxygen-containing plasma. Inducing oxygen to form ozone in autogenous cutting [17], allowed its speed to be increased by 15 %. With the ozone concentrations found by the hygienists in the plasma, a certain increase in the cutting speeds is possible, but this does not account for the change in the cutting speed with a typical plasma composition (N_2–O_2), either.

In the author's opinion, in nitrogen-oxygen plasma interaction with steel in its cutting, a special process of iron burning is possible, which is related to the high-temperature gas reactions proceeding in the plasma.

It is known that introduction of external source energy into a reacting system stimulates the reactions which proceed with energy absorption. Among the exoergic reactions in the plasma arc, the chief place is taken by the reaction of oxidation proceeding in the mixture of nitrogen with oxygen, $0.5N_2 + 0.5O_2 \rightleftarrows NO - 21.6 \cdot 4.1868 \cdot 10^3$ J/mol, running at high temperatures with equilibrium constant $K_{eq} = \frac{P^2_{NO}}{P_{N_2}P_{O_2}}$ with the yield of nitrogen oxide NO, which increases with temperature, pressure and nitrogen to oxygen ratio in the initial mixture. V.V. Frolov [18] gives data on the composition of gas atmosphere at temperatures of 2000 – 5000 K in the case of nitrogen oxidation by oxygen in the mixture of 1:1 composition. From his data, nitrogen oxide content is as follows: 5.3 % at $T = 3000$ K; 13.0 % at $T = 4000$ K; 9.4 % at $T = 3500$ K; 20.6 % at $T = 5000$ K. These data practically correspond to the results of thermodynamic calculations of L.S. Polak [19] for the same temperature interval, allowing for dissociation of oxygen and nitrogen into atoms. The greatest amount and highest concentration of nitrogen oxide in the plasma reactor are achieved at oxygen content in the initial mixture of 60 – 70 % [20]. Under the conditions of cutting the nitrogen-oxygen plasma flow with such a content of NO interacts with the iron melt by $2Fe + 2NO = 2FeO + N_2$ reaction.

Equilibrium constant $K_{eq} = \frac{P_{NO}}{P_N a_{FeO}}$ depends on the degree of metal saturation with iron oxide, whose solubility rises with temperature. If the melt saturation with the iron oxide $a_{Feo} = \frac{\% \, FeO}{\% \, FeO_{sat}}$ at a given temperature tends to zero, then the ratio of partial pressures P_{NO}/P_N should also tend to zero, i.e. even very small concentrations of NO already cause iron oxidation. V.V. Frolov states that nitrogen oxide is an active oxidant in relation to metals, even stronger than pure oxygen.

Thus, unlike oxygen cutting (in which oxygen dilution with nitrogen greatly reduces the number of oxygen and iron particle collisions, required for the reaction, while with a significant dilution it almost or completely eliminates them), in plasma arc cutting in nitrogen-oxygen mixtures, collisions of not only the oxygen particles, but (to a greater extent) also of nitrogen particles with iron particles are effective, thus intensifying iron oxidation even with a small content of oxygen in the plasma.

The proposed concept of the mechanism of iron burning in cutting of steel in nitrogen-oxygen plasma, which can be conditionally called a nitro-oxide effect of oxidation, provides an explanation for all the features of cutting in N_2-O_2 plasma, unlike other ones. Indeed, even small additions of oxygen to the plasma result in a replacement of the neutral particles of nitrogen by active particles of NO and start of exoergic oxidation of iron. Increase of oxygen concentration in the plasma enhances this effect. At plasma enrichment with oxygen, the content of actively oxidizing particles increases and the exoergic reaction develops, until NO yield has reached a maximum at oxygen content of 60 – 70 %. As was already mentioned, further on, the amount of NO is not increased because of the lack of nitrogen in the plasma; nitro-oxide effect is replaced by a traditional oxygen mechanism of oxidation. This adversely affects the intensity of steel burning and the cutting speed. In addition, the arc

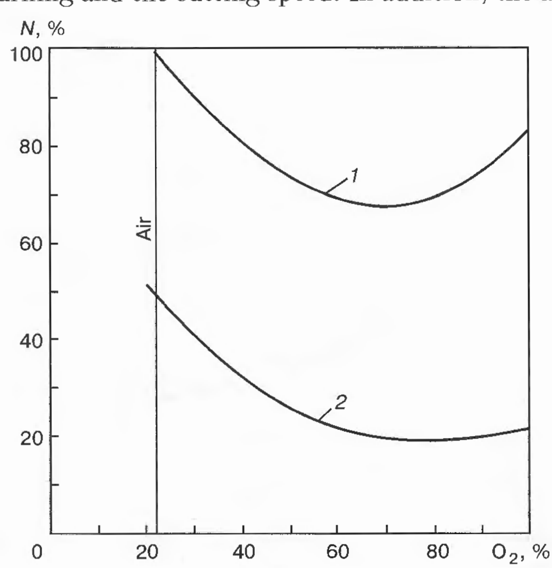

Figure 2. Relative cost of 1 m of cut N and specific power consumption in plasma arc cutting in nitrogen-oxygen mixtures; *1* — total cost; *2* — power cost

voltage in oxygen is reduced from 170 – 160 to 150 V. Both factors limit the cutting speed at oxygen concentration above 70 %.

The results of chemical analyses allow determination of the intensity of steel melting out g_c and of cutting speed W_c. Iron burning in oxygen-containing plasma complements the effective thermal power of the arc Q_{g_i}, by effective thermal power Q_{x_i} of exoergic reaction, which can be conditionally evaluated as the thermal effect of formation of α- and β-FeO and Fe_3O_4 fractions in the forming melt:

$$g_c = \frac{Q_{g_i} + Q_{x_i}}{S_{melt}} = W_c \delta b \gamma,\ Q_{x_i} = g_c(\alpha q_{FeO} + \beta q_{Fe_3O_4}),$$

$$g_c\, S_{melt} - g_c(\alpha q_{FeO} + \beta q_{Fe_3O_4}) = Q_{g_i} = 0.24 I U \eta_i - Q_m,$$

$$g_c = W_c \delta b \gamma = \frac{0.24 I U \eta_i - Q_m}{S_{melt} - (\alpha q_{FeO} + \beta q_{Fe_3O_4})},$$

$$W_c = \frac{0.24 I U \eta_i - Q_m}{\gamma b \delta [S_{melt} - (\alpha q_{FeO} + \beta q_{Fe_3O_4})]}.$$

The calculated curve of cutting speed, depending on oxygen concentration correlates well with the measured actual speeds (Figure 1, curve *4*). It is seen that the optimal speed of cutting is reached at oxygen concentration of 60 – 70 % in the plasma. The highest speeds also provide a saving of power and money, compared to cutting in air and in oxygen (Figure 2). As regards the quality of cutting carbon steels in nitrogen-oxygen plasma, in this case it is important to take into account the proneness of the formed cut surfaces to nitrogen saturation and formation of an anomalous porosity in the welds in subsequent welding. Our investigations [21] showed that this is caused by an abrupt (up to 50 times relative to the initial value) increase in the content of nitrogen in the cast zone of the HAZ metal in air-plasma cutting and coincidence of this cast region in welding with the boundary layer of the weld pool. Measures were determined that limit nitriding of the cut edges and formation of anomalous porosity in the welds after welding such edges, namely selection of the speed parameters, applying rigid stabilization of the arc, producing «reversed» welds and selection of the least gas-saturated cut edges for them opposite to the direction of the stabilizing eddy flow vector. The results of these investigations became used in our country and abroad [22, 23], thus promoting performance of sound welding after air-plasma cutting of the blanks. However, in order to prevent anomalous porosity, cutting with the oxygen-plasma arc is preferable in the most critical cases.

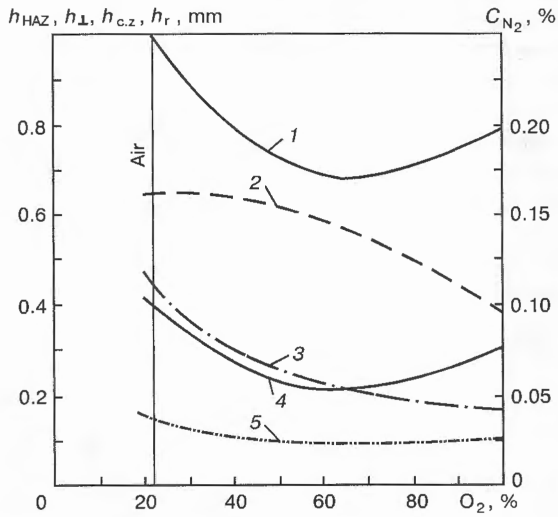

Figure 3. Quality characteristics of the cuts with the change of oxygen content in the mixture: *1* — HAZ depth (h_{HAZ}); *2* — non-perpendicularity of the cut surfaces ($h_\perp$); *3* — nitrogen content on the cut surface (C_{N_2}); *4* — depth of the cast zone of the HAZ ($h_{c.z}$); *5* — roughness (h_r)

On the other hand, investigations by Williamson [24] showed that oxygen cutting with a high content of oxygen (70 – 75 %) yield similar results both in terms of porosity prevention and the least non-perpendicularity and roughness of the cut surfaces (Figure 3). Thus, cutting in the optimal nitrogen-oxygen mixtures with 70 % oxygen is greatly superior to air-plasma cutting in efficiency and quality.

The restraining factors in application of the developed technology can be the need to use two gas sources (air and oxygen), as well as a certain increase of the intensity of the nozzle and cathode consumption. When this problem was solved, compressed air was used as the working gas, which was fed through a unit of diffusion enrichment with oxygen with diffusion membranes selective to it. This solution was verified in the pilot plants [25] and yielded positive results. However, oxymethyltriethylsilane membranes required supplying compressed air to them at the pressure of 1.5 MPa, which was only possible in individual enterprises, as well as a very thorough filtering and drying of air to extend the membrane service life, which was still limited. Their improvement will make this solution promising.

The simplest way is to supply gas to the cutting plasmatron from two sources, namely the compressor or the compressed air line, as well as a cylinder or supply line of oxygen. Our Institute, together with NPO «Kislorodmash» created in 1990 the first local combined autogenous-plasma Kentavr machine with numerical programmed control [26], which, having the oxygen and compressed air mains, enabled both gases to be used. The combined machines are becoming ever wider accepted. Use of plasma with 70 % oxygen, is not a problem in this case. A solution has been found which allows, when supplying oxygen to the plasmatron, replacing the compressor by a simple and inexpensive device for air feeding to create an optimal working medium.

The Institute has found solutions which allow reducing the wear of the nozzles and cathodes, based on increasing the intensity of heat removal from these elements into the cooling medium, eventually creating gas-dynamic cutting nozzles that will not wear in cutting [27, 28].

The developed equipment and technological solutions should become those of choice in the future, and ensure a wide acceptance of plasma arc cutting of carbon steels of small and medium thickness and its effectiveness.

REFERENCES

1. Gage, R.M. *Arc torch and process*. Pat. **2858411** USA. Publ. 1957.
2. *Investigation of gas-arc cutting of light metals and alloys and development of special equipment*. Certificate of the Committee on Inventions and Discoveries of the USSR Soviet of Ministers No.8923 on registering the work of NVIIavtogen. Prior. 28.02.58.
3. Vasiliev, K.V. (1963) *Gas-electric cutting of metals*. Moscow: Mashgiz.
4. Vasiliev, K.V. (1960) Investigation of oxygen-arc cutting of steel. *Transact. of VNIIavtogen*, Issue 6.
5. Vasiliev, K.V., Maslova, E.P. *Device for oxygen plasma arc cutting of steels with a tungsten electrode*. USSR author's certificate **181760**, Int. Cl. B 23 K 7/00. Publ. 21.04.66.
6. Browning, J.A. (1964) The dual-flow plasma torch. *Welding J.*, **4**, 5 – 10.
7. Khrenov, K.K. (1968) Plasma cutting of metals. *Avtomaticheskaya Svarka*, **1**, 39 – 40.
8. Dobrolensky, V.P. (1968) Gas-electric cutting of steel. In: *Abstr. of pap. XIX Session on R&D in Welding*.
9. O'Brien, R.L., Wichham, R., Keane, W. (1964) Advances in plasma arc cutting. *Welding J.*, **12**, 60 – 63.
10. Efimov, B.G., Kuzyayev, P.N. (1994) Some features of metal burning in N_2 + P_2 flow. *Fizika Goreniya i Vzryva*, **6**, 18 – 22.
11. Vasiliev, K.V., Isachenko, A.A. (1967) Plasma arc cutting of steels. *Transact. of VNIIavtogen*, Issue 14.
12. Bykhovsky, D.G. (1972) *Plasma cutting*. Leningrad: Mashinostroyeniye.
13. Sewerance, W.S., Anderson, D.G. (1984) How plasma arc cutting cases affect productivity. *Welding J.*, **2**, 79 – 83.
14. Heize, B. (1984) Plasmaschneiden mit Sauerstoff und Sauerstoff-Stickstoff-Gemischen. *ZIS-Mitteilungen*, **3**, 43 – 50.
15. Boschnakow, I. (1972) Thermishches Trennen mit erhitzten O_2-Strahlen. *Sweiβtechnik*, **12**, 9 – 12.
16. Kofstad, P. (1969) *High-temperature oxidation of metals*. Moscow: Mir.
17. Vasin, V.S. (1991) Cutting with activated oxygen. *Svarochnoye Proizvodstvo*, **5**, 17 – 23.
18. Frolov, V.V. (1954) *Physico-chemical processes in the welding arc*. Moscow: Mashgiz.
19. (1975) *Theoretical and applied plasmachemistry*. Moscow: Nauka.
20. Ganz, S.N. (1969) *Plasma in chemical technology*. Kyiv: Tekhnika.
21. Vasiliev, K.V. (1974) Saturation with gases of the edges in air-plasma cutting and its influence on porosity in welds. *Avtomaticheskaya Svarka*, **9**, 13 – 19.
22. Shirshov, I.G., Kotikov, V.N. (1987) *Plasma cutting*. Leningrad: Mashinostroyeniye.
23. Nakajima, M., Fujimura, H., Nitoh, H. (1978) Some aspects of blowhole formation in welding of air-plasma cut steel plates. *IIW Doc. 1B-396–78E*.
24. Williamson (1988) Plasma cutting with oxygen-nitrogen mixtures. *IIW Doc. 1-872–88/OE*.
25. (1982) Industrial application of a highly effective process of super air-plasma cutting. *Svarochnoye Proizvodstvo*, **6**, 3 – 6.
26. Vasiliev, K.V. (1992) Combined Kentavr machines for thermal cutting of metals. *Ibid.*, **1**, 17 – 19.
27. Vasiliev, K.V. *K.V. Vasiliev's method of arc column stabilization*. USSR author's certificate **1003461**, Int. Cl. 23 K 31/10, 9/00. Publ. 20.03.95.
28. Vasiliev, K.V., Zubkov, V.I. *A method to improve the fatigue life of electrode and nozzle units and a processing plasmatron for its implementation*. Pat. **2135629** RF, Int. Cl. C 23 C 4/00, NO5P 1/28. Publ. 27.08.99.

PLASMA WELDING (REVIEW)

V.S. GVOZDETSKY[1] and **N.A. MAKARENKO**[2]
[1]The E.O. Paton Electric Welding Institute, NASU, Kyiv, Ukraine
[2]Priazov State Technical University, Mariupol, Ukraine

ABSTRACT

Plasma arc process sequences and design features of plasmatrons are considered. Plasma process advantages compared to other arc welding processes are described. Illustrations of technological capabilities of plasma welding and its effective application in rocket engineering, ship-building, power generation and other industries are given. The effectiveness of application of combined plasma processing with two arcs, a plasma arc and laser beam is noted.

Key words: *plasma welding, microplasma welding, plasmatron, welding equipment, weldment, rocket engineering, ship-building, power engineering, automotive industry*

Plasma welding pertains to arc welding processes and is characterized by artificial constriction of the arc column in the nozzle channel by the gas flow or magnetic field. Microplasma welding is defined as «plasma welding at which the current value does not exceed twenty amperes» [1]. Unlike other welding processes, however, in plasma welding by a penetrating arc, the pool and the weld are formed under the additional impact of the plasma-gas flow.

Plasma welding development was reported for the first time in 1950s [2]. Several principles of the plasma-gas flow formation were proposed during 1960s [3, 4]. Over the same period the equipment and technology for microplasma welding of 0.2 – 1.0 mm thick metal were developed and introduced in a number of countries [5].

For fabrication of aluminium structures PWI for the first time in the world developed plasma arc welding at sinusoidal AC [6] and DCRP and AC microplasma welding [7]. Intensive research was performed in a number of industrial research institutes and factory laboratories both in the USSR and in the foreign companies, which led to development of the equipment and technology of plasma welding by a non-transferred arc, at DCSP and DCRP and by a transferred arc (Figure 1), three-phase arc (Figure 2), by twin arcs with non-consumable and consumable electrodes with separate power sources (Figure 3) [8].

Combined processes using two and more heat sources in the welding zone were developed to improve the efficiency of the plasma processes with a high quality of the welds. The sequence with twin arcs was implemented at the start of 1970s in the processes which were named plasma-MIG welding (Philips Company) [9, 10]. In 1960 PWI proposed plasma welding by a bipolar arc with a dual plasmatron or a plasmatron and an arc torch located on both sides of the item being welded (Figure 4) [11].

A number of requirements are taken into account in welding plasmatron design, and, primarily, the need to increase the plasma penetrability

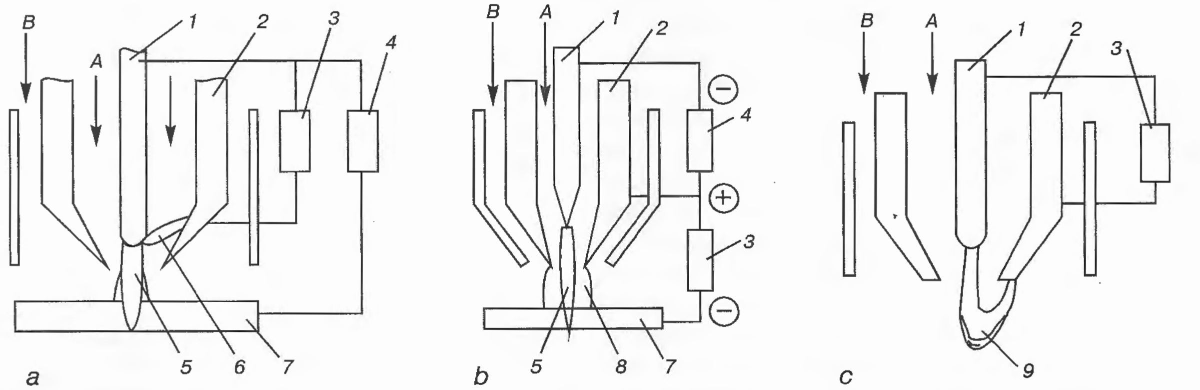

Figure 1. Schematic of plasma welding: transferred arc (*a*), reverse polarity microplasma (*b*), non-transferred arc (*c*): *1* — electrode; *2* — nozzle; *3, 4* — source of the auxiliary and the main arc, respectively; *5* — plasma arc; *6* — auxiliary arc; *7* — item; *8* — reverse polarity arc; *9* — arc column and flame; *A* — plasma gas; *B* — shielding gas

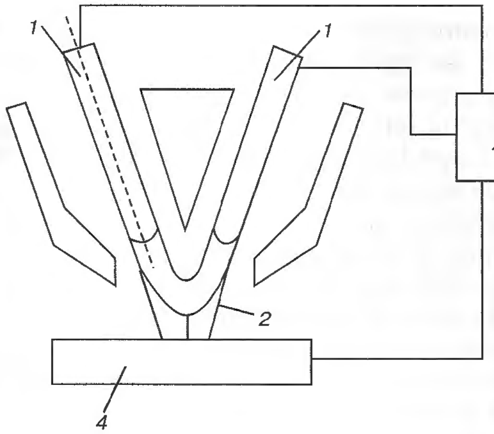

Figure 2. Schematic of plasma welding with a three-phase arc: *1* — electrodes; *2* — transferred and non-transferred arcs; *3* — power source; *4* — item

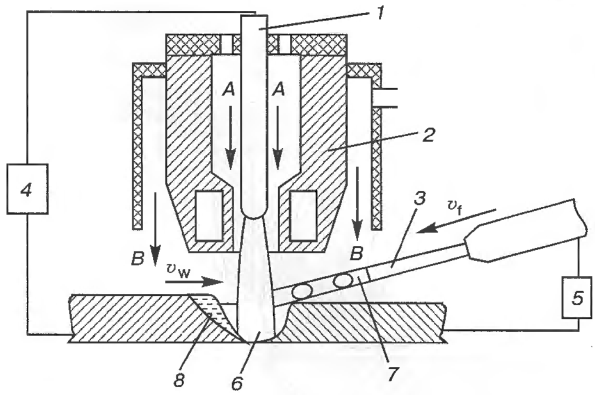

Figure 3. Schematic of plasma arc welding with a lateral feed of the consumable electrode: *1* — plasmatron electrode; *2* — nozzle; *3* — consumable electrode; *4* — plasma arc power source; *5* — consumable electrode power source; *6* — plasma arc; *7* — consumable electrode arc; *8* — item; *A* and *B* — as in Figure 1

and provide a good formation and quality of the weld metal. Therefore, the issues of geometry and design of the electrode and nozzle (shielding and plasma-shaping) components are solved as one package. Arc stabilization and improvement of its penetrability are achieved in several ways: 1) increase of electric power with preservation of the degree of constriction (i.e. with the constant density of current in the plasmatron channel); 2) increase of the degree of constriction by reducing the channel diameter, changing the geometry of the electrode-nozzle unit, etc.; 3) combination of connection to the power sources of the electrodes and the nozzle, interaction of the main, pilot and auxiliary arcs, as well as application of the pulsed power supply modes; 4) combination of the pro-cesses (with nonconsumable and consumable electrodes) under the conditions of blowing with a gas flow, etc.

Block diagrams of the electrode-nozzle unit have been developed. A nozzle with a long straight cylindrical channel with the diameter commensurate with that of the tungsten electrode, became accepted for AC and DCRP welding. Welded joints made with the plasma arc, are characterized by deep penetration and narrow weld, these parameters of the weld being provided at the speeds which are higher than those with other arc welding processes at the same arc power. In this connection, the high thermal effectiveness of the process is an advantage compared to these values for the known arc welding processes. Further constriction at the output of the channel can be achieved using the «focusing» gas flow.

The problem of sound formation of the weld metal should be solved simultaneously with provision of a sufficient penetration depth and high efficiency of the process. However, increase of the density of the plasma-gas jet and of its pressure, causes defects of formation, of which the weld undercuts and ridges are the most typical. The wish to reduce the dynamic head of the plasma-gas flow at a high enough degree of the arc column constriction, gave rise to the idea of drawing the constricting gas into the nozzle channel in the direction away from the item surface (Figure 5) [12]. A plasmatron with a system of feeding the constricting gas in the radial direction through the channel wall of a porous gas-permeable material has been developed with the same purpose (Figure 6) [13].

Use of a separate and independent control of heat content in the base and the liquid deposited metal opens up new technological capabilities, in particular, promotes less overheating of the weld pool and achievement of minimal mixing of the filler metal with the base meal. So, the process of plasma-MIG welding lends itself to separate control of the heat input into the base and the filler metal. For instance, in welding of 16 mm thick samples of a corrosion-resistant steel, the groove was filled in one pass. With minimal mixing of the base metal with the liquid filler metal, it becomes possible to make a weld, with any shape of the cross-section without changing the groove shape [14].

The plasma process was initially implemented using mass-produced power sources, usually ap-

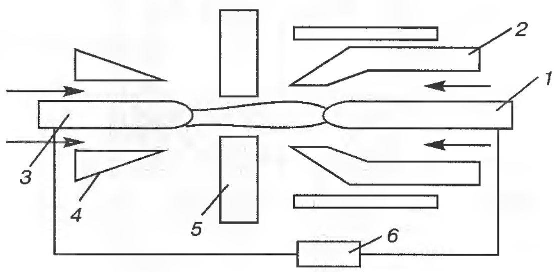

Figure 4. Schematic of plasma welding with a bipolar arc: *1* — plasmatron electrode; *2, 4* — nozzle; *3* — electrode; *5* — item; *6* — power source

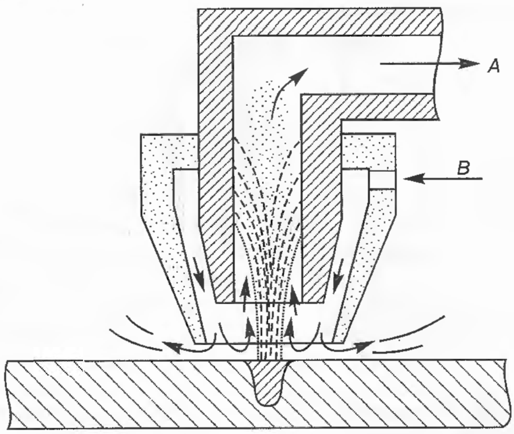

Figure 5. Schematic of plasmatrons with the reverse flow of plasma gas; *A* and *B* — as in Figure 1

plied for the regular arc welding processes with upgraded power and control circuits (windings were added to increase the voltage, auxiliary arc was powered from a special attachment) [15]. Fundamentally new thyristor-controlled power sources of the units were developed for pulsed microplasma welding and a number of other processes [5]. One of the first specialized power sources was the arc power source for AC welding, in which the transformer secondary winding is sectioned and in the branch through which the straight polarity current runs, the rectifier is made controllable [16]. In 1967 PWI developed a method of controlling the penetration of weld root in plasma welding by measuring the electrical conductivity of the ionized arc flame, passing through the weld pool [17]. Furtheron, this process was used for automation of the technology [18, 19].

It should be noted that already the first plasma welding processes became applied in fabrication of critical structures. In 1960–1970s, investigations in the field of plasma technologies both in the USSR and abroad were aimed at solving the problems of aircraft and rocket engineering, electronics, nuclear and cryogenic engineering. Special attention was given to improvement of the quality of welding of aluminium, corrosion-resistant and high-temperature alloys and titanium in a large range of thicknesses of various kinds of joints [20 – 22]. Argon or helium (with hydrogen addition in a number of cases) were used as plasma gases. Plasma welding at alternating current was applied in fabrication of machine clamps (contact tips) for high-voltage transmission lines, consisting of a copper-plated aluminium plate 6 mm thick and an extruded T-shaped aluminium part 12 mm thick [23]. The task of fabrication of cryogenic tubing up to 12000 mm long of 150 to 600 mm diameter and 2.0 to 8.0 mm wall thickness of 12Kh18N10T (C — ≤ 0.12; Cr — 17.0 – 19.0; Ni — 9.0 – 11.0; Si — ≤ 0.80; Mn — 1.0 – 2.0; S — up to 0.02; P — up to 0.035 wt.%) steel in NPO «Kriogenmash» (Russian Federation) was solved using gravity-position plasma welding [24]. Ten years after the introduction of welding by a penetrating alternating current plasma arc into production of rocket fuel tanks in the USSR [6], a similar technology began to be introduced in the US instead of argon-arc welding for outside aluminium tanks in the Space Shuttle [25]. This technology is believed to have a great role also in construction of space stations. In 1989 NASA selected plasma welding technology for manufacture of solid fuel engines of a space rocket for structure delivery to «Freedom» International Space Station. In 1979 PWI experimentally established the ability to perform CO_2-plasma welding with zirconium and hafnium cathodes and air ducts and canisters were welded of low-carbon and low-alloyed steels [26].

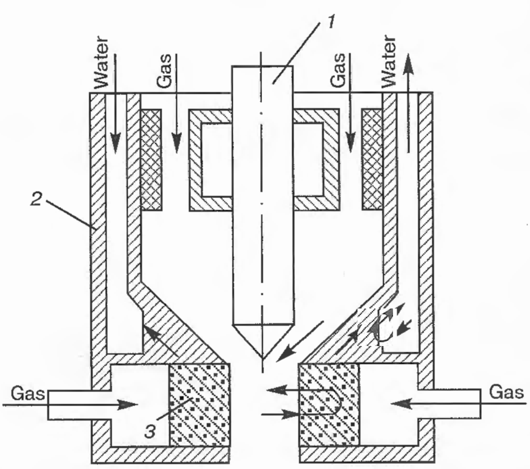

Figure 6. Schematic of plasmatrons with a porous nozzle and radial feed of «constricting» gas: *1* — tungsten electrode; *2* — nozzle; *3* — insert of a porous tungsten-copper alloy

For decades microplasma welding has been an indispensable process in fabrication and repair of items in the electronic, jewelry and watch industry, in manufacturing of instruments, thin-walled tubes, bellows, artificial teeth of many types of steels, gold, titanium, tungsten, vanadium, copper, molybdenum, nickel, tantalum, niobium, zirconium and a number of other metals.

Plasma-MIG welding allowed solving a number of problems in the technology of fabrication of heat-resistant and high-temperature high-alloyed steels. In particular, the high quality of butt joints of EP-202 (C — up to 0.8; Si — up to 0.6; Mn — up to 0.5; Cr — 17.0 – 20.0; Mo — 4.0 – 5.0; W — 4.0 – 5.0; Ti — 2.2 – 2.8; Al — 1.0 – 1.5; P — up to 0.015; S — up to 0.010; B — up to 0.01; Ce — up to 0.01; Fe — up to 4.0 wt.%) alloy 8 – 12 mm thick was achieved in single-pass plasma-MIG welding [27]. Schwelmer Eisenwerk/Müeller&Co. (FRG) has gained extensive experience of effective application of plasma-MIG welding of aluminium tanks. Applying Philips Company equipment allowed complete elimination of pores, undercuts and other defects in the weld metal with simultaneous increase of the welding speed compared to the earlier used consumable-electrode arc welding [28, 29]. Development of consumable-electrode plasma welding in Perm STU is reported [30], however, which provides sound welds with specified dimensions at high welding speeds (> 100 m/h) and thickness of the metal being welded (aluminium and titanium alloys, complex-alloyed steels) in one pass without edge preparation, of up to 15 mm, and with edge preparation of more than 20 mm. PWI developed plasma-powder welding process in which the powder is fed into the plasma and fills the groove. The process was verified in all-position mechanized and manual welding of 1 – 50 mm metal. Variation of the composition of filler powders opens up new possibilities for production of permanent joints of metallic, composite and ceramic materials [31].

A promising welding process is that based on a simultaneous heating of the weld pool by the plasma arc and the laser beam. The first investigations of such a «hybrid» welding process showed that it has a whole range of features which are not attributable to a simple superposition of the properties of the used heat sources, taken separately. So, a special kind of plasma discharge is implemented at the expense of laser radiation absorption in the plasma, namely a combined laser-arc discharge [32].

Plasma surgery has been developing for about three decades now. Equipment testing and surgical operations on animals demonstrated the good prospects for plasma technology application in medicine [33].

Arc welding of a number of complex-shaped items requires regulation of the heat flow power in keeping with the heat removal conditions varying along the weld length. In series and mass production of such items just the automatic control of the welding mode provides a high efficiency with good reproducibility of welding results and stability of the weld geometry. Compared to arc welding processes, plasma arc welding has a maximal number of parameters which can be diagnosed and changed during welding.

In connection with the fact that plasma welding with through penetration offers a unique possibility of monitoring the pool composition by the ionised flame, one of the research areas is study of this process and, finally, visualisation on the display and computer programming of the welding modes. In a brief review of welding technology advances

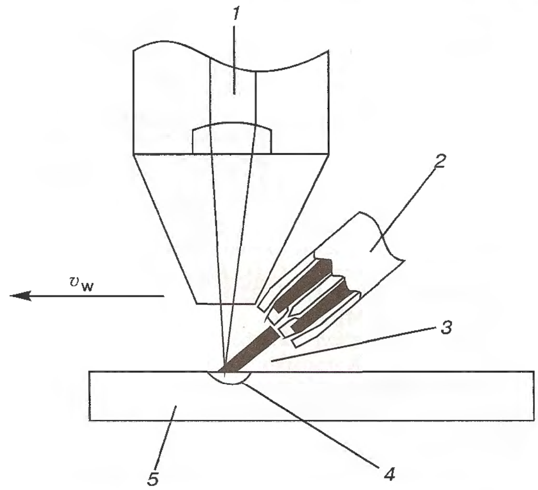

Figure 7. Schematic of a combined laser-plasma process of items processing: *1* — laser beam; *2* — plasmatron; *3* — plasma arc; *4* — weld pool; *5* — item

in 1999, the main area of research on plasma welding is indicated to be the study of the mechanism of through penetration, influence of the mode parameters on the technological properties with the aim of programming and computerization [29]. Arc Kinetic Company (Great Britain) has developed and is manufacturing computer-controlled plasma welding units. In particular, the company has computerized spot plasma welding applied in fabrication of the «Yaguar» car (instead of resistance welding) [34].

Metals science and metallurgy are entering the XXI century with new metallic materials, the majority of which acquires the required service properties in heat treatment. They are welded using processes which allow controlling the heat input without impairing the quality characteristics (absence of defects, minimal deformations, etc.). Electron beam, laser and other technologies are being developed along such principles. However, application of plasma welding, especially of the combined processes, can be simpler in terms of the required equipment, and performance technique. Plasma welding has good prospects for further development also due to the high efficiency and lower energy content.

REFERENCES

1. (1999) Welding and allied processes. Terms and definitions. In: *Derzhstandart of Ukraine 3761.2–98*. Kyiv: Derzhstandart.
2. Ludwig, H.C. (1959) Plasma energy transfer in gas-shielded welding arcs. *Welding J.*, **7**, 296 – 300.
3. Gage, R.M. (1960) The plasma arc torch: a new research tool. *Electric Manufacture*, **1**, 144 – 146.
4. Dudko, D.A., Lakiza, S.P. (1960) On new possibilities of welding by a high-temperature arc constricted by a gas flow. *Avtomaticheskaya Svarka*, **11**, 38 – 46.
5. Paton, B.E., Gvozdetsky, V.S., Dudko, D.A. *et al.* (1979) *Microplasma welding*. Kyiv: Naukova Dumka.

6. Dudko, D.A., Kornienko, A.N. (1968) Welding of aluminium-magnesium alloys by an alternating current plasma arc. In: *Constricted arc cutting, surfacing and welding*. Moscow: Mashinostroyeniye.
7. Gvozdetsky, V.S., Voropay, N.M., Kozlov, L.N. *et al.* (1969) Apparatus for alternating current microplasma welding of light metals and alloys. *Avtomaticheskaya Svarka*, **7**, 75 – 76.
8. Dudko, D.A., Kornienko, A.N., Esibyan E.M. *A method of plasma arc welding*. USSR author's certificate **294422**, Int. Cl. B 23 K 17/00. Approv. on 24.11.69.
9. Boughton, P., Bernard, C.D. *Plasma-MIG arc welding*. Pat. **1340794** UK, Int. Cl. 23 K 9/16. Publ. 12.12.73.
10. (1972) Plasma-MIG. En ny interessant svetsmetod. *Verkstadsinformation*, **12**, 365 – 367.
11. Dudko, D.A., Kornienko, A.N., Vinogradsky, F.M. *Method of plasma welding and cutting of metals*. USSR author's certificate **237568**, Int. Cl. B 23 K 35/02. Approv. on 17.06.67.
12. Cooper, C.H., Pabermo, G., Browning, G.A. (1965) Recent development in plasma welding. *Welding J.*, **4**, 268.
13. Dudko, D.A., Kornienko, A.N., Khurtsidze, G.S. (1981) Technological features of plasma arc welding by plasmatrons with porous nozzles. In: *Abstr. of Sci.-Techn. Conf. devoted to 100th anniversary of electric arc welding invention by N.N. Bernardos*. Ivanovo.
14. Alekseev, A.V., Shevchenko, A.E. (1992) Physico-technological characteristics of twin-arc plasma heat source. *Svarochnoye Proizvodstvo*, **8**, 20 – 22.
15. Paton, B.E., Dudko, D.A., Gvozdetsky, V.S. *et al.* *Power source for plasma welding*. Pat. **50-31105** Japan, Int. Cl. B 23 K 9/00. Publ. 07.10.75.
16. Paton, B.E., Dudko, D.A., Kornienko, A.N. *et al.* *Alternating current arc power source*. USSR author's certificate **1173429/25-27**, Int. Cl. 21, 32/04 B 23 K. Publ. 10.03.69.
17. Dudko, D.A., Vinogradsky, F.M., Kornienko, A.N. *Method of control*. USSR author's certificate **222152**, Int. Cl. B 23 K 9/00.
18. Fujioka, G., Kobayashi, S., Okuyama, H. *Method of control of plasma welding process with through penetration*. Pat. **62-93072** Japan, Int. Cl. B 23 K 9/00. Publ. 28.04.87.
19. Galaktionov, P.M., Ermakov, S.A., Sosnin, N.A. (1988) Constricted arc as a source of information on weld formation in plasma welding with a penetrating arc. In: *Proc. of Sci.-pract Conf. on Achievements of Leningrad Scientific and Production Teams in the Field of Welding in 1987*. Leningrad.
20. Ashauer, R.C. Goodman, J. (1967) Automatic plasma arc welding of square butt pipe joints. *Welding J.*, **5**, 405 – 415.
21. Miller, H.R., Filipski, S.P. (1966) Automatic plasma arc welding and cryogenic fabrication. *Ibid.*, **6**, 493 – 501.
22. Esibyan, E.M., Gvozdetsky, V.S. (1981) Plasma welding and cutting. In: *Welding in the USSR*. Moscow: Nauka.
23. Kornienko, A.N., Makarenko, N.A. (2000) Solving the problem of welding structures from blanks by a constricted arc using an asymmetrical heat removal. In: *Abstr. of pap. of Int. Conf. on Welded Structures*. Kyiv: PWI.
24. Astakhin, V.I., Nekrasov, S.A., Konovalov, V.A. *et al.* (1986) Plasma welding in production of cryogenic systems. In: *Pap. of Int. Conf. on Cryogenic Materials and their Welding*. Kyiv: Naukova Dumka.
25. Craig, E. (1988) The plasma arc process — a review. *Welding J.*, **2**, 19 – 25.
26. Esibyan, E.M., Malkin, V.B., Pestunov, V.G. *et al.* (1979) Dnepr-1 apparatus for plasma welding and cutting of sheet steel. *Avtomaticheskaya Svarka*, **5**, 55 – 56.
27. Shchitsyn, Yu.D., Tytkin, Yu. M. (1985) Investigation of the process of consumable electrode plasma welding of high-temperature alloys. In: *Abstr. of pap. of II All-Union Conf. on Problems of Technology of Welding Heat-stable, Heat-resistant and High-temperature Steels and Alloys*, Nikolaev. Kyiv: PWI.
28. Page, M. (1983) Modified plasma-MIG-torch welds Al tanks faster. *Iron Age Metal-working International*, **5**, 26 – 27.
29. Mattes, K., Kusch, M. (2000) Plasma-MIG-Schweißen. *Der Praktiker*, **5**, 182, 184, 186, 188.
30. Shchitsyn, Yu.D., Tytkin, Yu.M., Shchitsyn, V.Yu. *et al.* (2000) Improvement of the technologies of plasma welding of non-ferrous metals and complex-alloys. In: *Abstr. of pap. of Int. Conf. on Welded Structures*. Kyiv: PWI.
31. Yushchenko, K.A., Savchenko, V.S., Nakonechny, A.A. (2000) Plasma-powder welding of metallic and composite materials. *Ibid*.
32. Gvozdetsky, V.S., Krivtsun, I.V., Chizhenko, M.I. *et al.* (1995) Laser-arc discharge: theory and application. *Welding and Surfacing Rev*. Harwood.
33. Paton, B.E., Gvozdetsky, V.S., Dranovsky, V.I. *et al.* (2000) Plasma surgical system «Plasmamed». *Avtomaticheskaya Svarka*, **1**, 46 – 47.
34. Nefedov, B.V., Lyalyakin, V.P. (1998) Development of plasma welding-surfacing abroad. *Svarochnoye Proizvodstvo*, **3**, 21 – 27.

PLASMA-POWDER SURFACING IN SHIP MACHINE BUILDING

E.F. PEREPLYOTCHIKOV
The E.O. Paton Electric Welding Institute, NASU, Kyiv, Ukraine

ABSTRACT

The results of investigations of some properties and performance of Co-, Ni- and Fe-base alloys are given. Possibility of plasma surfacing of aluminium bronze parts with cobalt and nickel alloys is studied. The effectiveness of application of plasma-powder surfacing in ship machine building is demonstrated.

Key words: *plasma-powder surfacing, cobalt alloys, nickel alloys, aluminium bronze, fusion zone, corrosion, investigations, surfacing equipment, technology*

Surfacing of stop valve parts, valves and seats of internal combustion engines, as well as other items with Co-base alloys is widely used in ship machine building. Manual arc surfacing with TsN-2 electrodes (190Kh30K60V5S2 type) or argon-arc surfacing with V3K rods (110Kh30K60V5S2 type) are used, as a rule. Manual surfacing is a low-efficient and labour-consuming process (because of the high susceptibility of the deposited metal to cracking, surfacing with TsN-2 electrodes and V3K rods has to be performed with parts preheating up to 773 – 823 K) with a greater consumption of expensive and deficit surfacing consumables. The quality of the surfaced parts is highly dependent on the qualification and diligence of the welder. Therefore, a high reject rate and unstable quality of the surfaced parts are inevitable in manual surfacing. In addition, the metal deposited with V3K rods, has insufficient fretting resistance at high specific pressures, while the metal deposited with TsN-2 electrodes, in view of its higher brittleness, is prone to formation of cracks and spalling in service. A number of fitting parts, for instance, rods of the gates and valves, parts of the gate of clinket gate valves, despite their obviously insufficient service life, were not surfaced at all, because of the great technological difficulties involved.

Thus, neither the surfacing consumables, not the surfacing processes, earlier applied in ship machine building, met the increased requirements to the quality of the deposited parts and the technology of their manufacturing. Transition to advanced materials, mechanised and automated surfacing processes was necessary.

Analysis of the domestic and foreign experience [1 – 5] showed that the plasma-powder process is the most effective method of surfacing many parts of ship machinery, allowing an essential (2 to 5 times) improvement and stabilisation of the quality of surfaced parts, compared to manual surfacing, increase in efficiency and drastic improvement of the labour conditions, reduction of the surfacing consumables consumption and cost of machining the surfaced parts. Plasma surfacing lends itself easily to automation, therefore, it is especially effective under the conditions of batch production.

Materials and methods of investigation. The possibility and effectiveness of plasma surfacing application in ship machine building were investigated mainly for parts of the ship stop valves. Evaluation of the performance of alloys surfaced by various methods was carried out, bench and full-scale testing of the surfaced parts has been conducted, surfacing technology and specialised surfacing equipment have been developed. Grades of studied commercial and test alloys and their chemical compositions are given in the Table.

Tribotechnical testing was performed on flat samples in the form of discs of 95 mm diameter and 22 mm thickness with a deposit on the end face, as well as cylindrical samples (rods and bushings) with the diameter and length of the wearing surfaces of 25 and 110 mm, respectively. Powder of 110Kh30K60V5S2 Co-base alloy was used for surfacing the bushings. The base material for all the samples was steel of 08Kh18N10T grade.

Comparative testing of flat samples surfaced with the above alloys, was performed under the following conditions: temperature of atmosphere (air) T = 623 K, specific pressure P_{sp} = 5 MPa, 20 mm reciprocating travel of samples, travel speed v = 0.07 m/s, friction path S_{fr} = 100 m. Used as the main characteristics of wear resistance of the alloys were the loss of weight and the linear wear of the tested samples, as well as the intensity of linear wear, determined by the ratio of linear wear to the product of specific pressure by friction path.

Material grade	*Chemical composition, wt.%*									
	C	*Si*	*B*	*Cr*	*W*	*Fe*	*Ni*	*Co*	*Cu*	*Balance*
110Kh30K60V5S2	1.19	2.56	–	30.1	4.72	2.70	0.20	Base		
160Kh30K60V5S2	1.67	2.49	–	30.8	5.04	0.54	0.85	Same		
190Kh30K60V5S2	1.93	2.36	–	30.2	4.84	3.40	0.37	»		
90Kh30K55V5N7R	0.93	2.72	1.05	30.5	4.46	1.06	7.00	»		
85Kh30K55V5B5GS	0.85	1.47	–	32.1	5.38	0.61	2.21	»		Ni–5.48 Mn–1.16
90Kh30K50V5M5N5R	0.94	1.40	0.40	32.0	5.44	0.34	5.46	»		Mo–4.63
N77Kh15S3R2	0.60	3.53	2.64	18.0	–	–	Base			
N68Kh21S5R	0.60	4.73	2.41	18.7	–	4.82	Same			
Kh18FMN	2.30	0.70	–	19.1	–	Base	2.70			V–8.70
08Kh18N10T	0.08	0.04	–	19.5	–	Same	11.30			Ti–0.55 Mn–1.26
Br.AZhNMts 9-4-4-1	–	–	–	–	–	4.40	4.42		Base	Mn–0.96 Al–8.00

The standard were the samples surfaced with TsN-2 electrodes.

The fretting resistance was studied at different values of specific pressure, temperature and friction path in air. The specific loads for the flat and cylindrical samples were 2.5, 5.0 and 10.0 MPa, and the friction path was 1000 m. The testing temperature for the flat samples was 673 and 743 K, that for the cylindrical samples being 523, 623, 673 and 743 K, respectively.

Cyclic fatigue resistance of the gate components was also determined in addition to alloy testing for fretting resistance. Samples simulating the parts of the gate unit in D_n 50 valves were tested. Testing was performed at a constant load equal to 47 MPa, and temperature of 623 K in air for 6000 cycles. The alloy performance was evaluated by leakage. The minimal specific load on the sealing surfaces providing the maximal admissible leakage at normal temperature, was also determined during testing.

Depending on the purpose of the ship fittings, stainless steels or non-ferrous metals, in particular bronze, are used as the base metal of the surfaced parts. With plasma-powder surfacing of steels with cobalt or nickel alloys, no difficulties are encountered either in surfacing, or in subsequent service. In plasma-powder surfacing of bronze, it was necessary to perform additional investigations of the adhesion strength of the deposited and the base metals, as well as corrosion testing. Cobalt and nickel alloys of 90Kh30K55V5N7R, N77Kh15S3R2, N68Kh21S5R grades, the most widely used in fitting manufacture, were selected as the deposited metal for investigations, and Br.AZhNMts 9-4-4-1 aluminium bronze was selected as the base metal.

The adhesion strength of the deposited and the base metals was evaluated in samples testing for tearing-away strength. Corrosion resistance of the deposited metal for some kinds of corrosion (continuous, contact, crevice) and resistance to cavitation-erosion fracture were also determined. Testing for continuous and contact corrosion, as well as cavitation-erosion wear was performed in synthetic sea water at the temperature of 293 K for 2000 h. Testing for cavitation-erosion wear was conducted in a spindle machine with 12 m/s speed of samples rotation.

Samples for determination of the adhesion strength and corrosion testing were made of 20×40×140 mm blanks, surfaced with the plasma-powder process in the following mode: current of 240 – 280 A, powder feed rate of 3.7 kg/h, surfacing speed of 4.6 m/h, oscillation range of 30 mm, oscillation frequency of 50 min^{-1}. Surfacing was performed in one layer without preheating, with air cooling of the blanks after surfacing.

Investigation results. According to the data of tribotechnical testing of flat samples, in 110Kh30K60V5S2 alloy deposited with the plasma process, the wear resistance is 1.5 times higher than that of the metal deposited manually with TsN-2 electrodes. The maximal wear resistance is demonstrated by alloys of 85Kh30K55V5B5GS and 90Kh30K50V5M5N5R grades, further alloyed with niobium and molybdenum. Wear resistance of 90Kh30K55V5N7R, N77Kh15S3R2, N68Kh21S5R alloys is equal to 0.8 – 0.9, and that of Kh18FNM alloy is 0.5 of the resistance of the standard. Argon-arc surfacing with V3K rods provides a higher wear resistance of the deposited metal than surfacing with TsN-2 electrodes.

The metal deposited with the plasma process with TsN-2 type powder, is characterised by intensity of linear wear, friction coefficient and surface condition close to these values for the metal deposited with the electric arc process. The intensity of linear wear of this alloy (Figure 1), is noticeably decreased during surface mating, then wear is stabilised, which is indicative of the steady nature of the deposited metal fretting.

In testing cylindrical samples, the best results were obtained with a combination of dissimilar materials that form the rod–bushing friction pair. The least wear was found in the rods surfaced with the plasma process with powders which provided metals of the type of 90Kh30K55V5N7R (PN-AN34) and Kh18FMN (PN-AN2).

All the studied alloys after 6000 cycles provided the leak-proofness of the gate, specified by GOST 1926–80. Note, however, that the minimal values of specific pressure, required to achieve the leak-proofness, were derived on samples with the deposited 90Kh30K55V5N7R and 160Kh30K60V5S2 metal and the maximal values were derived on samples surfaced with PR-N68Kh12S5R powder.

Comprehensive studies and testing conducted at PWI in co-operation with the organisations in the ship machine building industry, allowed optimisation of the composition of the deposited metal of the traditional cobalt–chromium–tungsten–carbon alloying system. It is found that the metal deposited by the plasma process, with 1.3 to 1.7 % concentration of carbon, is characterised by a much higher cracking resistance, than the metal deposited with TsN-2 electrodes. As shown by bench testing for fretting resistance, even better wear resistance values can be achieved.

For plasma surfacing of the sealing surfaces of ship fittings, valves of combustion engines, including large ship diesels and other parts, exposed to elevated temperatures under the conditions of intensive wear, an alloy of the following composition, wt.%: C — 1.3 – 1.7; Si — 1.7 – 2.5; Cr — 28.0 – 32.0; W — 4.0 – 5.0; Co being the balance, and an appropriate PN-AN35 filler powder have been developed. The hardness of the deposited metal is HRC_e 42 – 48. Its structure consists of solid solution with the microhardness of HV 270 – 300 and an eutectic with HV 650 – 700.

As to corrosion resistance in sea water, 90Kh30K55V5N7R, N77Kh15S3R2, N68Kh21S5R alloys deposited on Br.AZhNMts 9-4-4-1 bronze, belong to the group of highly resistant (GOST 13819–68). Testing for contact corrosion showed

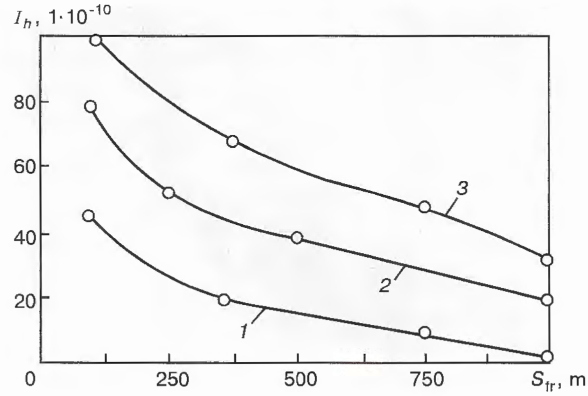

Figure 1. Intensity of linear wear I_h of samples deposited with 190Kh30K60V5S2 alloy, depending on the friction path S_{fr} at the temperature of 623 K and different specific loads: *1* — 2.5; *2* — 5.0; *3* — 10.0 MPa

that in all the cases the potential of the deposited metal shifts to the negative side from the stationary value. In this case, the corrosion rate of all the alloys decreases compared to corrosion without contact. The studied alloys in slot gaps are characterised by minor attack. Cavitation-erosion fracture is absent in all these alloys.

As shown by investigations of the properties of the zone of fusion of the cobalt and nickel alloys with Br.AZhNMts 9-4-4-1 bronze, the metal in the fusion zone is characterised by satisfactory strength. From Figure 2 it follows that in plasma surfacing of aluminium bronze with stellite, a minimal mixing of the base and the deposited metals is achieved. No pronounced solidification or diffusion interlayer was found on the interface.

The performed investigations allowed plasma-powder surfacing with alloys of 90Kh30K55V5N7R, N77Kh15S3R2 and N68Kh21S5R grades to be recommended for strengthening the sealing surfaces of parts of gate valves of Br.AZhNMts 9-4-4-1 aluminium bronze.

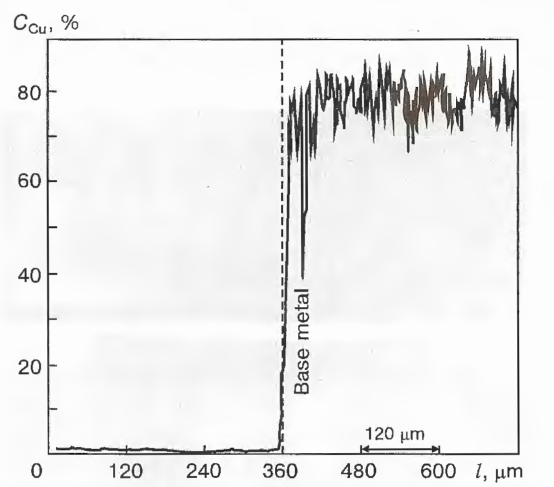

Figure 2. Copper distribution in the fusion zone of 90Kh30K55V5N7R alloy with Br.AZhNMts 9-4-4-1 bronze; l is the length of the studied section

Figure 3. Specialised UD-308 unit for plasma-powder surfacing

Equipment. All-purpose OB-2184 units for plasma-powder surfacing [6] and specialised UD-308 units have been introduced in several shipbuilding and ship-repair enterprises (Figure 3). The latter unit is designed for surfacing the end surfaces of discs and rings of up to 200 mm diameter and up to 150 mm height. The unit delivery set includes a cooling block, control cabinet and VDU-506 power source.

Specification of UD-308 unit

Surfacing current, duty cycle 100 %, A	not more than 300
Filler powder feed rate, kg/h	0.35 – 15
Capacity of feeder hopper, dm^3	3
Range of plasmatron oscillations, mm	25
Frequency of plasmatron oscillations, min^{-1}	40 – 110
Frequency of oscillations of the rotator faceplate, rpms:	
working	0.08 – 0.80
travel	0.8 – 2.0
Argon flow rate (total), l/min	16 – 20
Overall dimensions, mm	880×1400×1980
Plasmatron cooling	water, independent
Weight (set), kg	1180

Surfacing in UD-308 type unit is performed in a special chamber which reliably protects the operator from the light and thermal radiation of the arc, as well as dust and gas evolutions. The unit is fitted with a novel control system, which allows surfacing to be performed in the automatic mode.

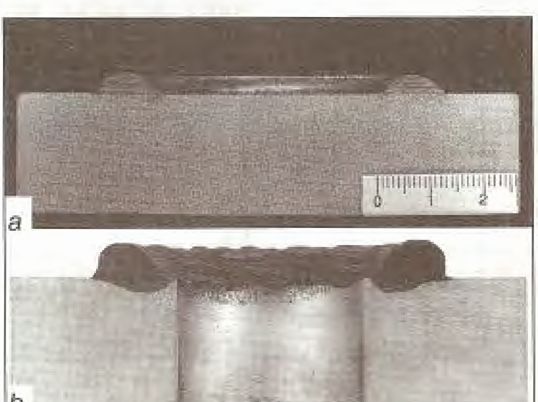

Figure 4. Macrosections of the parts deposited by the plasma-powder (*a*) and manual (*b*) process

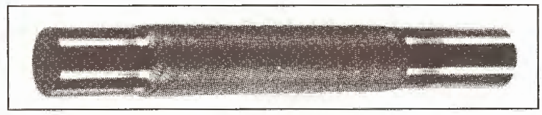

Figure 5. Surfaced billet of a rod of 25 mm diameter of an actuator valve with D_n 50

Technology. In surfacing with cobalt alloys the greatest difficulties are encountered in crack prevention and provision of a low content of iron in the deposited metal (not more than 5 %). A radical measure for prevention of cracks is the preheating and concurrent heating of the blanks being surfaced. In arc surfacing with preheating, however, the base metal penetration is abruptly increased, which makes it necessary to deposit 3 to 4 layers to obtain the specified composition, thus increasing the labour, material and power consumption in surfacing.

As was noted above, compared to those earlier applied, the developed Co-base alloys are less susceptible to cracking. In addition, plasma-powder surfacing provides a «soft» thermal cycle, good formation of the beads and high quality of the deposited metal, thus also promoting crack prevention.

In this connection, in plasma-powder surfacing with cobalt alloys, the temperature of the parts preheating can be significantly lowered, while the fitting parts with D_n below 100 can be surfaced without preheating.

An important advantage of plasma-powder surfacing is the ability to provide a small penetration of the base metal, irrespective of its preheating temperature [7]. For this purpose, an optimal ratio between the powder feed rate and effective thermal

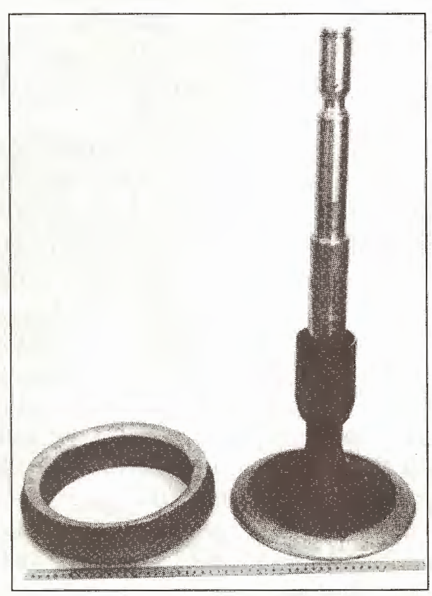

Figure 6. Seat and discharge valve of 258 mm diameter of the main engine of «Geroi Shipki» type ferry, surfaced with stellite (repair surfacing)

power of the arc determined by current, should be maintained during surfacing.

A feature of the design of ship fittings, valves and other parts, is a narrow sealing surface, the production of which requires deposition of narrow (not more than 6 – 8 mm) beads. Surfacing of such billets must be performed with plasmatron oscillations at the frequency of 80 to 100 min^{-1} and their minimal range. This does not require any forming devices. The mode parameters are selected depending on the typesize of the billet being surfaced. The arc current and powder feed should be selected so as to provide a good formation of the deposited beads and their reliable fusion with the billet surface with minimal dilution of the deposited metal with the base metal. The deposition rate is set to be such that with the selected powder feed rate, the deposited bead had the required height and width.

Due to small penetration of the base metal in plasma-powder surfacing, the required composition of the deposited metal is provided already in the first layer, therefore, plasma surfacing is, as a rule, performed in one layer. As the powder particles have the same composition and the plasma surfacing process proper is very stable, the metal deposited by this process is characterised by a high homogeneity, not achievable with manual surfacing. Depending on the sizes and shape of the deposited parts, the efficiency of plasma-powder surfacing is 2 – 6 kg/h. Despite the difference in the thermophysical and mechanical properties of the base and filler materials, in plasma surfacing a well-formed deposited layer is produced with a small share of the base metal (Figure 4). The deposited beads feature a high stability and reproducibility of their dimensions, which results in a smaller labour consumption for machining the surfaced parts. Small allowances for machining are also one of the ways to save the surfacing consumables.

Plasma surfacing of the parts of ship fittings with N77Kh15S3R2 and N68Kh21S5R nickel alloys can be performed by the same technology as surfacing with the cobalt alloys.

Surfacing of rods with PN-AN2 powder is performed along a helix without preheating. Rod billets of 25 to 30 mm diameter are surfaced with the rate of up to 3 kg/h, larger ones – with the rate of up to 6 kg/h. The appearance of some of the surfaced parts is shown in Figures 5, 6.

Recommendations on selection of the main parameters of the plasma-powder surfacing process and surfacing modes of the characteristic items, are contained in the technological instructions made available to the enterprises.

REFERENCES

1. Frumin, I., Gladkij, P., Jeremeev, W. *et al.* (1974) Auftragsschweißen hitzebeständigen Legierungen auf Dichtflächen der Hochparameterdampfarmaturen. *DVS-Berichte*, **32**, 331 – 339.
2. Frumin, I.I., Gladkij, P.V., Jeremeev, W.B. *et al.* (1980) Materials and methods for hard-facing of power engineering valves. In: *Colloque international sur les Materiaux durs pour Frottement dans les Reactures Nucleaires*. Avignon.
3. Zuchowski, R.S., Carrabrant, E. (1964) New developments in plasma arc surfacing. *Welding J.*, **1**, 13 – 26.
4. Kučera, L., Gladkij, P., Pereplotchikov, E. (1990) Skysegrosti z navarania plazmou na syčasti energetickeho zariadenia. In: *Renogacne metody. Welding'90*. Bratislava: Dom Techniky.
5. Frumin, I.I., Gladky, P.V., Pereplyotchikov, E.F. *et al.* (1981) Experience of application of plasma surfacing with stellite for repair of large gate valves. *Avtomaticheskaya Svarka*, **7**, 54 – 56.
6. Pereplyotchikov, E.F. (2000) Plasma surfacing. *Svarshchik*, **2**, 8 – 11.
7. Frumin, I.I., Pereplyotchikov, E.F., Gladky, P.V. *et al.* (1974) Plasma surfacing of stellite. *Avtomaticheskaya Svarka*, **2**, 54 – 56.

LASER + PLASMA: SEARCH FOR NEW POSSIBILITIES IN SURFACING

A.I. SOM[1] and **I.V. KRIVTSUN**[2]
[1]Plasma-Master Co., Ltd., Kyiv, Ukraine
[2]The E.O. Paton Electric Welding Institute, NASU, Kyiv, Ukraine

ABSTRACT

Method of combination of a laser beam and plasma arc for realization of a combined process of a laser-plasma cladding is suggested. A prototype of a laser-arc plasmatron for a powder cladding was designed and manufactured. A detailed computer modelling of a combined discharge in the given plasmatron and experimental studies of its characteristics and technological capabilities of the mentioned process were made. It is shown that the combined use of a laser beam and plasma arc increases the speed, stability and reproducibility of results of cladding, and also efficiency of using these sources of heating.

Key words: *plasma arc, laser beam, combined discharge, laser-arc plasmatron, plasma-laser cladding, filler powder, investigations*

More and more publications appear in a scientific and technical literature about application of combined processes of welding based on a combined use of a laser radiation and electrical arc, including plasma arc [1 – 7]. Such combination leads to the improvement of a space stabilization of an arc spot at the surface of metal being welded and to the increase in stability of its burning at low currents and high rates of displacement relative to the workpiece. Simultaneously, the coefficient of absorption of a laser radiation by the metal surface is increased that is especially important when the low-power lasers are used. All this provides, from the one hand, the significant increase in productivity and stability of arc (plasma) welding, and from the other hand, the increase in effectiveness and decrease in the cost of the laser welding.

Our work was aimed at the conductance of theoretical and experimental investigations of effect of a laser beam on the process of a plasma-powder cladding (PPC) and revealing of new technological capabilities of a combined method, i.e. laser-plasma powder cladding (LPPC). The most rational scheme of realization of this combined process is, in our opinion, a coaxial combination of a laser beam and plasma arc during a distributed feeding of a filler powder into a discharge plasma. As in this case the laser beam should pass a definite distance in the arc plasma, then, during development of the above-described method it is necessary to take into account not only the plasma and laser effect on the filler material and the surface treated, but also the direct interaction of the focused laser beam with a compressed arc plasma.

It is known that such interaction can lead to the occurrence of a special type of a gas discharge, i.e. a combined laser-arc discharge [5]. The necessary condition of its occurrence is the commensurability of energy, put into an arc plasma by a laser radiation, with an energy, generated in the plasma at the expense of the electric current passing. When this condition is fulfilled, a significant change in energy balance of the arc discharge takes place, thus resulting in the fact that both integral and local characteristics of the plasma of the combined discharge are differed greatly from the corresponding characteristics of the initial arc plasma. As to the characteristics of the laser beam, then they undergo the significant changes due to absorption of beam and its additional focusing in the plasma of the laser-beam discharge.

Unfortunately, it is almost impossible to use the traditional arc plasmatrons for the creation of a combined discharge and its use for LPPC according to the above-described scheme. The coaxial combination of the laser beam with a plasma arc requires the creation of special devices, i.e. laser-arc plasmatrons [8 – 10]. These devices are distinguished mainly by a design of the cathode unit (refractory tubular cathode or a system of pin cathodes located around the circumference). This peculiar feature makes it possible to introduce a focused laser beam to an arc plasma along the axis of the plasma-shaping channel.

For a practical realization of the LPPC process and revealing the technological capabilities of a combined use of the plasma arc and laser radiation, a prototype of a specialized laser-arc plasmatron LPP-22 was designed and manufactured (Figure 1). During its design a large experience of

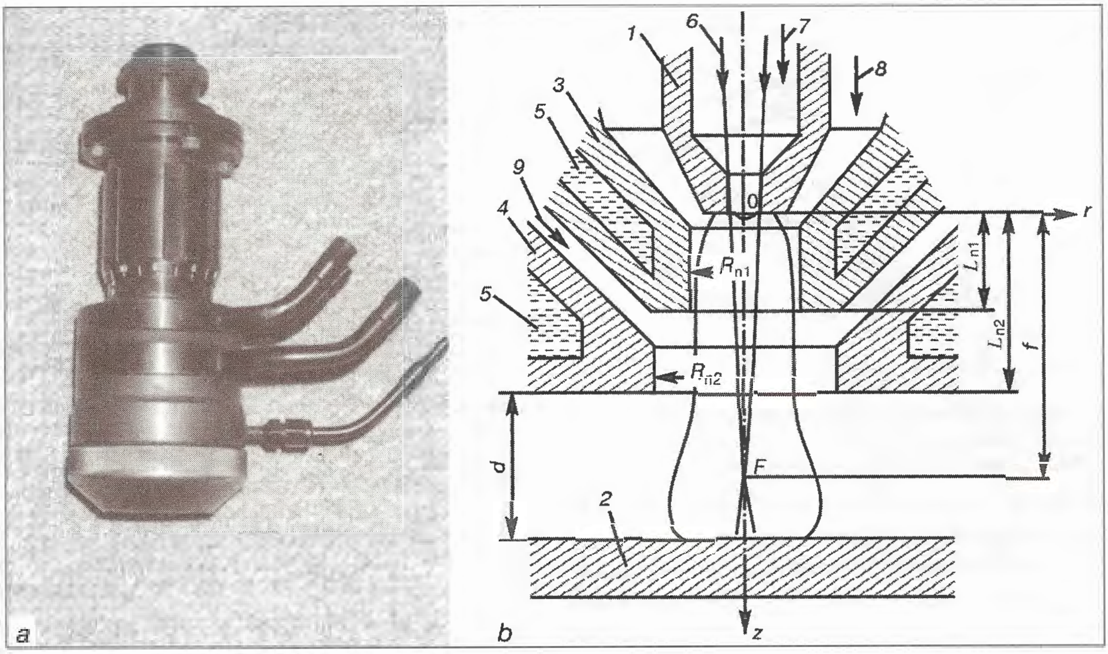

Figure 1. Appearance (*a*) and scheme of a nozzle part (*b*) of the laser-arc plasmatron LPP-22 (see designations in text)

Plasma-Master Co., Ltd. on the creation of plasmatrons for PPC [11], and also results of theoretical studies of a combined laser-arc discharge and devices for its realization, made at the E.O. Paton Electric Welding Institute, were used [5, 9].

In this plasmatron (Figure 1, *b*) the DC arc is burning in an axial flow of the plasma gas (argon) between the refractory (tungsten) tubular cathode *1* and the workpiece being subjected to cladding (anode) *2*. At initial region a discharge is stabilized by a wall of the plasma-shaping nozzle *3*, which is coaxial with a cathode. The nozzle *4* serves for a distributed feeding of the filler powder to the discharge. Both nozzles are made from copper and cooled by water *5*. The beam *6* of a continuous CO_2-laser radiation, focused by an optical system and spreading along the plasmatron axis, is introduced to the discharge through the cathode orifice. The plasma gas *7, 8* is supplied to a plasma-shaping channel both through the cathode orifice and to a gap between the cathode and a wall of the nozzle *3*. The gas consumption here may vary independently of one another. The filler powder is fed by a flow of the transporting gas *9* (argon) to the gap between nozzles *3* and *4*. The cladding zone is protected by an argon flow. To protect the laser focusing system in plasmatron LPP-22 an additional gas gate is provided, and also appropriate correctors of the cathode positioning relative to the beam axis are provided to provide the coaxiality of a laser beam and a plasma arc.

The plasmatron was designed for operation at the arc current of $100 \text{ A} \le I \le 300 \text{ A}$ using a laser beam having a mode $TEM_{2.0}$, power $Q_0 \le 5$ kW and angle of beam focusing $\theta = 0.053$. To define the optimum conditions of the LPP-22 plasmatron operation. characteristics of the generating plasma and an interacting laser beam, a detailed computer modelling of a combined discharge generated by the mentioned plasmatron without taking into account the feeding of the filler powder was made. Here, the following sizes of the nozzle *3* were used (Figure 1, *b*): 4.5 mm length of a cylindrical channel ($L_{n1} = 5.5$ mm), radius $R_{n1} = 5.0$ mm. Respectively, for nozzle *4*, the length of the outlet channel is 2.5 mm ($L_{n2} = 10.0$.mm), radius $R_{n2} = 5.0$ mm. Consumption of the plasma gas, supplied through the cathode orifice is $G_1 = 0.5$ l/min, while between the cathode and the channel wall it is $G_2 = 2.5$ l/min. Consumption of transporting gas was 5.0 l/min, and its initial temperature was taken equal to the temperature of water-cooled walls of the channels (300 K). Distance *f* from the cathode edge till the focus of the initial beam was varied within the range of 14 – 22 mm, and the length *d* of the open region of the discharge was 4 – 12 mm.

Calculations of characteristics of plasma and a laser beam, interacting with it, were carried out on the basis of a model of the combined discharge in a laser-arc plasmatron, described in detail in [9]. Results of numerical modelling of the discharge for different conditions of the plasmatron operation are presented partially in Figures 2 – 4. Thus, Figure 2 presents space distributions of plasma temperature *T*, while Figure 3 shows a distribution of gas-dynamic pressure of its flow $\rho u^2/2$ (ρ – density, kg/m^3; u – rate, m/s). According to curves given in Figure 2, the absorption of the laser ra-

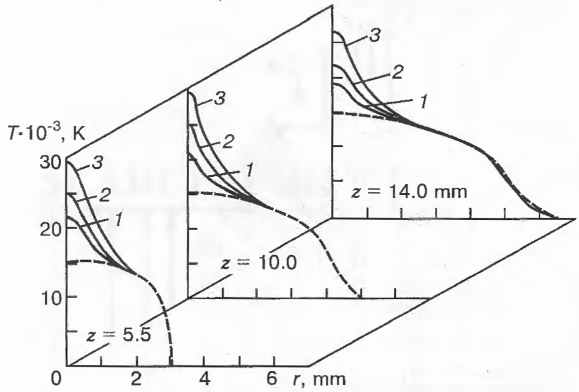

Figure 2. Space distribution of temperature of discharge plasma in laser-beam plasmatron (I = 200 A, d = 12 mm, f = 14 mm) at laser beam power 1 (*1*), 2 (*2*), 3 (*3*), 0 kW (dashed curve)

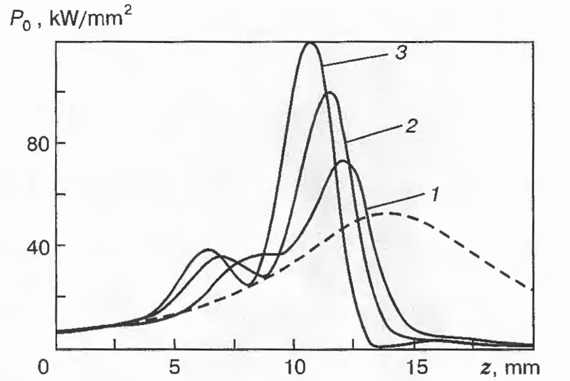

Figure 4. Distribution of intensity of laser radiation along the axis of a combined discharge (Q_0 = 3 kW, d = 12 mm, f = = 14 mm) at arc current 100 (*1*), 200 (*2*), 300 A (*3*), dashed curve — without plasma arc

diation by an arc plasma leads to a significant increase in temperature of its central regions. Moreover, the maximum achieved values T are increased with a growth in beam power Q_0. The mentioned growth in the plasma temperature promotes the increase in its electroconductivity and, consequently, to the increase in current density in a near-axial zone of the discharge. Thus, the discharge, generated by a laser-arc plasmatron, is characterized by an increased concentration of heat and electrical energy in that region of the plasma, which is subjected to the action of the laser beam and rigidly connected with its axis and also by a high space stability of this zone.

The described change in heat condition of the plasma arc burning under the action of the laser radiation causes a significant redistribution of gas-dynamic characteristics of the plasma flow with increase in Q_0. One of the main causes is the decrease in a viscosity of the argon plasma with the temperature increase. Another cause is the above-mentioned redistribution of current density in the discharge, thus increasing the role of electromagnetic forces in accelerating of the plasma flow [5].

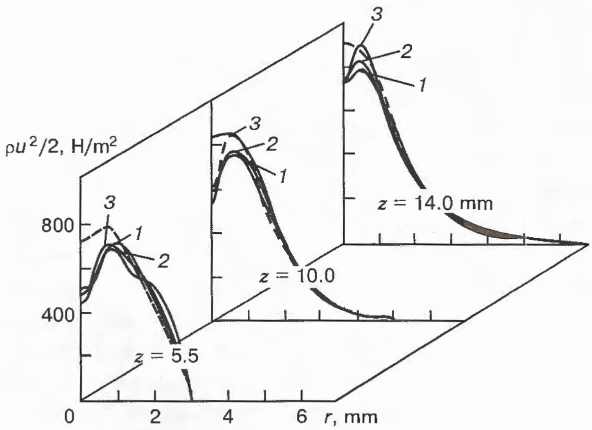

Figure 3. Space distribution of gas-dynamic pressure of plasma flow generated by laser-arc plasmatron (conditions and designations are the same as in Figure 2)

As a result, the axial component of the plasma rate at the discharge axis is increased noticeably. In spite of increase in rate, the decrease in plasma density at the temperature increase leads to the fact that the gas-dynamic pressure of the plasma flow $\rho u^2/2$ in a near-axial zone of the combined discharge is somewhat decreased (Figure 3). It should be noted that this decrease, which causes the dynamic action on the surface of the molten metal, is important for the cladding process using a laser-arc plasmatron [12].

The interaction of a laser radiation with an arc plasma, proceeding in the above-described plasmatron leads to the redistribution of not only its characteristics but also the laser beam itself (due to absorption and refraction in the discharge plasma). Thus, for example, the absorption of the laser radiation leads to the fact that at the distance of 20 mm from the cathode edge the beam power for the mentioned conditions is only about 30 % of its initial power Q_0, whereas the intensity of radiation, P_0, at its axis increases by more than twice (Figure 4). Thus, the interaction of the laser beam with plasma of a combined discharge causes its additional focusing, which is increased with a growth of I and Q_0. Consequently, by varying these two parameters, it is possible to control effectively the beam focusing in plasma of the combined discharge created with the help of a laser-arc plasmatron that is important when similar devices for welding and cutting are used.

Experimental investigations of the plasmatron LPP-22 were performed in Fraunhofer Institute of Technology (Germany) using CO_2-laser RS-5000 and plasma arc power source Messer Griesheim Uniting GW 30. The plasmatron was fastened to a focusing system by a special adapter which makes it possible to coincide the axis of the laser beam with the plasmatron axis. The movement of the workpiece to be treated with respect to the plas-

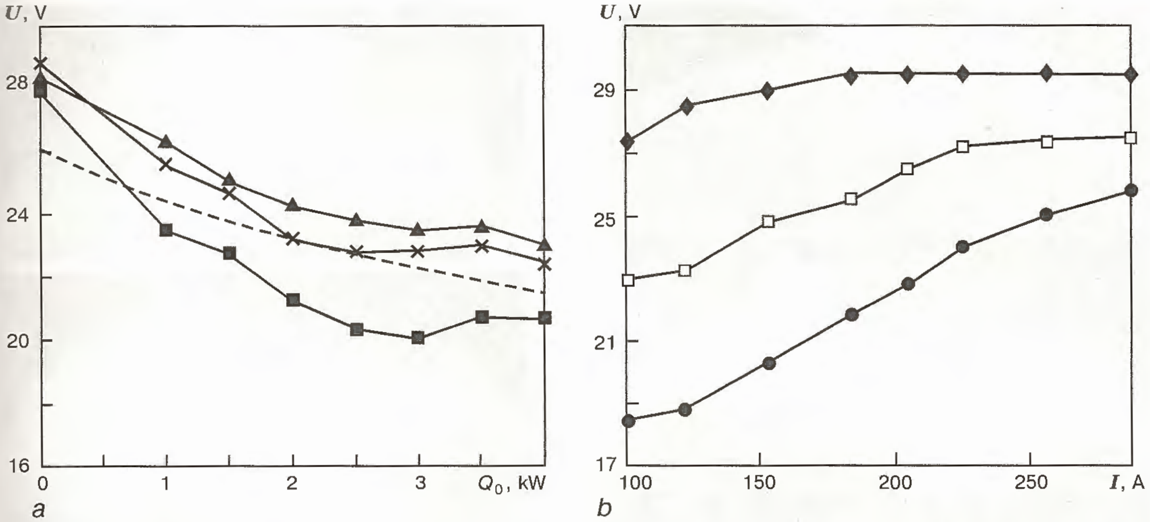

Figure 5. Dependence of discharge voltage in laser-arc plasmatron (d = 8 mm, f = 16 mm) on initial beam power Q_0 (a) and plasma arc current I (b): ■ — I_a = 150, × — 200, ▲ — 250 A; ◆ — Q_0 = 0, □ — 1, ● — 3 kW; dashed line — calculated data at I = 200 A

matron was realized by a programming welding manipulator.

Experiments were performed in two stages. First, the peculiarities of burning the combined discharge without feeding the filler powder were studied, then the laser-plasma cladding of steel samples at different conditions was performed. During all the experiments the arc current was varied in the range of 100 – 280 A, the laser beam power — 0 – 4 kW. The distance f was changed within 14 – 22 mm, and d (from the plasmatron edge to the anode-workpiece surface) was set equal to 4, 8 and 12 mm. Consumptions of transporting and plasma gas were constant and corresponded to the above-mentioned values.

The experiments showed that the plasmatron LPP-22 operated with a high space-time stability of parameters of the generating plasma within the entire examining range of arc current and laser beam power. Volt-ampere characteristics of dis-

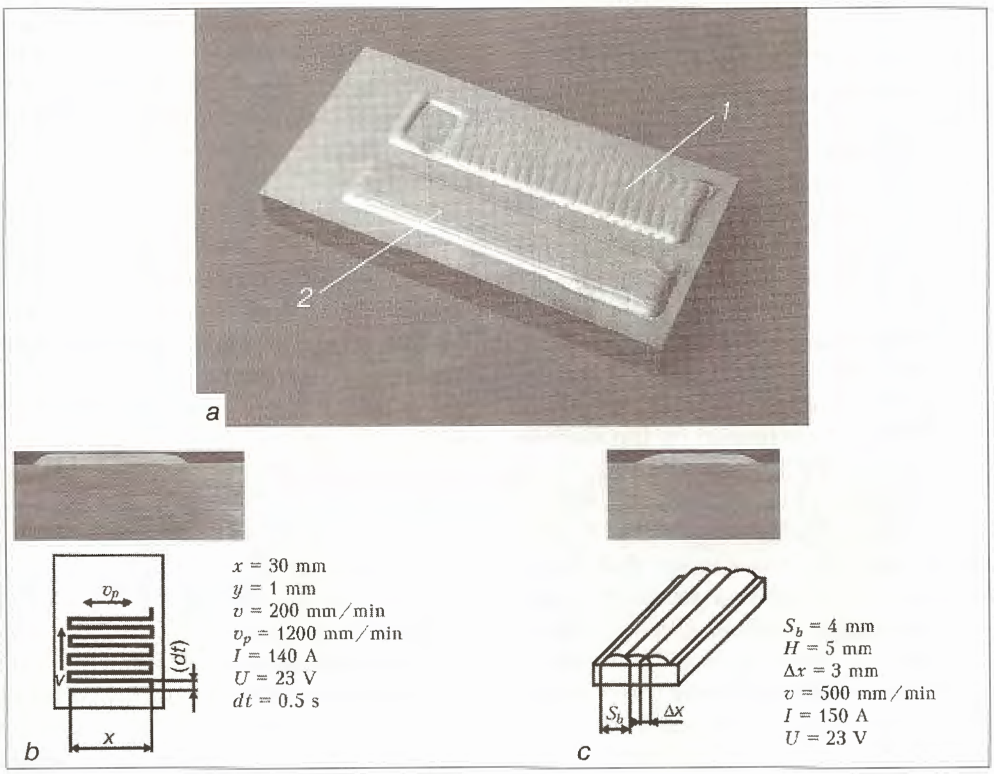

Figure 6. Appearance (a) of wide-layer laser-plasma deposits *1*, *2* and scheme of their cladding (b — *1*, c — *2*) with appropriate conditions and macrosections of transverse section of clad layers

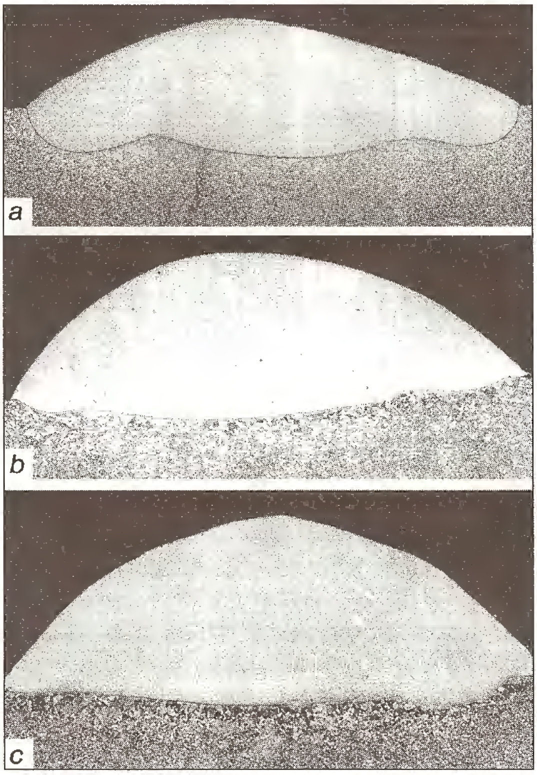

Figure 7. Macrosections of single beads at different speeds of cladding: *a* — 12 (γ = 40 %); *b* — 18 (γ = 15 %); *c* — 30 m/h (γ = 10 %) at I = 200 A, Q_0 = 3 kW, d = 8 mm, f = 16 mm

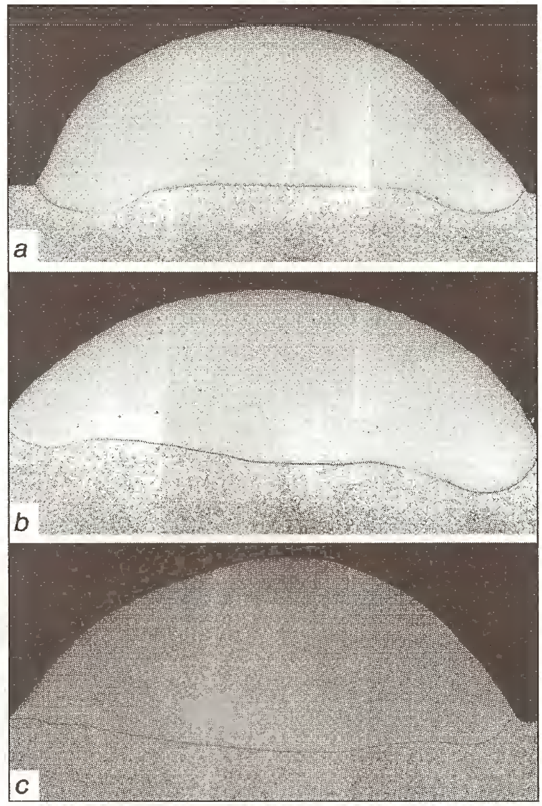

Figure 8. Macrosections of single beads after cladding at different powers of laser beam: *a* — 0 (γ = 5 %); *b* — 1 (γ = 10 %); *c* — 4 kW (γ = 10 %) at I = 200 A, d = 8 mm, f = 16 mm, v = 18 m/h

charge using a copper water-cooled anode at different values Q_0 and I were measured (Figure 5). The experimental data confirm the theoretical results [5]: under the action of the laser beam the arc voltage is decreased, and, as follows from Figure 5, *a* (solid curves), its main drop occurs at the laser power $Q_0 < 2.5$ kW. In the same Figure the calculated dependence (dashed curve) of a full voltage of discharge on the beam power demonstrates quite satisfactory its coincidence with experimental values. As to the plasma arc itself, then under the action of the laser radiation it is somewhat compressed that can be observed visually or from the rising volt-ampere characteristics of the discharge (Figure 5, *b*).

Investigation of technological capabilities of the plasmatron LPP-22 was performed on flat samples made from 20 mm thick low-carbon steel using LPPC. Powdered alloys of Hastelloy C and Stellite 6 grades of 20 – 63 μm fractions were used as filler materials. These investigations showed that the coaxial combination of the plasma arc with a laser beam in the laser-arc plasmatron gives an opportunity to increase the speed of cladding of single beads by 2 – 3 times as compared with conventional PPC due to improving the space stability of the arc burning. This is similar to the increase in productivity of cladding works for such parts as screw conveyors of extruding machines, flat and disc knives, milling cutters, etc. Simultaneously, the melting γ of the parent metal during cladding of separate beads was at the level of 5 – 10 %. This small value became possible due to the above-mentioned dynamic action of the plasma flow to the melt surface.

In addition, the above-mentioned decrease in arc voltage in the combined process reduces the risk of a double arcing that is especially important in operation at high currents (more than 300 A). This is a good premise for increasing the cladding efficiency by increasing the arc current. Unfortunately, it was not possible to realize this opportunity in our series of experiments, as the available power source could not operate at currents of more than 300 A.

Figure 6 presents two examples of a wide-layer LPPC, made at Q_0 = 2 kW, 18 l/min, full gas (argon) consumption and 2.7 kg/h powder (Hastelloy C) consumption. In one case the cladding was performed with transverse oscillations of the workpiece relative to the plasmatron (Figure 6, *b*), and in the second case — with longitudinal overlap beads (Figure 6, *c*). In both cases a good formation of the deposited layer was provided at minimum melting of the parent metal ($\gamma \le 5$ %). This method of surfacing opens up the feasibility of cladding of large surfaces of the products using wear- and corrosion-resistant alloys providing a high efficiency and quality, for example, in production of bimetals. For comparison, such efficiency of cladding (2.7 kg/h) can be attained in case of using only a laser radiation at the beam power of not less than 10 kW.

In the work, the effect of LPPC speed (Figure 7) and laser beam power (Figure 8) on the formation of single beads and also on the melting γ of the parent metal was also investigated. In experiments, with increase of the cladding speed the section of the beads tried to be kept constant by the appropriate increase in the powder consumption.

As follows from the appearance of beads and macrosections of their transverse section, a good formation of beads is provided in the wide range of cladding speeds (from 10 to 50 m/h). In addition, the nature and level of melting of the parent metal depends both on a total power of the laser beam and plasma arc and also on their ratio. With increase of the laser beam power a peak of melting of the parent metal is shifted from the edges of the bead to its axis (Figure 8). The structure of metal deposited with LPPC method (Figure 9) is similar to that produced by using the conventional PPC.

Thus, the combined application of the laser beam and plasma arc opens up new possibilities in cladding, consisting of increase in speed, stability and reproducibility of the process results, reducing in its cost, as well as in improving the use of the laser energy. However, the authors understand that the results given in this article are preliminary. For a practical realization of the combined process the further investigations are required both from the point of view of optimizing the process parameters and also the selection of rational fields of its application.

CONCLUSIONS

1. Throughout the entire range of conditions the created laser-arc plasmatron LPP-22 has a stable operation with high space-time stability of parameters of the generating plasma and can serve a prototype for making the new designs of such devices for different technological processes.

2. Interaction of the laser beam with a plasma arc leads to the decrease in arc voltage that reduces the risk of a double arcing.

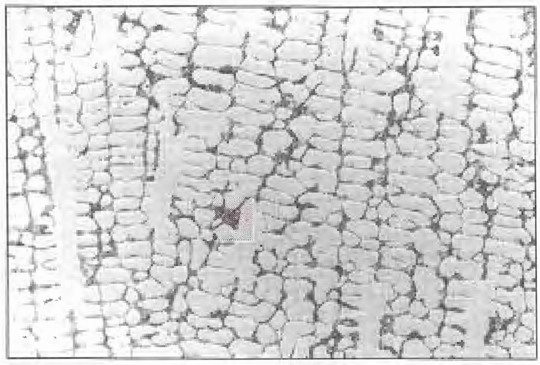

Figure 9. Microstructure of clad metal (Stellite 6) (×500) (reduced by 2/3)

3. It is possible to increase the speed of cladding of single beads in the combined process by 2 – 3 times as compared with a conventional PPC at the expense of increasing the space stability of the arc.

4. The parent metal melting at the LPPC optimum conditions can amount to 5 – 10 %.

The authors thank Dr.-Ing. T. Cheliker for participation and assistance in conductance of the experimental investigations.

REFERENCES

1. Steen, W.M. (1980) Arc augmented laser processing of materials. *J. of Appl. Phys.*, **11**, 5636 – 5641.
2. Diebold, T.P., Albright, C.E. (1984) «Laser-GTA» welding of aluminium alloy 5052. *Welding J.*, **6**, 18 – 24.
3. Matsuda, J., Utsumi, A., Katsumura, M. *et al.* (1988) TIG or MIG arc augmented laser welding of thick mild steel plate. *Joining and Materials*, **1**, 31 – 34.
4. Walduck, R.P., Biffin, J. (1994) Plasma arc augmented laser welding. *Welding and Metal Fabrication*, **4**, 172 – 176.
5. Gvozdetsky, V.S., Krivtsun, I.V., Chizhenko, M.I. *et al.* (1995) Laser-arc discharge: theory and applications. In: *Welding and Surfacing Rev.* Harwood.
6. Tusek, J. (1996) Sinergic operation of welding arc and laser beam for practical application or for scientific research only? *Varilna Tehnika*, **2**, 39 – 46.
7. Dilthey, U., Lueder, F., Wieschemann, A. (1998) Process-technical investigations on hybrid technology of laser beam-arc welding. In: *Proc. of 6th Int. Conf. on Welding and Melting by Electron and Laser Beams*. Toulon, France.
8. Paton, B.E. (1995) Improvement of methods of welding — one of the ways of improving quality and cost-effectiveness of welded structures. *Avtomaticheskaya Svarka*, **11**, 3 – 11.
9. Krivtsun, I.V., Chizhenko, M.I. (1997) Fundamentals of calculation of laser-arc plasmatrons. *Ibid.*, **1**, 16 – 23.
10. Dykhno, I.S., Krivtsun, I.V., Ignatchenko, G.N. *Combined laser and plasma arc welding torch*. Pat. **5700989** USA, Int. Cl. B 23 K 26/00, 10/00. Publ. 23.12.97.
11. Som, A.I. (1999) New plasmatrons for plasma-powder surfacing. *Avtomaticheskaya Svarka*, **7**, 44 – 48.
12. Krivtsun, I.V., Som, A.I. (1998) Modelling of the laser-arc plasma torch. In: *Proc. of 5th Int. Conf. on Thermal Plasma Processes*, St.-Petersburg, Russia. New-York: Begelhouse.

COMPUTER MODELLING OF THE PLASMA SPRAYING PROCESS

Yu.S. BORISOV[1], **I.V. KRIVTSUN**[1], **A.F. MUZHICHENKO**[1], **E. LUGSCHEIDER**[2] and **U. ERITT**[2]
[1]The E.O. Paton Electric Welding Institute, NASU, Kyiv, Ukraine
[2]University of Technology, Aachen, Germany

ABSTRACT

Mathematical models have been constructed and software has been developed for computer modelling of the turbulent plasma jets formed during plasma spraying and behaviour of the spray particles in such jets. Detailed computer modelling of the processes of plasma spraying of particles of nickel and aluminium oxide using argon and nitrogen as the plasma gas, and corresponding experimental studies of these processes have been conducted. The ISSO-1 device has been used to measure velocities and paths of the spray particles. The computer modelling results are in good agreement with the experimental data.

Key words: *plasma spraying, plasma jet, spray particles, mathematical models, computer modelling, software*

Until recently a direct experiment intended for finding optimal conditions has been the basic method for development of commercial technologies of plasma spraying. This approach is time consuming and involves considerable costs, and one cannot always be sure that results obtained are really the best. In this connection, an increasingly high attention is given to development of systems of computer modelling [1, 2] of the process of plasma spraying, allowing an objective analysis of the effect of different factors on conditions of heating and movement of particles in the plasma jet, as well as the most reasonable combination of these factors. This application of computer modelling is a realistic way of changing from a pure experimental approach used for optimization of the plasma spraying technology to a computerized selection of its optimal parameters.

Two approaches can be distinguished in development of the computer models of the plasma spraying process: detailed theoretical investigation and numerical modelling of individual physical-chemical phenomena, on the one hand, and development of mathematical models and software for computer simulation of the process as a whole, on the other hand. An example of the second approach is the CASPSP software (versions 2.0 [3] and 3.1) developed by the E.O. Paton Electric Welding Institute. It is designed for computer simulation of turbulent plasma jets used for application of coatings, and for simulation of heating and movement of the spray particles in such jets.

This software is a package of applied programs, consisting of two inter-related modules:

- modelling of the plasma jet;
- modelling of spray particles.

The first module is intended for modelling of subsonic plasma jets generated by the non-transferred type plasmatrons and emitted into the open atmosphere (Figure 1). This module allows calculation and display of spatial distributions of temperature and velocity of a free plasma jet (Figure 2) depending upon the geometrical dimensions of the anode nozzle of the plasmatron and its operating parameters (arc current, plasma gas composition and flow rate).

The second module serves for modelling of behaviour of the spray particles (Figure 3) in the plasma jet with the preliminarily computed spatial distributions of temperature and velocity. It allows calculation and display of the path, velocity and parameters of the thermal state of a spray particle (Figure 4) depending upon the composition of its material, initial diameter and conditions of its introduction into the jet. It should be noted that in a new version of CASPSP (3.1) a provision is made for a decrease in temperature and velocity of the plasma jet caused by its dusting with a material being sprayed.

The software developed is equipped with Windows 9×/NT/2000 user's interface (English), which includes the following systems for each module:

- control menu;
- system for data input-output and processing (see Figures 1 and 3);
- system for graphical display and printing out of results (see Figures 2 and 4);
- help system.

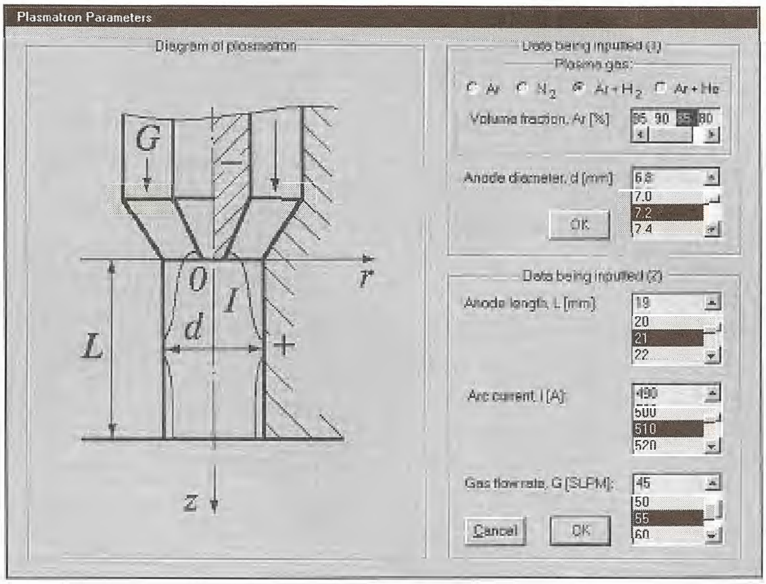

Figure 1. Computed diagram of the plasmatron and parameters used for modelling of plasma jets

The new version of the software has an option of different measurement units for the input and output data:

- sizes (cm\in);
- temperatures (K\F\C);
- gas flow rates (l/min\SCFH);
- powder consumption (kg/h\lb/h).

Finally, it allows simulation of the plasma spraying process using different plasma-forming environments:

• Ar • N_2 • Ar + H_2 • Ar + He (Figure 1),
and different spray materials:

• Al • Cu • Mo • Ni • Ti • Al_2O_3 • Cr_2O_3 • • Fe_3O_4 • TiO_2 • ZrO_2 • Cr_3C_2 • TiC • WC • CaF_2 • • AlCuFe (Figure 3).

Modelling of the plasma jet. Calculation programs for the first module of CASPSP are based on a mathematical model of gas dynamics and heat transfer for the turbulent flow of the arc plasma, described by a system of magnetic-gas-dynamic (MGD) equations [4]. It is known that peculiarity of the plasma flows generated by the non-transferred type plasmatrons is the presence of two flow regions differing in a character of the occurring physical phenomena. Region one includes heating and acceleration of the plasma gas by the electric arc (electric-arc region), and region two includes an inertia movement of the currentless plasma (inertia region). Thermal and gas-dynamic characteristics of the plasma jet are determined primarily by the processes occurring in the electric-arc region,

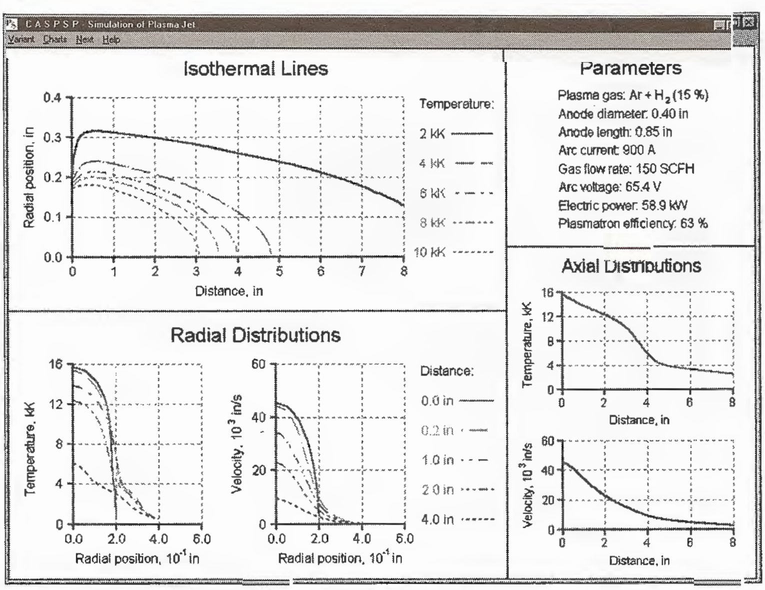

Figure 2. Graphical visualization of the results of modelling of the plasma jet

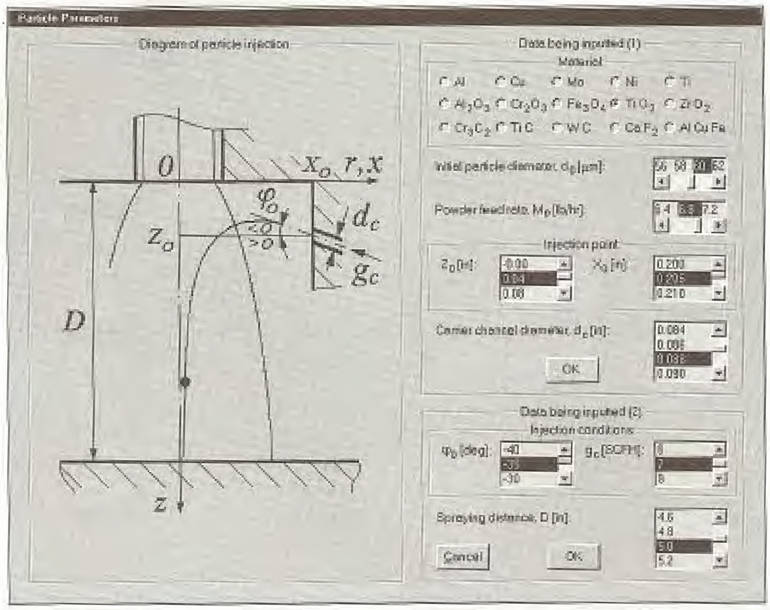

Figure 3. Diagram of introduction of the spray particles into the plasma jet and parameters used for modelling of the spray particles

which in turn depend upon the design and operational conditions of the plasmatron. Therefore, a correct description and computer modelling of the plasma jets used for application of coatings are impossible without allowance for the entire package of the electric-arc processes occurring in the plasmatron.

Consider first the electric-arc region of the plasma flow in the plasmatron with a smooth channel whose schematic is shown in Figure 1. Assume that the arc burns in a turbulent flow of the plasma gas between a refractory pin cathode and a copper cylindrical nozzle serving as the anode. For this we will use the following designations: d — diameter of the plasma-shaping channel, L — its length, I — arc current and G — volume flow rate of the plasma gas (conditions being standard), and make the following assumption for mathematical description of physical processes occurring in the plasmatrons with an axial feed of the plasma gas:

1) the plasma system under consideration has a cylindrical symmetry and the processes occurring are stationary;

2) the plasma is in the state of a local thermodynamic equilibrium and its natural radiation is volumetric;

3) the pressure energy and viscous dissipation can be ignored, while the Joulean heat release (in the arc region), thermal conductivity and convection (natural convection is neglected) are regarded as the main mechanisms of generation and transfer of energy in the plasma;

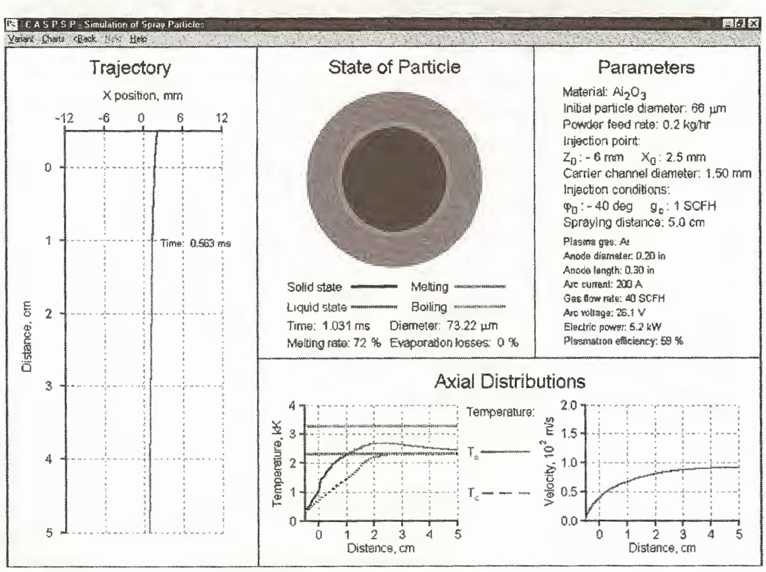

Figure 4. Graphical visualization of the results of modelling of the spray particles

4) the plasma flow is viscous and subsonic, the mode of the flow is turbulent and there are no external magnetic fields.

Given also that in the plasmatrons of the design considered the gas flows primarily in an axial direction and the radial temperature and velocity gradients are much larger than the axial ones, for the calculation of thermal and gas-dynamic characteristics of the plasma we will use approximation of a boundary layer [5]. Assuming the turbulence to be hydrodynamic (ignoring pulsations of electromagnetic values) and considering pressure pulsations to be small, it can be shown, using the Boussinesq's hypothesis, that the system of MGD equations in an approximation of the turbulent boundary layer for time-averaged values of temperature and velocity of the plasma has the following form [2, 4]:

$$\rho C_p\left(\bar{v}\frac{\partial T}{\partial r}+u\frac{\partial T}{\partial z}\right)=\frac{1}{r}\frac{\partial}{\partial r}\left(r\bar{\chi}\frac{\partial T}{\partial r}\right)+\sigma E^2-\psi, \quad (1)$$

$$\rho\left(\bar{v}\frac{\partial u}{\partial r}+u\frac{\partial u}{\partial z}\right)=\frac{1}{r}\frac{\partial}{\partial r}\left(r\bar{\eta}\frac{\partial u}{\partial r}\right)-\frac{\partial}{\partial z}\left(p+\mu_0\frac{H^2}{2}\right), \quad (2)$$

$$\frac{1}{r}\frac{\partial}{\partial r}(r\rho\bar{v})+\frac{\partial}{\partial z}(\rho u)=0. \quad (3)$$

Here T is the averaged temperature of the plasma; $\bar{v}=(\rho v+\rho' v')/\rho$, where v and ρ are the averaged radial velocity and density of the plasma; ρ' and v' are the density and radial velocity pulsations; u is the averaged axial velocity of the plasma; p is the pressure; σ and C_p are the electrical conductivity and heat of the plasma under the constant pressure; ψ is the volume density of power of a natural radiation; $\bar{\eta}$ and $\bar{\chi}$ are the total coefficients of dynamic viscosity and thermal conductivity of the plasma, which are the sums of molecular and turbulent viscosity and thermal conductivity, respectively; E is the axial component of the electric field intensity; μ_0 is the universal magnetic constant and H is the azimuthal component of the magnetic field of the arc current

$$H=\frac{1}{r}E\int_0^r\sigma r dr. \quad (4)$$

Within the frames of the used approximation of the boundary layer the axial component of the arc electric field intensity is almost constant across the section of the channel [4] and determined from the condition of conservation of the total flow

$$I=2\pi E\int_0^{R_C}\sigma r dr, \quad (5)$$

where R_C is the radius of the calculation domain for the arc region, $R_C = d/2$.

In the arc region of the flow the distribution of pressure is determined with allowance for its magnetic component:

$$p=p_{ext}-\int_z^L\frac{dp_C}{dz}dz+\mu_0 E\int_r^{R_C}\sigma H dr, \quad (6)$$

where p_{ext} is the external medium pressure. The gas-static pressure gradient dp_C/dz in an approximation of the boundary layer is also constant across the channel section [5] and determined from the condition of conservation of the total flow rate of gas through the plasmatron:

$$\rho_0 G=2\pi\int_0^{R_C}\rho u r dr, \quad (7)$$

where ρ_0 is the mass density of the plasma gas under standard conditions.

The system of equations (1) through (7) should be supplemented by an equation of state and dependencies of the molecular coefficients of transfer, thermal-physical parameters and radiation losses of the plasma gas upon the temperature and pressure

$$\rho=\rho(T,p),\ C_p=C_p(T,p),\ \chi=\chi(T,p),$$
$$\eta=\eta(T,p),\ \sigma=\sigma(T,p),\ \psi=\psi(T,p). \quad (8)$$

The detailed tables of the above values for the used plasma gases and mixtures are given, e.g. in [4, 6]. It should be reminded here that the total coefficients of dynamic viscosity and thermal conductivity of the plasma, which are included into equations (1) and (2), have the following form:

$$\bar{\eta}=\eta+\eta_t,\ \bar{\chi}=\chi+\chi_t, \quad (9)$$

where index t refers to turbulent components of the said transfer coefficients.

To determine turbulent viscosity η_t, we will use a combined algebraic model of turbulence. As it is shown in [4], it is in the best agreement with experiment for the entire set of parameters of the electric-arc flows in the channel purged with the turbulent gas flow. The following models are used in this case:

1) for the central portion of the channel — the Prandtl model [7]:

$$\eta_t = \rho l_m \left| \frac{\partial u}{\partial r} \right|, \qquad (10)$$

where $l_m = 0.41(R_c - r)$ is the length of the mixing path;

2) for the near-wall portion — the Deissler model [8]:

$$\frac{\eta_t}{\eta} = 0.0154 u^+ Y^+ [1 - \exp(0.0154 u^+ Y^+)], \qquad (11)$$

where

$$u^+ = \frac{u}{v^*}, \quad Y^+ = \frac{\rho(R_C - r)}{\eta} v^*, \qquad (12)$$

$$v^* = \sqrt{(\eta \frac{\partial u}{\partial r})_{R_C} / \rho_{R_C}}.$$

The limits of applicability of formula (11) are determined from condition $0 < Y^+ < 26$. Formula (10) is used at $Y^+ > 26$.

The coefficient of turbulent thermal conductivity χ_t can be expressed in terms of the coefficient of turbulent viscosity using the following relationship:

$$\chi_t = \eta_t \frac{C_p}{\mathrm{Pr}_t}, \qquad (13)$$

where Pr_t is the Prandtl turbulent number, which is selected according to recommendations [9] or is assumed to be equal to one [4].

To describe characteristics of the turbulent plasma flow in an inertia region of the flow inside the anode nozzle of the plasmatron ($L_a < z < L$, where L_a is the arc length), it should be set in the above equations that $E = H = 0$. In this case the system of equations (1) through (3) together with relationships (6) and (7) is transformed into a conventional system of gas-dynamic equations of the turbulent boundary layer for the internal flows [10]. Expressions for the turbulent coefficients of transfer in the inertia region of the plasma flow inside the channel remain as they are in the arc region — (10) through (13).

This system of gas-dynamic equations can be used also for description of the inertia region of the plasma jet outside the plasmatron channel ($z > L$). Assuming that the subsonic jet flows into a quiescent medium in which the pressure is constant, $dp/dz = 0$ and $p = p_{\mathrm{ext}}$ are set in equation (2). Then the initial system of equations at $E = H = 0$ will describe the currentless jet in an approximation of the turbulent boundary layer.

To determine turbulent viscosity in the case of a free immersed (emitted into the quiescent medium) jet, we will use the model given in [11]

$$\eta_t = \rho \gamma F r_{1/2} \hat{u}. \qquad (14)$$

Here the intermittence function is as follows:

$$\gamma = \begin{cases} 1, & 0 < r/r_{1/2} < 0.8, \\ 0.5^m, & r/r_{1/2} > 0.8, \end{cases} \qquad (15)$$

where $m = r/r_{1/2} - 0.8$; $F = 0.015(1 + 2.13\hat{u})$ and $\hat{u}$ is the ratio of the axial velocity in the jet to the averaged velocity of the plasma flowing from the anode nozzle opening. Parameter $r_{1/2}$ is the distance from the jet axis to a point at which the axial velocity decreases to a value equal to half that at the jet axis. As to the coefficient of turbulent thermal conductivity for an exposed portion of the jet, it can still be calculated using relationship (13).

To solve the system of parabolic equations (1) through (3) within the plasmatron channel, it is necessary to set the corresponding boundary and initial (input) conditions at the limits of the calculation domain: $0 < r < R_C = d/2$ and $0 < z < L$ (Figure 1). Boundary conditions at the channel axis are selected on the basis of considerations that the system features a cylindrical symmetry, i.e. at $0 < z < L$, $r = 0$

$$\frac{\partial T}{\partial r} = 0, \quad \frac{\partial u}{\partial r} = 0, \quad \bar{v} = 0. \qquad (16)$$

At the external limit of the calculation domain outside the anode spot of the arc the gas temperature is assumed to be equal to temperature of a cooled wall of the channel and the «sticking» condition is met, i.e. at $r = R_C$

$$T = T_{\mathrm{w}}, \; u = 0, \qquad (17)$$

where T_{w} is the wall temperature. It is assumed that within the region of the anode fixation of the arc $T = T_a$, where T_a is the temperature of the plasma near the copper anode surface determined from the experimental data [12, 13].

At the initial section of the channel at $0 < r < R_C$ and $z = 0$, it holds that

$$T(r, 0) = \begin{cases} T_0 [1 - (r/r_c)^4] + T_{\mathrm{w}}, & 0 < r < r_c, \\ T_{\mathrm{w}}, & r_c < r < R_C, \end{cases} \qquad (18)$$

where r_c is the radius of the cathodic region of the arc determined from the following condition:

$$I = \pi r_c^2 j_c. \qquad (19)$$

Here j_c is the cathode current density set on the basis of experimental data for refractory (tungsten) cathodes operating in different gases [13]. The radial distribution of the axial velocity of the plasma gas at the initial section of the calculation domain is also set by the model dependence to be equal to

$$u(r, 0) = u_0 \left[1 - \left(\frac{r}{R_C} \right)^2 \right]. \quad (20)$$

Parameters T_0 and u_0 in distributions (18) and (20) are selected so that the following relationship is met:

$$IU_c - Q_c = 2\pi \int_0^{R_C} \rho u h r dr, \quad (21)$$

which corresponds to an integral balance of energy between the cathode and plasma, and also that condition (7) is satisfied. In it U_c and Q_c are the cathodic voltage drop and power introduced into the cathode by the arc, respectively, their values being taken from the experiment, depending upon the arc current and kind of the gas [13], and h is the enthalpy of the plasma gas.

The following condition is used as the ratio determining the arc length L_a (boundary of the arc and inertia regions of the plasma flow):

$$U_c + \int_0^{L_a} E dz + U_a = U, \quad (22)$$

where U_a is the anode voltage drop (its value for the arc burning in different plasma gases, using a copper water-cooled anode, can be found, e.g. in [12]); U is the total voltage of the arc depending upon its current, composition and flow rate of the plasma gas. Generalized volt-ampere characteristics $U = f(d, I, G)$ for the considered plasmatron with a smooth channel, operating with different gases, are given in [14, 15]. They are used for calculation of the overall electric power of the plasmatron, $P = IU$, and its efficiency equal to W/P, where W is the flow of enthalpy of the plasma determined by the right part of equation (21) at $z = L$.

Boundary conditions for the exposed portion of the plasma jet are selected as follows. At its axis, i.e. at $r = 0$, the boundary conditions remain as they are inside the channel of the plasmatron. At the external boundary of the calculation domain the conditions assumed are those of a smooth interface with the environment. It holds for the immersed jet at $r = R_C$ and $z > L$ that

$$T = T_{ext}, \quad u = 0. \quad (23)$$

The R_C value in the exposed portion of the jet is selected such that at $r = R_C$ and at any z

$$\frac{\partial T}{\partial r} = \delta, \quad \frac{\partial u}{\partial r} = \delta, \quad (24)$$

where δ is a certain small value.

The system of equations (1) through (3), as well as relationships (4) through (15) and boundary conditions (16) through (24) determine in full the thermal and gas-dynamic characteristics of the turbulent plasma flow both in the arc and inertia regions of the flow. Therefore, the above equations make the base of the mathematical model for the calculation of spatial distributions of temperature and velocity of the subsonic turbulent plasma jets generated by the spraying plasmatrons, depending upon the mode of operation and kind of the plasma gas.

Characteristics of the subsonic argon plasma generated by the Miller SG-100 plasmatron were calculated to compare results of computer modelling of the plasma jet with known experimental data using the developed software. Investigated was the stationary turbulent plasma jet flowing into the argon atmosphere under the following conditions: diameter of the anode nozzle of the plasmatron — 8.5 mm, its length — 30 mm, arc current — 400 A, argon flow rate — $9.57 \cdot 10^{-4}$ kg/s (35 l/min). Results of the probe and spectrometry measurements of temperature and velocity of the plasma for such a jet are given in [16]. As shown by the calculations, the integrated characteristics (arc voltage — 24.0 V, plasmatron efficiency — 44 %) are in good agreement with the experimental data given in [16] (23.9 V and 42.2 %, respectively).

Distributions of the axial values of temperature and velocity of the plasma along the length of the jet for the plasmatron under consideration (calculated and experimental) are shown in Figure 5. The calculated axial temperature (*top curve*) is in good agreement with the experimental one. As far as the axial velocity of the plasma (Figure 5, *bottom curve*) is concerned, its values measured at the initial sections of the jet are a bit higher than the calculated ones. In addition, an actual decrease in the axial velocity along the length of the jet occurs more rapidly than it is predicted by the mathematical model. This discrepancy can be associated, e.g. with the fact that the Miller SG-100 plasmatron uses a vortex feed of the plasma gas, whereas the mathematical model considered describes the jet with an axial gas flow in the plasmatron.

The calculated radial profiles of temperature and velocity of the plasma at different distances from the exit section of the anode nozzle of the

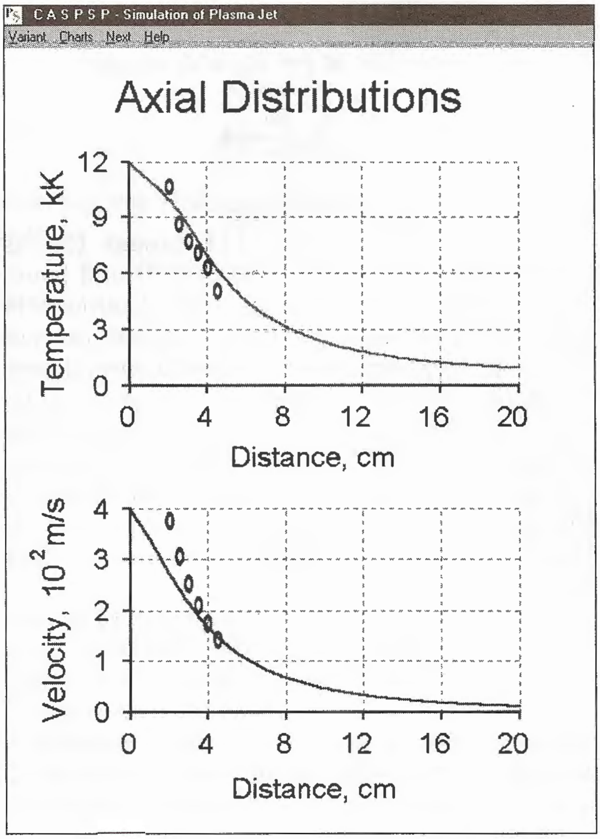

Figure 5. Calculated distributions of the axial values of temperature (*top*) and velocity (*bottom*) of the plasma along the length of the argon jet; 0 — experimental data [16]

plasmatron almost coincide with the respective distributions obtained as a result of the probe measurements and can be represented with a sufficient accuracy as the Gaussian curves [16]. Therefore, results of modelling of the turbulent plasma jet using the CASPSP software are in good agreement with the experimental data.

Modelling of the spray particles. Calculation programs for the second module of CASPSP are based on a mathematical model of heating and movement of a spray particle, which is described by a non-stationary non-linear equation of movement of the particle in the plasma flow [2]. The basic assumption used for development of this mathematical model is that the particle has a spherical shape and distribution of temperature in the bulk of this particle is spherically symmetrical.

Consider behaviour of one such spherical particle in the plasma jet with known distributions of temperature and velocity of the plasma depending upon the properties of the particle material, initial diameter and conditions of introduction of the particle into the plasma jet. Assume that the particle with an initial diameter d_0 is introduced into the jet as it is shown in Figure 3. In this case X_0 and Z_0 are the coordinates of the introduction point, φ_0 is the angle at which the particle is introduced (counted off from the horizontal line), d_c is the diameter of the transportation channel, g_c is the volume flow rate of the transporting gas and D is the spraying distance. In this case the calculation of heating of the spray particle in the plasma jet is reduced to integration of the non-stationary equation of thermal conductivity:

$$\rho_p C_{ep} \frac{\partial T_p}{\partial t} = \frac{1}{r^2} \frac{\partial}{\partial r} \left(r^2 \chi_p \frac{\partial T_p}{\partial r} \right). \qquad (25)$$

Here $T_p(r, t)$ are the space-time distribution of temperature in the bulk of the particle; t is the time from the moment of its ejection from the transportation channel; $\rho_p(T_p)$ is the density; $\chi_p(T_p)$ is the coefficient of thermal conductivity and C_{ep} is the effective heat capacity of the particle material determined by allowing for the latent heat of melting and vapour formation:

$$C_{ep} = c_p + W_m \delta(T_p - T_m) + W_b \delta(T_p - T_b), \qquad (26)$$

where $c_p(T_p)$ is the specific heat; W_m and W_b are the latent heat of melting and vapour formation; T_m and T_b are the temperatures of melting and boiling of the particle material and $\delta(x)$ is the delta function.

Equation (25) is solved provided the following initial condition is met:

$$T_p(r)|_{t=0} = T_0, \qquad (27)$$

where T_0 is the initial temperature of the particle (assumed to be equal to the temperature of the transporting gas) and the following boundary conditions hold:

$$\frac{\partial T_p}{\partial r}|_{r=0} = 0, \quad \left(-\chi_p \frac{\partial T_p}{\partial r} \right)|_{r=a} = q. \qquad (28)$$

Here $q(t)$ is the heat flow introduced by the plasma through the particle surface; $a(t)$ is its current radius which can vary with time during evaporation and melting of the particle due to differences in density of the material in solid and liquid states. It is assumed that evaporation of the material occurs from the surface of the particle as soon as its temperature, according to (26), becomes higher than T_b. It is also assumed that the rate of evaporation is not limited by the velocity of dissipation of the vapour and the velocity of the particle is determined at each time moment as the distance from its centre to points at which the said temperature is achieved. In addition, it is assumed that the presence of the vapour around the particle does not limit the heat flow coming into it.

Exchange of the energy between the plasma and particle is described on the basis of the combined model of convective-radiation exchange [17], according to which

$$q = \alpha(\tilde{T} - T_s) + \xi\sigma_0(\tilde{T}^4 - T_s^4), \quad (29)$$

where $\tilde{T}$ is the temperature of the plasma at the point of location of the particle calculated with allowance for a local decrease in temperature of the initial jet caused by its dusting with the spray material; T_s is the temperature of the particle surface; α is the heat transfer coefficient; ξ is the emissivity factor of the particle material and σ_0 is the Stefan-Boltzmann constant. The convective heat exchange coefficient for a spherical particle can be calculated from the criterial dependence [18] for a flow around the sphere

$$\mathrm{Nu} = 2\,\frac{\chi_s}{\chi} + 0.5\mathrm{Re}^{0.5}\mathrm{Pr}^{0.4}\left(\frac{\rho\eta}{\rho_s\eta_s}\right)^{0.2}. \quad (30)$$

Here $\mathrm{Nu} = 2\alpha a/\chi$ is the Nusselt number; $\mathrm{Re} = (\rho\,|\,\tilde{\mathbf{u}} - \mathbf{w}\,|\,2a)/\eta$ is the Reynolds number, both calculated from the current values of radius and velocity of the particle; $\mathrm{Pr} = (C_p\eta)/\chi$ is the Prandtl number; χ, η, ρ, C_p are the transfer coefficients, density and heat capacity of the plasma determined at the point of location of the particle (index s designates the respective properties of the plasma at the particle surface temperature); $\tilde{\mathbf{u}}$ is the velocity of the plasma flow at the point of location of the particle, calculated with allowance for a decrease in the plasma velocity due to dusting the jet with the spray material and $\mathbf{w} = (w_x, w_y, w_z)$ is the particle velocity.

To describe movement of the spray particles, assume that each of them in the plasma flow is affected only by the aerodynamic drag force:

$$\mathbf{F} = 0{,}5C_dS\rho(\tilde{\mathbf{u}} - \mathbf{w})|\tilde{\mathbf{u}} - \mathbf{w}|, \quad (31)$$

where C_d is the coefficient of the head resistance; $S = \pi a^2$ is the midship section of the particle. To determine C_d of a spherical particle, we will use the following criterial dependencies [18]:

$$\begin{aligned} &C_d = 24\mathrm{Re}^{-1}, \quad \mathrm{Re} < 0.2, \\ &C_d = 24\mathrm{Re}^{-1} + 3.6\mathrm{Re}^{-0.317}, \quad 0.2 < \mathrm{Re} < 4, \quad (32) \\ &C_d = 24\mathrm{Re}^{-1} + 4\mathrm{Re}^{-0.333}, \quad 4 < \mathrm{Re} < 400. \end{aligned}$$

Then the calculation of velocity and path of the spray particle in the plasma jet is reduced to solution of the following system of differential equations:

$$\frac{d(m\mathbf{w})}{dt} = \mathbf{F}, \quad \frac{d\mathbf{r}}{dt} = \mathbf{w}, \quad (33)$$

where $m(t)$ and $\mathbf{r}(t) = (x, y, z)$ are the current values of mass and radius vector of the particle.

Equations (27) are integrated under the following initial conditions:

$$\begin{aligned} &x|_{t=0} = X_0, \; y|_{t=0} = 0, \; z|_{t=0} = Z_0, \\ &w_x|_{t=0} = -w_0\cos\varphi_0, \; w_y|_{t=0} = 0, \quad (34) \\ &w_z|_{t=0} = w_0\sin\varphi_0. \end{aligned}$$

Here w_0 is the initial velocity of the particle in a flow of the transporting gas

$$w_0 = k\,\frac{4g_c}{\pi d_c^2}, \quad (35)$$

where $k \approx 0.5$ is the coefficient which depends upon the size of the transportation channel, composition and flow rate of the transporting gas, spray material and diameter of the particles.

The following relationships are used for an approximate determination of a decrease in temperature and velocity of the plasma in the initial jet caused by its dusting with the spray material:

$$\begin{aligned} &\int_{\tilde{T}}^{T} C_p dT = K\,\frac{h_p}{m_0}, \quad (36) \\ &\tilde{u} = u - K(w_z - w_0\sin\varphi_0), \quad K = \frac{M_p}{\rho_0 G}, \end{aligned}$$

where T and u are the non-disturbed values of temperature and velocity of the plasma at the point of location of the particle; h_p is the current value of enthalpy of its material; K is the coefficient of dusting the jet with a powder; M_p and $\rho_0 G$ are the mass flow rates of the spray material and plasma gas, respectively.

This settles description of the mathematical model of heating and movement of a spherical particle in the plasma jet with known (preliminarily calculated) spatial distributions of temperature and velocity of the plasma. This model allows determination of path and velocity of the spray particles, distribution of temperature in the bulk of these particles, degree of melting and losses of mass for evaporation (depending upon the type of the spray material and its consumption, initial diameter and condition of introduction of the particles into the jet).

To compare results of computer modelling with the experimental data, the processes of plasma spraying of nickel and aluminium oxide particles were simulated using the developed software [19]. In the calculations the required parameters of

Table 1. Experimental conditions of plasma spraying of Ni and Al_2O_3 particles

No. of experiment	Plasma gas		Elecrtical parameters		Spray particles		Spraying distance, mm	Coating thickness, μm
	composition	flow rate, l/min	current, A	voltage, V	material	size, μm		
1	Ar	50	300	35	Al_2O_3	16 – 40	125	–
2	Ar	50	400	34 – 35	Al_2O_3	16 – 40	125	5
3	Ar	30	520	31 – 33	Al_2O_3	16 – 40	125	30 – 35
4	N_2	30	300	70	Al_2O_3	16 – 40	125	50
5	Ar	50	300	35	Ni	40 – 70	150	12
6	Ar	50	380	35	Ni	40 – 70	150	40
7	Ar	30	520	31 – 32	Ni	40 – 70	150	120
8	N_2	30	300	70	Ni	40 – 70	150	60 – 68
9	Ar	30	600	25 – 27	Al_2O_3	45 – 50	150	–
10	Ar	30	600	25 – 27	Ni	40 – 50	150	–

spraying corresponded to the experimental parameters given in Table 1. The plasmatron with a smooth channel of the anode nozzle 6 mm in diameter and 12 mm long for argon and 21 mm for nitrogen was used in the experiments. The powder feed conditions (Figure 3) were as follows: $X_0 = 4$ mm, $Z_0 = 2$ mm, $\varphi_0 = 0$, $d_c = 2$ mm, $g_c = 4$ l/min and $M_p = 1$ kg/h for aluminium oxide and 2 l/min and 2 kg/h for nickel. Velocities of the particles were measured in experiments No.9 and 10, but in this case conditions of introduction of the particles were a bit different: $X_0 = 10$ mm, $Z_0 = 6$ mm and $\varphi_0 = -15°$.

Table 2. Results of computer simulation of the processes of plasma spraying of Ni and Al_2O_3 particles

No. of experiment	Electrical parameters		Spray particles		Temperature, K		Melting degree, %	Evaporation losses, %	Particle velocity, m/s	Particle distance from jet axis, mm
	voltage, V	power, kW	material	size, μm	particle surface	particle centre				
1	34.4	10.3	Al_2O_3	16	820	820	0	0	12.2	5.1
				30	2000	2000	0	0	128.9	1.5
				40	2330	2330	0	0	155.1	–0.1
2	33.6	13.4	Al_2O_3	16	750	750	0	0	7.6	6.0
				30	2300	2310	0	0	131.8	4.8
				40	3040	3070	100	0	167.8	0.8
3	27.4	14.2	Al_2O_3	16	1270	1270	0	0	12.8	5.3
				30	3250	3230	100	55	110.0	2.4
				40	3250	3260	100	99	53.3	1.3
4	69.9	21.0	Al_2O_3	16	3220	3250	100	46	78.5	3.0
				30	3270	3230	100	66	194.2	–0.3
				40	3250	3230	100	49	155.4	–3.0
5	34.4	10.3	Ni	40	1630	1630	0	0	92.8	0.8
				60	2230	2230	100	0	94.7	–1.7
				70	2510	2520	100	0	88.2	–3.0
6	33.7	12.8	Ni	40	1720	1720	0	0	95.7	1.8
				60	3050	3050	100	0	103.6	–0.8
				70	3050	3050	100	0	98.1	–2.1
7	27.4	14.2	Ni	40	3070	3070	100	0	100.8	1.4
				60	3080	3060	100	0	93.6	–2.3
				70	3080	3060	100	8	83.0	–4.0
8	69.9	21.0	Ni	40	3070	3070	100	0	107.4	–2.4
				60	3070	3060	100	0	77.8	–6.3
				70	3060	3060	100	0	65.8	–8.3
9	27.1	16.3	Al_2O_3	48	1850	1860	0	0	46.4	4.9
10	27.1	16.3	Ni	46	1560	1560	0	0	41.6	4.9

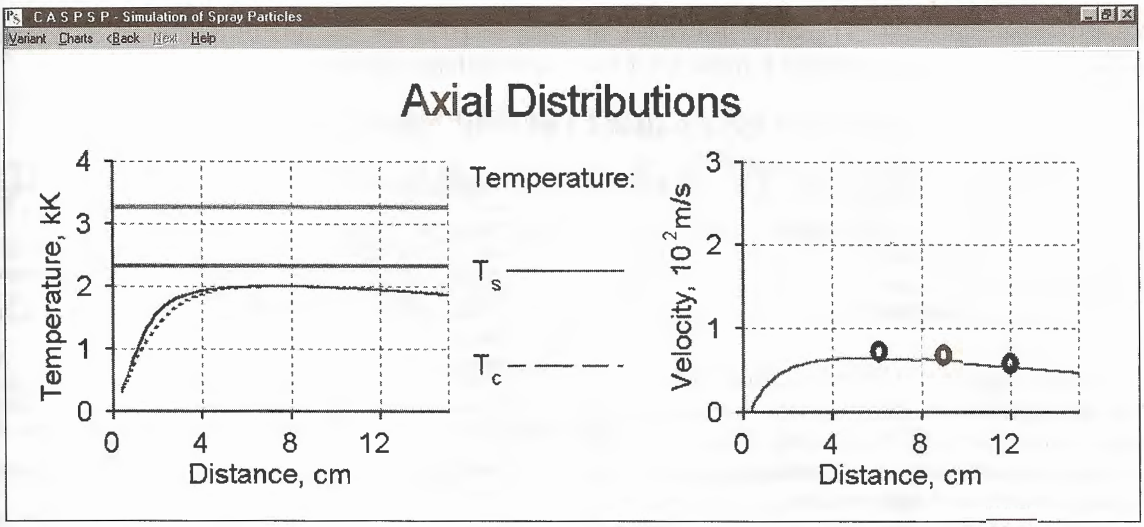

Figure 6. Dependencies of the calculated temperatures at the centre, T_c, and surface, T_s, of a particle of Al_2O_3 (*in the left*) and its velocity (*in the right*) upon the distance to the exit section of the plasmatron (initial diameter of the particle is 48 μm, conditions of experiment No. 9); 0 — experimental data [19]

Metallography of the samples sprayed in experiments No.1 – 8 showed that coatings were formed in all cases, except for experiment No.1. In this case thickness of the sprayed layer depends upon the experiment conditions (Table 1). The quality of the resulting coating depending upon the spraying conditions was determined from porosity of the sprayed layer and presence of the non-melted particles in it. The best results were obtained in experiments No.4 for aluminium oxide and No.7 for nickel.

Results of the calculations of characteristics of the spray particles near the sample surface for the above experimental conditions are given in Table 2. Comparison of the simulation results with the experimental data shows that the calculated characteristics of the spray particles (temperature, velocity and melting degree) are in a sufficiently good agreement with the quality of the coating provided in a given experiment. Thus, it was found for experiment No.1 that the degree of melting of the aluminium oxide particles approaching the sample surface was equal to zero (Table 2). This corresponds to the fact that under the given spraying conditions no coating is formed. It turned out in experiment No.2 that only some of the particles were fully melted (Table 2), which corresponded to a small thickness of the coating produced under these conditions (Table 1). The best results in simulation of the process of spraying aluminium oxide were obtained under conditions of experiment No.4. All particles were fully melted and had rather high velocities (Table 2), which corresponded to the largest thickness and the high quality of the coating

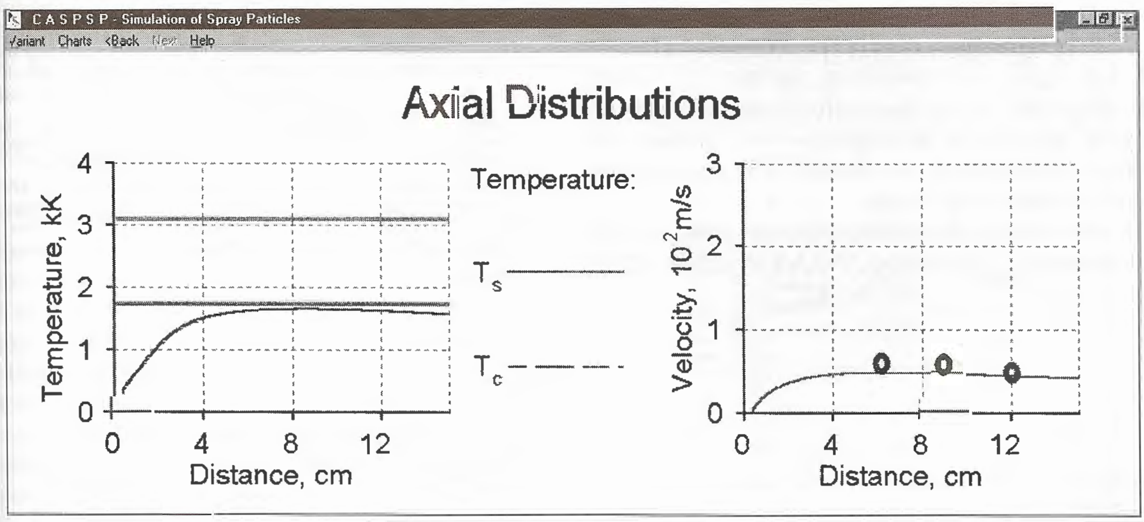

Figure 7. Dependencies of the calculated temperatures at the centre, T_c, and surface, T_s, of the particle of Ni (*to the left*) and its velocity (*to the right*) upon the distance to the plasmatron exit section (initial diameter of the particle is 46 μm, conditions of experiment No.10); 0 — experimental data

produced experimentally. The only drawback of these conditions is evaporation of particles (Table 2).

In the case of spraying nickel the calculation results are also in a sufficiently good agreement with the experimental data. Thus, a decrease in the quantity of the non-melted particles and increase in their temperature and velocity near the sample surface correspond to an increase in thickness of the coating and its density observed in experiments No.5 – 7 (Table 1).

To check results of the calculation of velocity of the spray particles, the velocity was measured directly using the ISSO-1 device. This device is based on the principle of a rotating mirror. To prevent formation of light marks on the image of particles under the plasma jet radiation, in experiments on the velocity measurement the particles were added to the jet at the lowest initial velocities (g_c = 1 l/min). The calculated values of temperature and velocity of the particles along the length of the jet, as well as the corresponding experimental values of the velocity for conditions of experiments No.9 and 10 are shown in Figures 6 and 7, respectively [19]. As it is seen from the plots shown in the left parts of these Figures, there is a good agreement between the calculated and experimental values.

CONCLUSIONS

Comparison of results of computer simulation of the processes of plasma spraying of the coatings of nickel and aluminium oxide under different spraying conditions with the experimental data indicates to their satisfactory agreement. This suggests that the CASPSP software can be successfully used for computer estimation of basic characteristics of the plasma jet and the spray particles, depending upon the plasma spraying conditions. The software can be helpful also for production engineers involved in development of various technologies for plasma spraying, and it can be employed as a manual for training of engineers and technicians specializing in the corresponding fields.

In conclusion, the authors express gratitude to the European Commission, INTAS Program (Project 94-672) for the financial support of the work on development of the CASPSP software.

REFERENCES

1. Pfender, E., Chang, C.H. (1998) Plasma spray jets and plasma-particulate interaction: modelling and experiments. In: *Proc. of 15th Int. Thermal Spray Conf.*, Nice, France.
2. Borisov, Yu.S., Chernyshov, A.V., Krivtsun, I.A. *et al.* (1994) Computer-aided simulation and experimental study of dusted plasma jets emitting into limited space. In: *Proc. of the Nat. Thermal Spray Conf.*, Boston, USA.
3. Borisov, Yu.S., Krivtsun, I.V., Muzhichenko, A.F. (1998) Software package for computer-aided simulation of plasma spraying process. In: *Abstr. of 5th Europ. Conf. on Thermal Plasma Processes*, St.-Petersburg, Russia.
4. (1990) *Theory of the electric arc column.* Ed. by M.F. Zhukov. Novosibirsk: Nauka.
5. Lojtsyansky, L.G. (1973) *Mechanics of fluid and gas.* Moscow: Nauka.
6. Boulos, M.I., Fauchais, P., Pfender, E. (1994) *Thermal plasmas: Fundamentals and applications.* New York-London: Plenum Press.
7. Prandtl, L. (1926) Über die ausgebildete Turbulenz. In: *Proc. of 2nd Int. Congr. on Applied Mechanics*, Zürich.
8. Deissler, R.D. (1959) *Analysis of turbulent heat transfer, mass transfer and friction in smooth tubes at high Prandtl and Schmidt numbers.* NASA Report.
9. Ievlev, V.M. (1975) *Turbulent movement of high-temperature continuum.* Moscow: Nauka.
10. Anderson, D., Tannekhil, J., Pletcher, R. (1990) *Calculation hydrodynamics and heat transfer.* Moscow: Mir.
11. Hwang, S.S., Pletcher, R.H. (1978) Prediction of turbulent jets and plumes in flowing ambient. In: *Engineering Research Institute Technical Rep. 79003/HTL-15.* Des Moines: Iowa State University.
12. Dyuzhev, G.A., Nemchinsky, V.A., Shkolnik, S.M. *et al.* (1983) Anodic processes in high-current arc discharge. *Khimiya Plazmy*, **10**, 169 – 209.
13. Zhukov, M.F., Kozlov, N.P., Pustogarov, A.V. *et al.* (1982) *Near-electrode processes in arc discharges.* Novosibirsk: Nauka.
14. Zhukov, M.F., Smolyakov, V.Ya., Uryukov, B.A. (1973) *Electric-arc gas heaters (plasmatrons).* Moscow: Nauka.
15. Donskoj, A.V., Klubnikin, V.S. (1979) *Electric-plasma processes and units in machine-building.* Leningrad: Mashinostroyeniye.
16. Chen, W.L.T. (1990) Enthalpy probe and spectrometric measurements for Miller SG-100 subsonic plasma jet. In: *High Temperature Laboratory, Department of Mechanical Engineering.* Minneapolis: University of Minnesota.
17. Kutateladze, S.S. (1979) *Fundamentals of the heat transfer theory.* Moscow: Atomizdat.
18. Tsvetkov, Yu.V., Panfilov, S.A. (1980) *Low-temperature plasma in reduction processes.* Moscow: Nauka.
19. Borisov, Yu., Krivtsun, I., Muzhichenko, A. *et al.* (1999) Comparison of computer modelling and measurements in plasma spraying of Ni and Al_2O_3. In: *Proc. of 13th Int. Conf. on Surface Modification Technologies*, Singapore.

MODELLING OF HEATING AND MOVEMENT OF PARTICLES IN ARC PLASMA AT SUPERCRITICAL PRESSURE GRADIENT

S.V. PETROV[1], A.G. SAAKOV[1], O.L. KOTLYAROV[2] and V.P. YATSENKO[2]
[1]RPC «TOPAS», Kyiv, Ukraine
[2]Institute for General Power Engineering, NASU, Kyiv, Ukraine

ABSTRACT

Results of calculation of the electric arc burning under conditions of a supercritical pressure gradient in a blocked nozzle and with dispersed particles injected in it are given. It is shown that a plasmatron based on this principle is an efficient means for heating and acceleration of the spraying powder. Molten particles which are not subjected to splitting in flight leave the arc plasma in such a plasmatron at a velocity of about 1000 m/s, which provides a substantial improvement in properties of the sprayed coatings.

Key words: *mathematical model, plasmatron arc, plasma flow, spraying powder, particle size, supersonic velocity*

The supersonic plasma flow is reported [1] to be an efficient means for acceleration of particles. However, the efficiency of their heating decreases with an increase in the Mach number. A method which provides a radical elimination of this disadvantage is an injection of the spraying powder into the arc of the plasmatron that burns at a supercritical pressure gradient.

Consider theoretical conditions which allow the basic estimates to be made and relationships to be derived for the first stage of development of supersonic spraying devices involving injection of the spraying powder into the plasmatron arc burning at a supercritical pressure gradient (Figure 1). It should be noted here that numerous attempts to inject the spraying powder into the channel of an exit electrode of the plasmatron without an anode fixation of the arc and at a subsonic velocity failed. Fast obstruction of passage in the channel made further operation of the plasmatron impossible. Today the cause of this phenomenon is clear, it results primarily from dissipation of the dispersed particles due to a pulsating component of the dynamic head. Results of our investigations show that the situation is different in the case of operation at a velocity close to the sound one. In this case dissipation of the dispersed phase is fundamentally decreased owing to laminarization of the flow. Thus, the angle of opening of the dispersed phase that moves with sliding in the supersonic plasma flow is 3 – 5°, whereas that in the subsonic plasma flow is 15 – 25°. In this situation, by regulating parameters of injection of the spraying material into the drifting flow it is possible to avoid hitting the walls of the plasmatron nozzle channel by molten droplets.

The mathematical model of processes occurring in the plasmatron nozzle can be represented as the one consisting of two independent parts. The first part is an attempt to theoretically describe the supersonic plasma flow in a cylindrical channel (exit portion of the nozzle), which contains the electric arc in its near-axis region. The second part is an investigation of movement and heating of the powder fed to the nozzle by lateral injection (normal to the axis) and estimation of the position of the point of splitting of a molten particle under the effect of aerodynamic forces of the drifting flow. As a rule, the mutual effect of the particles and their coagulation is ignored, which suggests a very small volume concentration of the powder in the flow.

The problem of transition over the sound velocity involves a known idea of a decisive role of the boundary layer for the flow in the cylindrical chan-

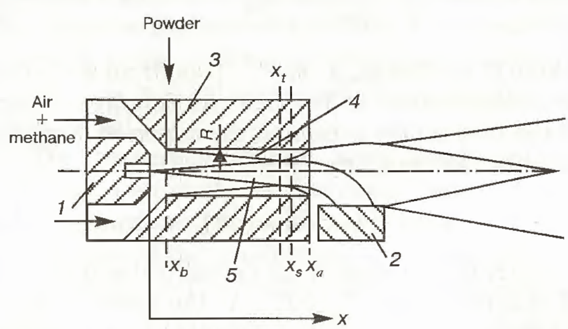

Figure 1. Schematic of the plasmatron with the arc in a blocked nozzle: *1* — cathode; *2* — anode; *3* — inter-electrode insert; *4* — boundary layer; *5* — arc

nel. In consideration of the model of transition over the sound velocity for the plasma arc flow in the Laval nozzle the effect of the boundary layer can be ignored. The flow in a radial direction is conditionally subdivided into a near-axis region of displacement of the arc with a cross section area of Θ_d, region of displacement of the boundary layer with thickness of δ^* and a unidimensional, non-viscous and adiabatic outward flow with an adiabatic exponent of $\gamma = 1.4$ located between the above regions. The bounds of the region of displacement of the boundary layer act as the Laval nozzle wall. In a longitudinal direction the boundary layer is divided into a region of growth, which ends at section x_t, and a «reset» region, at which thickness δ of the layer decreases from a maximum value of $\delta_m = \delta(x_t)$ to a value of $\delta_a = 0$ at the nozzle exit section. Therefore, the longitudinal profile of the nozzle and its boundary point x_t are the assigned values, while the sound point x_s is to be determined. In the problem considered in this article the situation is reverse: position of the sound point is taken from the experiments and profile of the boundary of the displacement region and, in particular, position of point x_t are to be calculated.

As the region of growth of the boundary layer is in the subsonic zone of the flow, then $x_t < x_s$ and dependence $\delta(x)$ is assumed to be as follows:

$$\delta/(x - x_b) = 4.6\mathrm{Re}_x^{-0.2}, \quad \mathrm{Re}_x = [\rho_\infty u_\infty \mu_\infty]\,(x - x_b), \tag{1}$$

which is valid for the required boundary layer with the incompressible air flow moving along the surface. Here ρ_∞, u_∞, and μ_∞ are, respectively, the density, velocity and viscosity of the outward flow, and all geometrical designation are given in Figure 1. Therefore, assuming that $\delta^* \approx 0.13\delta$, the expression for thickness of displacement of the boundary layer in the region of its growth is as follows:

$$\delta^* = C(x - x_b)^{0.8}, \quad x \le x_t, \tag{2}$$

where $C = 0.598(\mu_\infty \rho_\infty u_\infty)^{0.2}$. Therefrom we derive the x dependence of the cross section area of part of the flow which is beyond the region of displacement of the boundary layer:

$$A(x) = F\,[1 - 2\delta^*(x)/R], \quad x \le x_t, \tag{3}$$

where R is the radius of the cylindrical exit portion of the nozzle and $F = \pi R^2$. As the model is of an estimation character, in equation (1) for a specific pulse the use was made of its value at the sound point $(\rho_\infty u_\infty)_s$ and for viscosity the value of $\mu_\infty = 1.81\cdot10^{-5}$ Pa·s at 300 K was used.

For a region of decrease of the boundary layer we estimate thickness δ^* in a general form

$$\delta^* = \delta^*_m[1 - (x - x_t)/(x_a - x_t)]^\chi, \quad x \ge x_t, \ \chi > 1, \tag{4}$$

where x_t and χ are the parameters to be determined. As they are complementary, two experimental facts were taken from [1], which were established for ranges of variations in the operation conditions and nozzle geometry close to those under consideration: distance of the sound point from the exit section of the nozzle and Mach number of the flow at the exit section can be considered constant and equal to the following:

$$x_a - x_s \approx 0.8R, \quad \mathrm{M} \approx 1.3.$$

Cross section area $A(x)$ at $x > x_t$ is related to δ^* through the same equation (3) as at $x \le x_t$.

Allowing for the abovesaid, we obtain the system of equations for dimensionless values

$$\xi_t = x_t/x_s,$$

$$\chi = K_1(1 - \xi_t)/[K_2(\xi_t - K_3)^{0.8} - 1], \tag{5}$$

$$\chi = \ln\{1 - [1/K_2(\xi_t - K_3)^{0.8}]\}/[(1 - \xi_t)/(K_4 - \xi_t)].$$

Here $K_1 = [1 - \Theta_{ds}/A_s]/[n(\Theta_{ds}/A_s)(1 - A_s/F)]$ (index s marks values of the parameters at the sound point); $n = 10Gh_0/(\Theta_a/F)W_a x_s$; G is the plasma gas flow rate; h_0 is the enthalpy of its deceleration; W_a is the net power per unit length of the arc; $K_2 = 2Cx_s^{0.8}/R(1 - A_s/F)$; C is the constant taken from [1]; $K_3 = x_b/x_s$ and $K_4 = x_a/x_s$.

In addition to the aerodynamic force, equations of the two-dimensional dynamics of particles injected in a normal direction into the axisymmetrical flow make allowance also for the Saffman force [1], whose impact on the particles is directed along a radius of the flow to its axis. The aerodynamic drag factor is estimated using V.M. Pusyrev's formulae [2]

$$C_d = \begin{cases} C_{d0}/[1 - 0.00673\,\gamma^{0.5}(\mathrm{Re} - 24)\mathrm{M}C_{d0}], & \mathrm{Re} < 24, \\ C_{d0} + 0.00299\,(\mathrm{Re} - 24)\mathrm{M}, & 24 < \mathrm{Re} < 100, \\ C_{d0} + 0.00079\,(\mathrm{Re} + 187.6)\mathrm{M}, & \mathrm{Re} < 100, \end{cases}$$

where γ is the adiabatic exponent of the flow; $\mathrm{Re} = d_s v_r \rho/\mu$ is the Reynolds number of a particle with a diameter of d_s; $\mathrm{M} = v_r/a$ is the Mach number of a particle; v_r is the velocity of the plasma and a is the sound velocity.

The following diagram of the flow was assumed to hold at the exit cylindrical portion of the plasmatron channel. As the flow is unidimensional, its

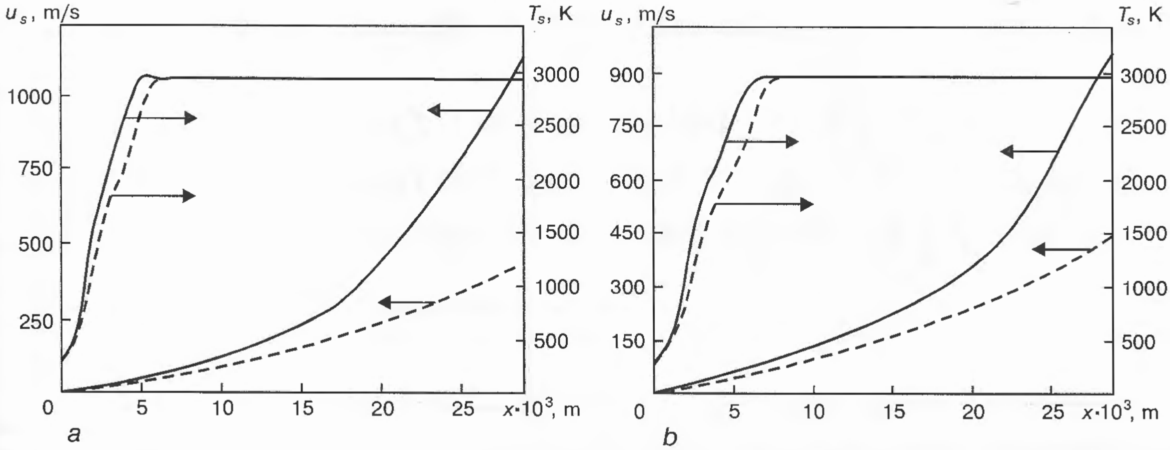

Figure 2. Distribution of velocities and temperatures along the flow of particles 20 μm (solid curve) and 30 μm (dash curve) in size at a plasma temperature of 12,000 (*a*) and 10,000 K (*b*)

enthalpy first grows in a linear way from a «cold» value of h_1 at the beginning of the entrance portion of the channel to a maximum value of h_s and then decreases also in a linear way to h_a at the nozzle exit section. The effect of pressure on thermodynamic and thermal-physical properties of the air plasma (parameters characterizing them were taken from Tables in [3]) was allowed for only for density ρ. The values of $P_1 = 405.3$ kPa and $h_1 = 4\cdot10^5$ J/kg were taken for pressure and enthalpy of the «cold» gas, and values of $4.65\cdot10^7$ and $6.18\cdot10^7$ J/kg at temperature T equal, respectively, to 10,000 and 12,000 K, [3] were taken for enthalpy h_s in a critical section. Pressure at the nozzle exit section and position of the critical values were taken from experimental data [1, 4]: $P_a = 0.3P_1$ and $x_s = L - 0.4d$, where d and L are the diameter and length of the exit portion of the channel, respectively, and x_s is the distance from its beginning to the critical section.

The rest of the parameters of the flow were calculated on the basis of the mathematical model that included two equations, i.e. continuity equation

$$\rho u = \text{const} \qquad (6)$$

and equation of pulses

$$P + \rho u^2 = \text{const}, \qquad (7)$$

which are valid for the flow in the cylindrical channel. In view of the estimation character of the model the equation of state was taken in its usual form

$$P = [(\gamma - 1)/\gamma]\rho h. \qquad (8)$$

For the adiabatic exponent the value of γ was assumed to be constant and equal to 1.3.

Expression for the velocity of the flow is derived from equations (6) through (8)

$$\bar{u} = \left(1 + \gamma \pm \sqrt{(1+\gamma)2 - 4\gamma\bar{h}}\right)\Big/2\gamma, \qquad (9)$$

where sign «+» corresponds to the supersonic region and sign «−» corresponds to the subsonic region. Here $\bar{u} = u/a$, where $\bar{h} = h/h_s$. Expression (6) also determines the density as $\bar{\rho} = 1/\bar{u}$, where $\bar{\rho} = \rho/\rho_s$. Movement of particles entering the flow was regarded as the unidimensional one with a longitudinal zero starting velocity.

Convective heat transfer between the flow and a particle was calculated from the Nusselt number [5]:

$$\text{Nu} = 2\lambda_{\text{surf}} + 0.6\text{Re}^{1/2}\text{Pr}^{1/3}(\rho\mu/\rho_{\text{surf}}\,\mu_{\text{surf}})^{0.2},$$

where λ and μ are the thermal conductivity and viscosity of gas, Pr is the Prandtl number and index «surf» indicates that values of the parameters were calculated at a temperature of the particle surface. In this case allowance was also made for the effect of evaporation of a particle on heat transfer.

The program of numerical calculation of movement and heating of particles in the plasma flow involved continuous calculation of the Weber number, We, for the molten particles. Upon reaching a critical value of We_c, splitting of such particles by the flow was calculated following the diagram given in [6].

The numerical studies were conducted for spherical iron particles (physical characteristics were taken from [7]) with a size of d_s = 30 μm, which entered the plasma flow at the beginning of the entrance portion of the channel with diameter d (3.4 and 5.0 mm) and length L equal to 10 gauge sizes. Results of the calculations for a channel of d = 3 mm are shown in Figures 2 – 4, where coordinate x is counted off from the beginning of the exit portion of the channel.

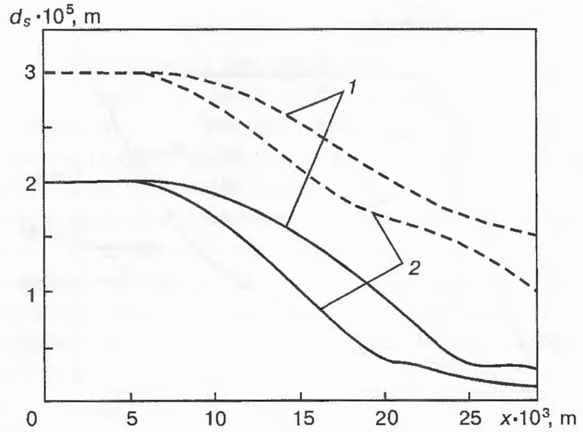

Figure 3. Variation in diameter of the iron particles along the flow at a plasma temperature of 10,000 (*1*) and 12,000 K (*2*)

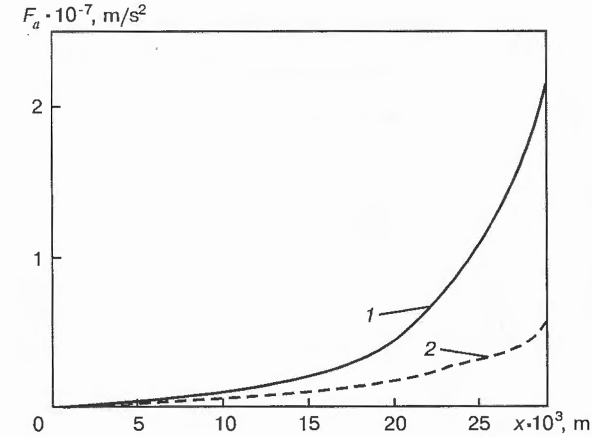

Figure 4. Distribution of accelerations along the flow of iron particles 20 (*1*) and 30 μm (*2*) in size

Analysis of the results obtained shows that heating and acceleration of particles injected into the plasmatron channel are of a gradual character. The particles are rapidly heated to the boiling temperature and, while moving in the acceleration region, fundamentally decrease in size (Figures 3 and 4), which is caused by an intensive evaporation of the material. In this case the relative decrease in number of finer particles is more intensive, i.e. the share of coarse particles in the powder increases. Corresponding changes in the particle size composition of the powder can be readily predicted, unlike the other mechanism which relates to splitting of the molten particles by the flow. However, with the diagram of heating and acceleration of the powder in the plasmatron channel under consideration, the latter does not show up because of low values of the Weber number (maximum values of We_{max} equal to about 1 – 2 are far from the critical ones).

Higher values of the final velocity of the particles, which for d_s = 20 μm is always in excess of that for particles with d_s = 30 μm, correspond to a higher temperature T and larger length L. Thus, at d = 3 mm and T = 10,000 K the final velocity d_{sa} is 698 m/s for particles with d_s = 20 μm and 300 m/s for particles with d_s = 30 μm. Accordingly, at d = 4 mm and T = 12,000 K, u_{sa} = 1100 and 438 m/s.

On the contrary, the rate of heating of the particles characterized by a relationship of x_{boil}/L, where x_{boil} is the coordinate of beginning of boiling of a particle, has just a slight dependence upon size d_s, temperature T (Figure 2) and channel diameter d.

CONCLUSIONS

1. In the case where the dispersed particles are injected into the region of the near-cathode expansion of the arc that burns in a blocked nozzle, intensive heating of these particles is accompanied by their gradual acceleration to a supersonic velocity. Therefore, unlike traditional methods, this method is an efficient means for heating and acceleration of the powder.

2. Gradual acceleration of molten particles prevents their splitting.

3. Velocity of the molten particles at exit from the arc plasma reaches 1000 m/s.

REFERENCES

1. Petrov, S.V., Karp, I.P. (1993) *Air-gas plasma spraying*. Kyiv: Naukova Dumka.
2. Stornin, L.E., Shraiber, A.A. (1994) *Multiphase flows of gas with particles*. Moscow: Mashinostroyeniye.
3. Engelsht, V.S., Gurovich, V.Ts., Desyatkov, G.A. *et al.* (1990) *Theory of the electric arc column*. Novosibirsk: Nauka.
4. Lukianov, G.A. (1985) *Supersonic plasma jets*. Leningrad: Mashinostroyeniye.
5. Donskoj, A.V., Klubnikin, V.S. (1979) *Electric plasma processes and units in machine building*. Leningrad: Mashinostroyeniye.
6. Nigmatulin, R.I. (1978) *Fundamentals of mechanics of heterogeneous media*. Moscow: Nauka.
7. Zinoviev, V.E. (1989) *Thermal-physical properties of metals at high temperatures*. Handbook. Moscow: Metallurgia.

INVESTIGATION OF AMPLITUDE-TIME CHARACTERISTICS OF THE CURRENT PULSE IN PLASMA-DETONATION TREATMENT OF ITEMS

Yu.S. BORISOV and **O.V. KOLISNICHENKO**
The E.O. Paton Electric Welding Institute, NASU, Kyiv, Ukraine

ABSTRACT

The results of the work on creation and development of plasma-detonation technology based on the detonation wave transformation into a plasma pulse, are described. The current discharge between the electrode of the plasma generator and the part being processed provides an integrated action of the convective, beam and electronic types of heat transfer on the surface. Brief comparative analysis of plasma detonation treatment and laser technology of strengthening the item surface is given.

Key words: *plasma-detonation treatment, laser strengthening, mechanism of surface heating, current pulse, amplitude-time characteristics, Rogowsky belt procedure, technological modes*

Treatment with high energy density sources (laser, electron beam, plasma, etc.) [1 – 3] is extensively used in mechanical engineering. It allows giving the material surface a high hardness, resistance to wear, corrosion, etc. Use of pulsed plasma technologies is one of the areas of surface engineering [4, 5]. Over the last years PWI has performed a series of studies on creation and development of the plasma-detonation technology based on transformation of the detonation wave into a plasma pulse [6, 7]. Application of the above technology for surface strengthening of a certain type of metal-working parts, demonstrated its practicability and cost-effectiveness [8]. The Table gives some technical and economic parameters of plasma-detonation and laser strengthening technology.

In order to produce modified layers with the specified properties, it is necessary to select the type of the heating source with the required specific heat flow, duration of its impact and other parameters, as well as evaluate the possibility of their regulation. The experience of pulsed laser strengthening (τ_p = 0.1 – 10.0 ms) shows that a rather narrow range of the pulse energy values, as well as of its duration, is used to achieve a positive effect in treatment of a number of materials [9]. This is especially important in treatment of items of high-speed and alloying steels. It is found that in pulsed laser quenching of high-speed steels the high hardness can be achieved, if the surface temperature does not exceed the melting temperature of the processed material, but is close to it. In this case the structure of the heated zone includes latent crystalline martensite, secondary and eutectoid carbides, while its microhardness is up to *HV* 1.0 – 10.5 GPa for P6M5 (C – 1; W – 6; Mo – 5 wt.%; Fe – balance) steel [10].

In pulsed plasma-detonation treatment (PDT), the mechanism of structure formation in the surface layers and their physicomechanical properties are close to those in laser treatment. This enables PDT to be used for treatment of the surface of items of various materials, proceeding from the experience of laser technology application. In keeping with [11], the mechanism of surface heating by pulses of shock-compressed plasma, can include both the convective and beam heat transfer, and heat conductivity. In this case one of the fundamental differences of PDT from laser treatment is the presence of a current discharge between the electrode of the plasma generator and the part being processed. In order to evaluate the influence of this component in pulsed treatment, it is necessary to determine the amplitude-time characteristics of the current pulse in PDT, which was exactly the aim of this study.

Plasma-detonation generator (Figure 1) consists of detonation chamber *1*, where the combustible gas mixture (C_3H_8, O_2, air) is formed and its combustion is initiated in the detonation mode; coaxial electrodes *2* and *3*; and power source *4*. When detonation is initiated, the partially ionised combustion products penetrate from the detonation chamber into inter-electrode gap *5* and close R–L–C loop (Figure 2) of the power source. This is followed by a discharge of a capacitor bank. The current runs between coaxial electrodes *2* and *3* through a certain conducting volume of gas *6*. An azimuthal magnetic field *B* (Figure 2) is induced

Technical-economical parameters of plasma-detonation and laser strengthening technologies

Parameters	*PDT*	*Laser strengthening with laser of «Kvant» or «Karat» type*
Treatment mode	Pulsed	Pulsed and continuous
Mechanism of heating the surface being strengthened	Integral impact of convective, beam and electronic mechanisms of heat transfer	Beam
Pulse duration, ms	0.2 – 1.0	0.1 – 10.0
Pulse repetition frequency, Hz	1 – 6	1 – 150
Pulse energy, J	Up to 3000	10 – 200
Area of the zone processed in one pulse, mm^2	60 – 200	0.6 – 10.0
Specific heat flow, W/cm^2	$1\cdot10^4 - 1\cdot10^6$	$1\cdot10^3 - 1\cdot10^7$
Consumed power, kW	27	20 – 100
Efficiency, %	65	6 – 10
Area taken up by the unit, m^2	12	25 – 30
Level of equipment complexity	Easy service	High qualification of servicing personnel is required
Ability of treating complex surfaces	Limited capability	Treatment of surfaces of any configuration

around the central electrode, which interacts with current I, running in the inter-electrode gap, and generates force F [12]

$$F = \frac{\mu_0}{4\pi} I^2 \ln\left(\frac{r}{r_0}\right),$$

where r, r_0 are the diameters of the external and internal coaxial electrodes, respectively.

The direction of this force action does not depend on the current direction, as B changes with the change of I sign. The current loop, consisting of the electrodes and the plasma gap, is trying to expand in a way, and increase its linear dimensions. The conductivity of the plasma through which current runs, is not infinite. Therefore, when electric current runs through it, Joule heat is evolved, a certain portion of which is entrained into the process of acceleration with expansion of the heated gas volume. With plasma pulse *7* interaction with the item surface, a shock-compressed plasma layer forms in the contact zone. The electric circuit between the central electrode and the surface of item *8* is closed (Figure 1). This results in heating of the material surface at the expense of the convective, beam and electronic mechanisms of heat transfer [11].

The PDT process is influenced by the number of pulses, their repetition rate, composition and consumption of combustion products, capacity of the capacitor bank, distance from the nozzle edge to the item, as well as the distance from the central electrode tip to the nozzle edge. In this connection, it is necessary to have precise concepts of the influence of the above parameters on the energy and duration of interaction of the plasma pulse with the surface of the item being processed. The data

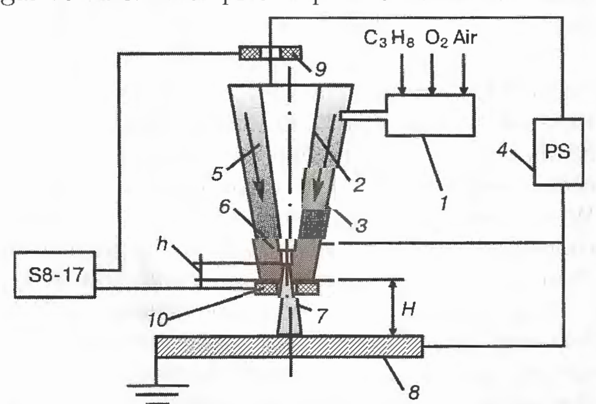

Figure 1. Diagram of a pulsed plasma generator (for nomenclature see the text)

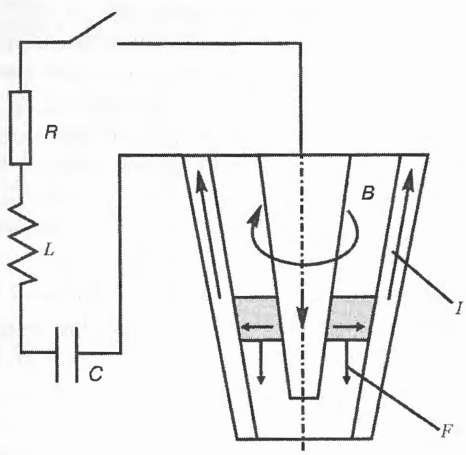

Figure 2. Diagram of plasma formation acceleration at the expense of the electromagnetic component

on the amplitude-time characteristics of current between the central electrode and the item will provide the required information.

Experimental studies of the parameters of plasma in pulsed electric gas-dynamic accelerators are important in view of the absence of reliable calculation procedures of the processes running in the type of devices under consideration.

The aim of this study consists in application of the Rogowsky belt procedure for determination of the duration of the impact of a plasma pulse on the item surface, its shape, as well as the degree of influence of the technological parameters on the amplitude-time characteristics of current and the heat flow $q \sim I$, respectively.

The methods of recording the integral parameters of the discharge and of the plasma flow generated by it are predominantly used now to measure the current, voltage of the discharge, pressure, and geometry of the plasmoid.

It is simpler to record the current in the discharge circuit with current transducers, shunts connected in series into the circuit. The currently available shunt designs and connection diagrams [12] are numerous, their application range being limited, however, by the thermal and mechanical conditions of operation. Water or gas cooling is used in a number of cases, especially in measurement of high currents (tens of kiloamperes). In this case conducting the experiment proper is made more complicated, and its accuracy also becomes worse. Therefore, inductive coils (Rogowsky belts) are often used to perform the measurements, in which the alternating magnetic field induces the voltage, proportional (depending on the design parameters of the measuring circuit), either to I, or to dI/dt [13].

Rogowky belt can be connected into the measuring circuit as the current transformer circuit or as an integrating circuit, the former being preferable. The measuring circuit of the Rogowsky belt used for $I(t)$ determination in the plasma-detonation generator is shown in Figure 3.

Equation [14] is valid for current in this circuit

$$\frac{di}{dt}L + (R_0 + Z_1 + Z_2)\,i = E_i, \qquad (1)$$

where i is the current in the measuring circuit; R_0 is the coil resistance; Z_1 is the sum of impedances of the measuring circuit and the ballast resistor (if included); Z_2 is the load impedance of the measuring circuit; L is the coil inductance; E_i is the induced voltage, equal to

$$E_i = \frac{d\Phi}{dt}; \qquad (2)$$

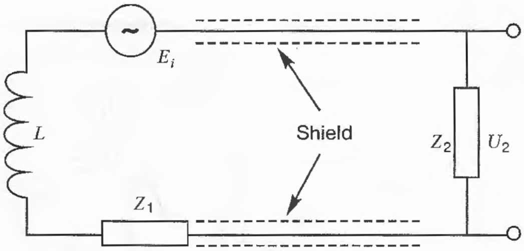

Figure 3. Diagram of measuring circuit of Rogowsky belt

Φ is the flux of the vector of magnetic induction B through the coil turns

$$\Phi = n\int_s B(r)dS = n\frac{h\mu_0 I}{2\pi}\ln\left(\frac{r_2}{r_1}\right); \qquad (3)$$

S is the turn area; n is the number of turns; r_1, r_2, h are the geometrical dimensions of the coil (Figure 4); I is the measured current; μ_0 is the magnetic constant equal to $4\pi\cdot10^{-7}$ H/m.

Taking into account expression (2) and that $U_2 = iZ_2$, let us rewrite equation (1) so that

$$\frac{d\Phi}{dt} = \frac{L}{Z_2}\frac{dU_2(t)}{dt} + \left(\frac{R_0 + Z_1}{Z_2} + 1\right)U_2(t),$$

where U_2 is the voltage read from the oscillograph, or in the integral form

$$\Phi(t) = \frac{L}{Z_2}U_2(t) + \left(\frac{R_0 + Z_1}{Z_2} + 1\right)\int_0^t U_2(t)dt.$$

Then, allowing for expression (3)

$$I(t) = \frac{2\pi\left(\frac{L}{Z_2}U_2(t) + \left(\frac{R_0 + Z_1}{Z_2} + 1\right)\int_0^t U_2(t)dt\right)}{hn\mu_0\ln\left(\frac{r_2}{r_1}\right)}. \qquad (4)$$

Thus, using equation (4), the nature of current distribution can be determined from the measured voltage on the load resistor U_2.

Measurements were taken using two identical coils with the following parameters: $n = 146$ turns; $h = 7\cdot10^{-3}$ m; $r_1 = 22\cdot10^{-3}$ m; $r_2 = 50\cdot10^{-3}$ m (Figure 4); $R_0 = 0.9$ Ohm. The calculated inductance of the coils is equal to

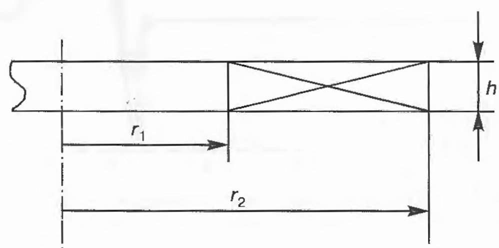

Figure 4. Geometrical dimensions of the coil

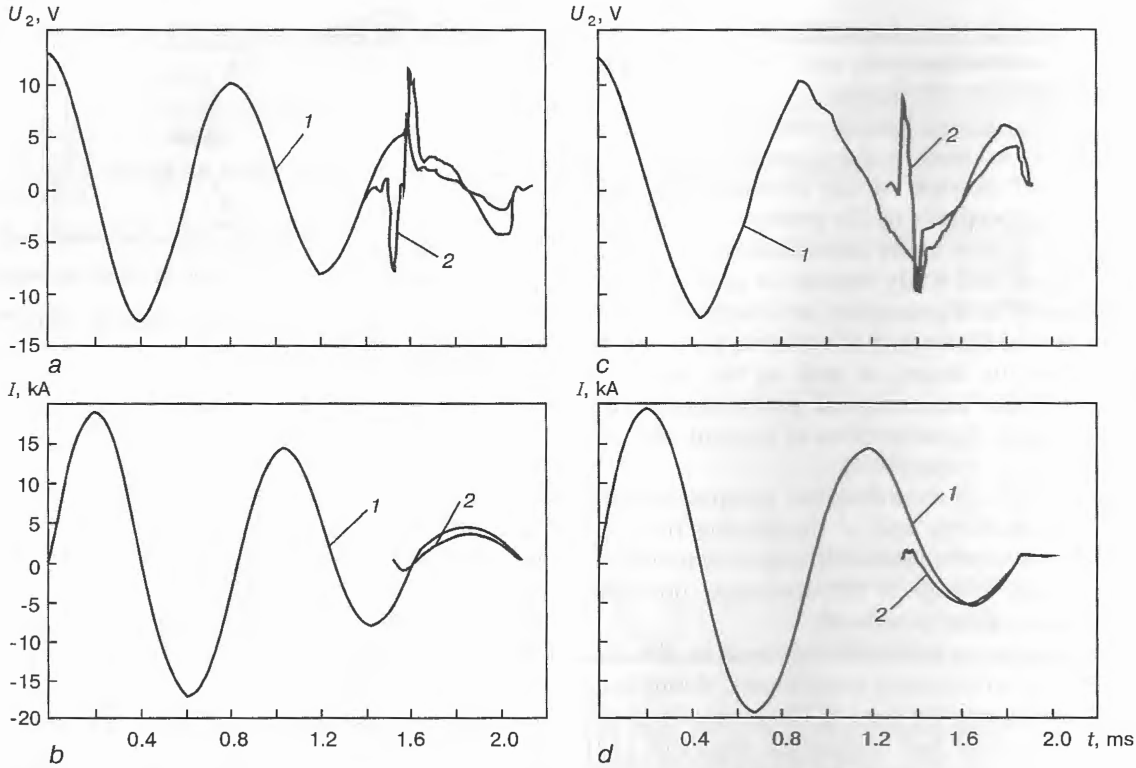

Figure 5. Curves taken from the oscillograph (*a, c*) and calculated curves (*b, d*) in the inter-electrode gap (*1*), as well as between central electrode and item (*2*)

$$L = 2 \cdot 10^{-7} n 2 h \ln \left(\frac{r_2}{r_1} \right) = 2.45 \cdot 10^{-5} \text{ H}.$$

The number and dimensions of the turns were selected so as to minimise the influence of electrical noise on the oscillograph readings.

Each coil is connected into the circuit separately (Figure 3) with $Z_2 = 96$ Ohm. In the measuring system of coils *9, 10* (Figure 1), $Z_1 = 52$ and $Z_2 = 0$ Ohm, respectively. The signals from the measuring systems come to the input of a double-beam memorising S8-17 oscillograph. With the discharge running between coaxial electrodes *2* and *3*, the signal comes to the oscillograph from coil *9*. When the circuit is closed, electric current runs between item *8* and central electrode *2*, which is recorded by the oscillograph through the measuring system of coil *10*.

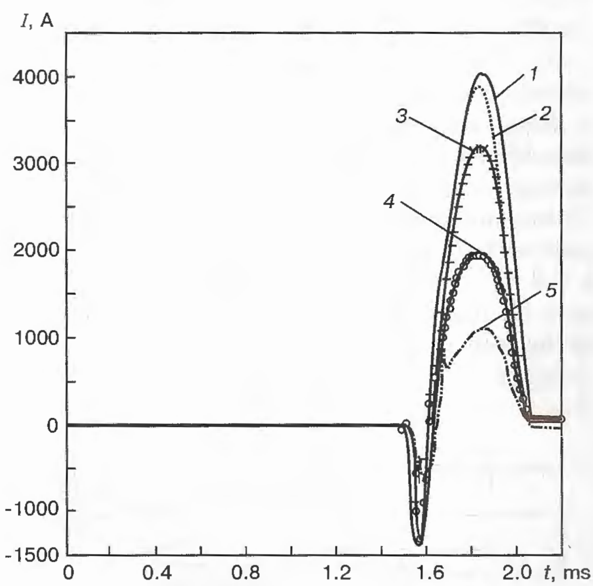

Figure 6. Influence of process parameters on the dynamics of current variation in time between central electrode and item: *1* — $h = 20$, $H = 40$; *2* — $h = 0$, $H = 70$; *3* — $h = 20$, $H = 70$; *4* — $h = 40$, $H = 70$; *5* — $h = 20$ mm, $H = 100$ mm; $C = 800$ μF

Having the oscillograph readings, equation (4) can be used to determine the current amplitude, pulse shape, as well as its duration.

Integration of the curves obtained in the oscillograph, using equation (4), was performed in the Mathcad-7 mathematical processor. The discharge circuit inductance did not change and was ≈ 20 μH. When operating in up to 10 Hz frequency range, the used capacitor batteries have enough time to be fully charged in the intervals between the pulses. Therefore, in operation at 2 Hz frequency the factor of its influence on the current pulse was not taken into account. Preliminary experiments showed that the change in the flow rate of C_3H_8 (0.24 – 0.48 m^3/h), O_2 plasma gases and air (1 – 2 m^3/h) influences the current, although much less than other factors. When measurements were taken, the values of capacity of the capacitor bank ($C = 600 - 1200$ μF), distance from the nozzle edge to the item ($H = 40 - 100$ mm) and distance from the central electrode tip to the nozzle edge ($h = 0 - 40$ mm) were varied. The gas flow rate did not change and was 0.35 (C_3H_8), 1.4 (O_2), 1.3 (air) m^3/h, respectively.

Figure 5, *a* gives the curves taken from the oscillograph at $C = 800$ μF, $h = 20$ mm, $H = 40$ mm and Figure 5, *c* — at $C = 1000$ μF, $h = 10$ mm, $H = 55$ mm. Figure 5, *b, d* shows the curves derived as a result of integration by equation (4).

Variation of the values of parameters H and h leads to change of the amplitude of current between the item and the central electrode (Figure 6), while capacity variation influences the frequency of the capacitor bank recharging. Figure 5, *b, d* shows the dependence of the bank capacity on the item polarity relative to the central electrode. Thus, treatment at $C = 800$ μF is preferable to that at $C = 1000$ μF, as in this case the item is the cathode relative to the central electrode. A greater intensity of the processes of alloying the surface layers with the plasma components can be also anticipated. In PDT of items the pulse duration can be regulated by varying in a broad range the bank capacity and the discharge circuit inductance. In the considered case $\tau_p \approx 0.5$ ms. The current amplitude in the item at $C = 1200$ μF can be up to 7 kA. The current density is equal to $J \approx \approx 11$ kA/cm^2 with 8 mm diameter of the matching spot of the current channel.

CONCLUSIONS

1. The current discharge between the plasma generator electrode and the part being treated is responsible for an integrated impact of the convective, beam and electronic mechanism of heat transfer on the surface. Despite the fundamental differences in surface heating at PDT and laser strengthening, the mechanisms of structure formation in the surface layers and their physicomechanical characteristics are similar. This enables PDT to be used for treatment of the surface of items of various materials, using the experience of laser quenching.

2. The procedure of measurement with Rogowsky belts was used to determine the influence of technological parameters on the dynamics of current variation in time between the coaxial electrodes, as well as between the central electrode and the item in PDT.

3. The extent of the influence of various technological parameters in PDT on the current amplitude in the item and on the heat flow $q \sim I$, respectively, was studied. The taken measurements showed that the current value is influenced by the capacity of the capacitor bank, distance from the nozzle edge to the item, distance from the central electrode tip to the nozzle edge, while the plasma gas flow rate does not have any significant influence on current.

4. The duration of the plasma pulse impact on the item surface in PDT was determined. With unchanged inductance it depends only on the capacity of the capacitor bank. The bank capacity influences the item polarity relative to the central electrode of the plasma generator. In order to improve the surface heating conditions, it is rational to conduct PDT, when the item is the cathode.

REFERENCES

1. Safonov, A.N. (1997) Main directions of effective use of laser equipment for heat treatment of alloys. *Metallofizika i Term. Obrabotka Metallov*, **7**, 2 – 6.
2. Leshchinsky, L.K., Samotugin, S.S., Pirch, I.I. (1990) *Plasma surface strengthening*. Kyiv: Tekhnika.
3. Gusev, O.A., Lazarenko, A.V., Ivanov, B.A. *et al.* (1984) Use of pulsed electron beam for heat treatment of metals. *Metallofizika i Term. Obrabotka Metallov*, **9**, 23 – 26.
4. Lebedev, V.K., Kaleko, D.M. (1998) Pulsed arc heat treatment of metal surface. *Ibid.*, **6**, 8 – 12.
5. Budkovskikh, E.A., Nazarova, N.N., Nosarev, P.S. (1994) Phase composition and microstructure of surface layers of iron, carburized by pulsed impact of heterogeneous plasma beams. *Izv. Vuzov, Chernaya Metallurgia*, **12**, 29 – 33.
6. Borisov, Yu.S., Tyurin, Yu.N. (1991) *Strengthening treatment of parts by high-energy plasma*. Kyiv: PWI.
7. Yushchenko, K.A., Borisov, Yu.S., Tyurin, Yu.N. (1994) Theory and practice of plasma-detonation modification of the surface of parts of machines and tools. *Svarochnoye Proizvodstvo*, **5**, 23 – 25.
8. Grigoriants, A.G., Safonov, A.N., Ivashov, G.P. *et al.* (1987) Investigation of pulsed laser quenching of stamping dies. *Kuzn.-Shtamp. Proizvodstvo*, **12**, 21 – 23.
9. Kovalenko, V.S., Golovko, L.F., Chernenko, V.S. (1990) *Strengthening and alloying of machine parts with the laser beam*. Kyiv: Tekhnika.
10. Sultanov, M.A. (1981) *Shock-compressed plasma in powerful pulsed discharges*. Dushanbe: Donish.
11. Lebedev, A.D., Uryukov, B.A. (1990) *Pulsed accelerators of high pressure plasma*. Novosibirsk: Nauka.
12. Andelfinger, K. (1971) Methods of investigation of fast processes in plasma physics. In: *Physics of fast processes in plasma physics*. Moscow: Mir.
13. Saveliev, I.V. (1989) *A course of physics*. Moscow: Nauka.

TECHNOLOGY OF RESTORATION AND STRENGTHENING OF SURFACES OF BODIES OF ROTATION AND FLAT SURFACES USING PLASMA SPRAYING

G.M. RUSEV, V.V. OVSYANIKOV, S.M. KISELYOV and **N.F. GALYUK**
NPF «Ornotof», Zaporozhje, Ukraine

ABSTRACT

Technology of plasma arc spraying with a feeding of a current-carrying wire sprayed and mechanical treatment of each layer of the multilayer coating using a rotating metallic brush. Examples of its application are given.

Key words: *plasma arc spraying, low-temperature plasma, wire materials, fine-dispersed particles, mechanical treatment*

The negative effect of the surfacing thermal cycle on the mechanical strength of the parent metal of the product is often one of causes of reducing the strength of round-section steel components whose surfaces are strengthened or restored using arc surfacing. In restoration of cast iron rolls by surfacing their fatigue strength can be decreased by 30 – 70 %.

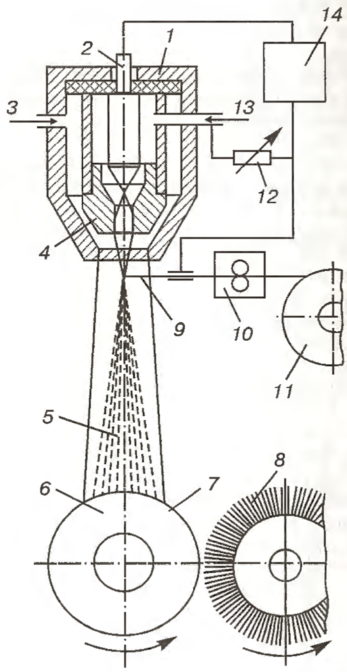

Figure 1. Schematic diagram of plasma arc spraying of coatings from wire materials: *1* — plasmatron; *2* — cathode; *3* — compressed air; *4* — plasma shaping nozzle; *5* — flow of particles of material sprayed; *6* — workpiece; *7* — coating; *8* — rotating metallic brush; *9* — wire sprayed; *10* — feeding mechanism; *11* — cassette with wire; *12* — ballast resistance; *13* — plasma gas; *14* — power source

The suggested technology is based on spraying of the standard wire by a low-temperature plasma, formation and transfer of the high-speed flow of fine-dispersed particles of the sprayed material in a molten (liquid) state on the component being treated and formation of the layer of coating on the component surface.

The process of spraying does not reduce the strength properties of the products restored, because the temperature of the product during spraying does not exceed 250 °C, therefore, there are no residual deformation in the product.

The principle of the described technology of the plasma spraying (development of the E.O. Paton Electric Welding Institute) consists in the fact that the current-carrying wire sprayed is fed to a working edge of the plasmatron nozzle which forms a plasma-arc discharge. The spraying is performed by layers of 0.05 – 0.10 mm thickness with a simultaneous treatment of each next layer using a special rotating metallic brush (Figure 1). The specific consumptions of electric energy for spraying of 1 kg of initial material are decreased by 30 – 45 % as compared with a plasma spraying with powder materials and, therefore, the cost of the final product is also reduced. In addition, it is possible to spray coatings of 15 – 20 mm thickness without a danger of their spontaneous damage or separation.

The treatment of the layer with the metallic brush during its formation, and also the reduction of the flow of particles of the material sprayed by an external concentrated jet of the compressed gas provided a noticeable increase in strength of the coatings due to interaction of the melted particles of the spraying material with a material of the base

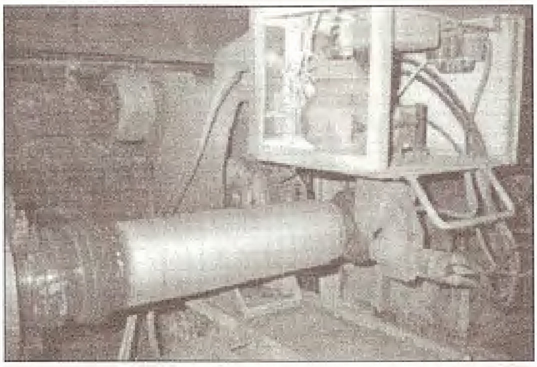

Figure 2. Plasma arc spraying of steel shaft

and layer-by-layer relaxation of stresses in thin intermediate layers of the multilayer coating. Thus, the continuous mechanical treatment of the surface layer of the base metal, combined in time with the process of spraying, provides favourable conditions for spraying coatings of almost unlimited thickness. In addition, it is possible to extend time of the technological break between the operations of a shot-blasting treatment of the workpiece surface and spraying to up to 3 – 5 days without a risk of decrease in strength of joining the particles of the material sprayed to the base material.

The rupture strength of the coating (tests according to pin method) is 40 – 55 MPa. The density of the coating produced by spraying of wires made from steel 65G (C — 0.6; Mn — 1.0 wt.%) is 93 – 96 % of the theoretical density of the initial material, while the density of wire 04Kh20N11MZDT (C — 0.04; Cr — 20.0; Ni — 11.0; Mo — 3.0; Cu — 3.0; Ti — 0.6 wt.%) is 98 %, the porosity of coatings is 1 – 4 %.

The introduction of an additional gas flow will decrease the power loading of the plasmatron, increase the stability and efficiency of the process and, in combination with the mechanical treatment of the forming layer of the coating, provide a high degree of the reproducibility of the coating characteristics.

The selection of the optimum density of the current in the material sprayed (current-carrying wire) depends in each definite case on the physical properties of the initial material used (temperature of melting, electrical conductivity) and other factors determined by the conditions of the process and parameters of the plasma arc device.

Unlike the traditional methods of coating the spraying is performed on steel and cast iron bases (Figure 2) without using additional technological procedures (for example, preheating of the product, deposition of a sublayer of thermoreactive material, etc.) used for increasing the strength of joining the coating material to the base metal.

The process possesses a high stability. The service life of the nozzle, which forms a plasma jet, and the plasmatron cathode (before resharpening) is not less than 100 h of the machine time. The typical parameters of the UN-126 installation used in plasma spraying are given below:

operating current of plasmatron, A	100 – 300
operating voltage, V	50 – 70
power of plasmatron, kV·A	25
consumption of plasma gas, m^3/h	0.5 – 1.3
pressure of plasma gas, Pa	1.0 – 2.5
cooling of plasmatron	air
consumption of cooling air, m^3/h	16 – 20
pressure of cooling air, Pa	4 – 6
diameter of wire sprayed, mm	0.8 – 3.0

In this case the productivity of the process is 2 – 10 kg/h.

The present technology makes it possible to spray coatings on metal products using any wire, including flux-cored wire and wire of non-ferrous metals and their alloys; multilayer coatings of different materials, including anticorrosion coatings; metallic coatings on non-metallic products (plastics, concrete, brick, graphite, etc.); composite coatings by a simultaneous spraying of several wires of different composition; coatings on inner surfaces of bodies of rotation of diameters of above 200 mm.

The shape-forming surfaces of press-forms can also be produced using the above-described technology.

This technology was implemented successfully at several car-repair enterprises of Russia and Ukraine.

In collaboration with Zaporozhje Abrasive Plant an experimental work was carried out on spraying the lateral surface of the graphitized electrodes of 300 mm diameter with aluminium to protect it from oxidizing during melting (Figure 3). From the preliminary data of eleven melts the mass-saving of electrodes was 25 – 30 %.

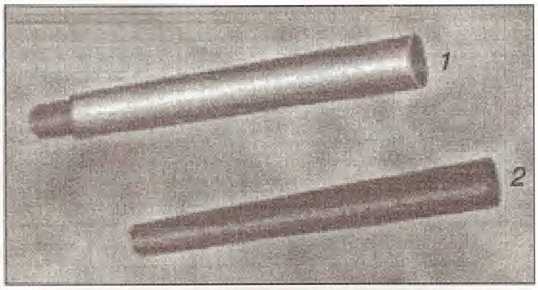

Figure 3. Appearance of graphite electrodes with coatings (*1*) and without them (*2*)

Transition contacts of copper–aluminium and aluminium–copper busbars of current-conductors of melting furnaces were sprayed for the pilot production of UkrNIIspetsstal in Zaporozhje city. As compared with the earlier used copper–aluminium and aluminium–copper welded joints the heating of contacts was reduced and their service life was increased. The application of spraying of contacts could simplify the design of busbars and decrease their cost.

MICROPLASMA SPRAYING OF BIOCERAMIC COATINGS

Yu.S. BORISOV[1], S.G. VOJNAROVICH[1], V.G. BOBRIK[1], V.A. DUBOK[2] and N.V. ULIANCHICH[2]
[1]The E.O. Paton Electric Welding Institute, NASU, Kyiv, Ukraine
[2]Closed Joint Stock Company «KERGAP», Kyiv, Ukraine

ABSTRACT

Peculiarities and characteristics of the method of microplasma spraying allowing a reduction of up to 5 – 15 % in powder losses in spraying on small objects are given. The process of production and properties of microplasma coatings of bioactive ceramics, i.e. hydroxyapatite (HA) are investigated. Phase and structural transformations occurring in the HA particles during their heating in a microplasma jet and conditions of formation of the coatings are studied. The feasibility of spraying HA coatings with a low degree of dissociation and amorphization is shown.

Key words: *microplasma spraying, hydroxyapatite, process parameters, spraying spot, phase composition, investigations*

One of the intensively progressing areas of the thermal spraying technology is application of bioceramic coatings. These coatings can be subdivided into bio-inert and bio-active ones. The bio-inert coatings include, for example, coatings of aluminium or zirconium oxides. Among the bio-active coatings the widest acceptance has been gained by coatings of HA ($Ca_5(PO_4)_3OH$), which are almost identical in their chemical composition to human bones.

Metallic implants with coatings of HA are characterized not only by high biological activity but also by high mechanical properties of the metal base. The coatings of HA on metallic implants lead to an increase in the rate of formation of bone tissues, provide the possibility of formation of a bond with a bone (osteointegration) and decrease the probability of formation of the corrosion products on metal base of the implants.

The plasma method of spraying of bioceramic coatings is the key method employed for commercial manufacture of implants with coatings. However, intensive heating of the HA particles in the plasma jet and their rapid cooling on the substrate surface lead to the probability of formation of an amorphous phase in the coating structure, which is characterized by an increased rate of dissolution (resorption) in a human organism. In addition, overheating of the HA particles in the plasma jet can cause partial dehydration of HA to form oxyhydroapatite or oxyapatite, as well as phase transformation of HA into tricalcium phosphate (TCP) or tetracalcium phosphate or even toxic calcium oxide (CaO). These phases have a decreased resorption resistance, as compared with stoichiometric HA, which leads to changes during the osteintegration process.

Therefore, the process of plasma spraying of HA leads to formation of a coating which actually consists of several phases and whose bio-active properties depend upon its composition. Several research works have been conducted in the last years on application of bioceramic coatings by different spraying methods: traditional plasma spraying in the atmosphere [1 – 9], plasma spraying in a dynamic vacuum [9, 10], high-frequency plasma spraying [11] and high-velocity oxygen spraying [6, 9, 12]. However, the drawback of all these technologies is that during the spraying process a substantial part of the bioceramic powder is lost, which is especially essential in spraying on surfaces of small objects, such as dental endoprostheses. The main cause of such losses is related to a comparatively large size of the spraying spot (15 – 25 mm). These losses can be fundamentally reduced using the microplasma spraying technology [13 – 15].

The task of this investigation was to study conditions of formation of a bioceramic coating in microplasma spraying of the HA powder and determine the possibility of controlling the phase composition of the coating by varying the spraying process parameters.

Microplasma spraying machine. The microplasma spraying machine MPN-003 consists of a power supply with a control panel, plasmatron and a special device for powder feeding. Design and parameters of operation of the plasmatron provide formation of a laminar plasma jet (Reynolds crite-

Table 1. Comparison of microplasma and traditional plasma spraying parameters

Parameter	*Microplasma spraying*	*Traditional plasma spraying*
Power, kW	0.5 – 3.0	25 – 40
Gas flow rate, l/min	0.1 – 0.5	30 – 40
Productivity, kg/h	0.25 – 2.50	3 – 6
Spraying spot size, mm	1 – 5	12 – 30
Noise level, dB	30 – 50	100 – 130
Specific power consumption, (kW·h)/kg	0.8 – 1.5	8 – 10
Velocity of particles, m/s	15 – 60	100 – 150

rion is 0.10 – 0.55). This factor is responsible for a number of peculiarities of the microplasma spraying process:

as the angle of opening of the laminar plasma jet is only 2 – 6° (instead of 10 – 18° for turbulent plasma jets) and diameter of the nozzle is small (1 – 2 mm or less), the size of the spraying spot is 1 – 5 mm;

low thermal power of the microplasma spraying jet allows heating of the substrate to be decreased, which makes it possible to apply coatings to items of small sizes and with thin walls by avoiding a substantial local overheating and buckling;

noise level in spraying with the laminar plasma jet is no more than 30 – 50 dB.

Specifications of the MPN-003 machine are given below:

working gas .... argon
transporting gas .... argon or air
shielding gas .... argon
power, kW .... up to 3.0
current, A .... 10 – 50
voltage, V .... up to 60
gas flow rate, l/min:
working gas .... 0.10 – 0.50
shielding gas .... 1.0 – 4.0
productivity, kg/h .... 0.25 – 2.50
material utilization factor .... 0.6 – 0.8
dimensions, mm .... 265×560×800
weight, kg 50

Comparison of characteristics of the processes of microplasma and traditional plasma spraying is given in Table 1.

The MPN-003 machine was used for spraying narrow-strip coatings [15]. The important component of the machine is a unit for feeding the powder into the plasma jet. It is intended for ensuring a precise feed of the powder (along the jet axis), small diameter of the powder jet, controllability and consistency of the powder feed.

Different types of powder feeders for microplasma spraying were made and tested during the experiments. It was established that in the case of using powders with good flow characteristics (10 ÷ ÷ 30 s/50 g) the powder could be fed using no transporting gas. With powder materials having lower flowability, such as HA, the feeding system uses a transporting gas which is ejected into the atmosphere before the powder is introduced into the plasma jet.

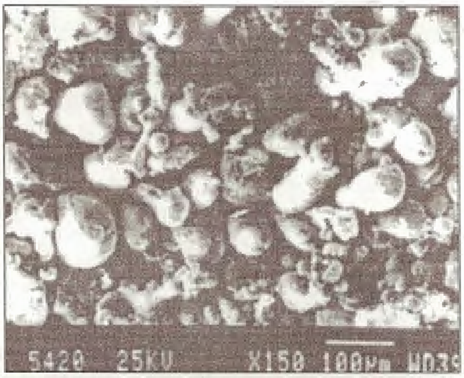

Figure 1. Appearance of the HA powder particles

Spraying material. The HA powder used for microplasma spraying was produced by two-stage synthesis of HA from aqueous solutions of calcium nitrate and ammonium hydrophosphate, drying of the sediment, its grinding, pelletization and sintering of the pellets. This technology provides powder with good flow characteristics and dense particles. The technology for production of the HA powder was developed by the KERGAP Company (also it made experimental batches of the powder which were used in this work).

Apparent density of the HA particles was 3.15 g/cm^3 and flowability was 70 ÷ 80 s/50 g (for particles less than 80 μm in size). Chemical composition and properties of this powder are in compliance with ASTM F1185–88. Appearance of the HA powder particles is shown in Figure 1.

The α-TCP phase $Ca_3(PO_4)_2$ content of the powder is less than 5 wt.%. Results of X-ray phase analysis of the initial HA powder are shown in Figure 2. The HA powder particles used for microplasma spraying were 40 – 63 and 100 – 125 μm in size.

Investigation of the spraying spot in microplasma spraying of HA. A series of experiments the design of which is given in Table 2 were carried out to evaluate the effect of the microplasma spraying parameters on size of the spraying spot.

Spraying was conducted on one spot with the plasmatron in a fixed position. After that the vertical and horizontal axes of the spraying spot, as well as maximum height of the sprayed hill were measured. It was established as a result of statistical analysis of characteristics of the sprayed hill profiles that the latter could be described by the Gaussian function $y = y_0 e^{-kx^2}$. For hills no more than

Table 2. Effect of the microplasma spraying parameters on size of the spraying spot

Sample No.	*Spraying process parameters*			*Spraying spot size, mm*			*Sprayed hill height h_0, mm*
	I, A	*Distance h, mm*	*Size of powder particles, μm*	*Vertical axis b_1*	*Horizontal axis b_2*	b_1/b_2	
1	30	60	100 – 125	6	4.0	1.50	0.8
2	50	60	100 – 125	10	8.0	1.25	6.0
3	30	120	100 – 125	5	3.5	1.43	0.1
4	50	120	100 – 125	11	7.0	1.57	3.0
5	50	60	40 – 63	11	8.0	1.37	6.5
6	30	60	40 – 63	10	7.0	1.43	6.0
7	30	120	40 – 63	10	8.0	1.25	2.0
8	50	120	40 – 63	12	8.0	1.50	7.0
9	40	90	40 – 63	10	6.0	1.67	2.5
10	40	120	40 – 63	10	7.5	1.33	1.5

Note: U = 40 – 43 V, working and shielding gas – argon, working gas flow rate – 0.2 l/min, shielding gas flow rate – 2.8 l/min, nozzle diameter – 1 mm, spraying time – 20 s, substrate – titanium alloy VT-6.

0.8 mm high k = 0.5 – 0.6, and for high hills (3 – 7 mm) k = 0.15 – 0.20. It means that at a diameter of the spraying spot equal to about 3 mm, in the case of relatively thin coatings of the HA powder (0.5 mm and less) the losses of the spraying material caused by a geometrical factor are 5 – 15 %. Appearance of the hills of the HA coatings sprayed for 15, 10 and 5 s is shown in Figure 3.

Structure and phase composition of the microplasma HA coatings. Parameters of microplasma spraying of the HA powder on a titanium substrate and results of X-ray phase analysis of the resulting coatings are given in Table 3 and shown in Figure 2, and microstructure of these coatings is shown in Figure 4. It follows from these figures that structure of the coatings is relatively dense, having no visible boundaries between lamellae and layers inside the coatings. Porosity of the coatings produced from coarse particles (100 – 125 μm) is somewhat higher than in spraying powder with a particle size of 40 – 63 μm. These coatings have similar X-ray patterns. In many cases the main phase is $Ca_5(PO_4)_3OH$ (HA). In addition to HA, the phases detected were α–$Ca_3(PO_4)_2$ and β–$Ca_3(PO_4)_2$. The α-TCP phase was detected only in sample No.9, and the α-TCP content of sample No.10 was lower than of sample No.9, which is associated with a decrease in amperage from 50 to 40 A and, accordingly, with a decrease in the intensity of heating of the HA particles. Another factor that affects the α-TCP content is the spraying distance the increase in which from 70 to 90 mm leads to a decrease in the α-TCP content of the coating. The presence of a small halo in regions 2θ equal to 23 – 27 and 44 – 54° is indicative of a slight amorphization of the coating material.

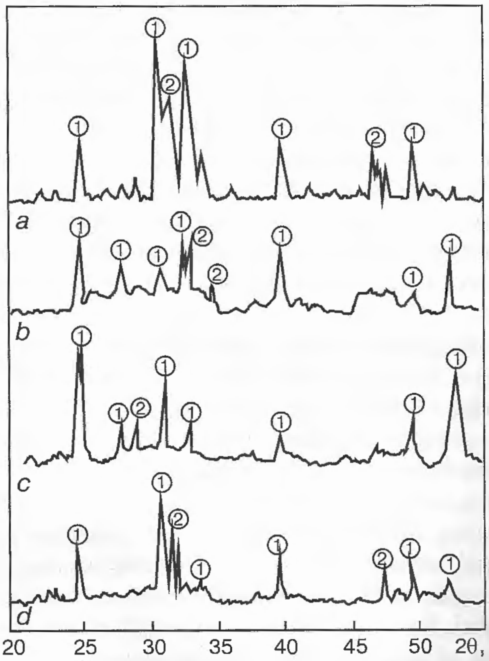

Figure 2. X-ray phase analysis of the HA powder (*a*) and microplasma HA coatings on samples No.9 (*b*), 10 (*c*) and 15 (*d*): *1* – HA; *2* – α-TCP; *3* – β-TCP

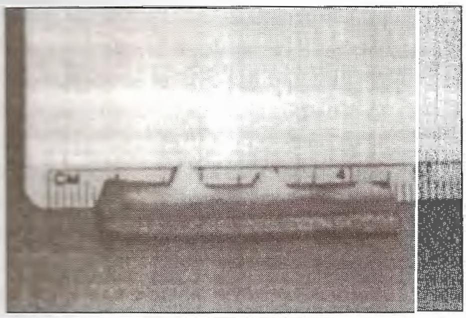

Figure 3. Appearance of the hills sprayed for 15, 10 and 5 s (*from left to right*)

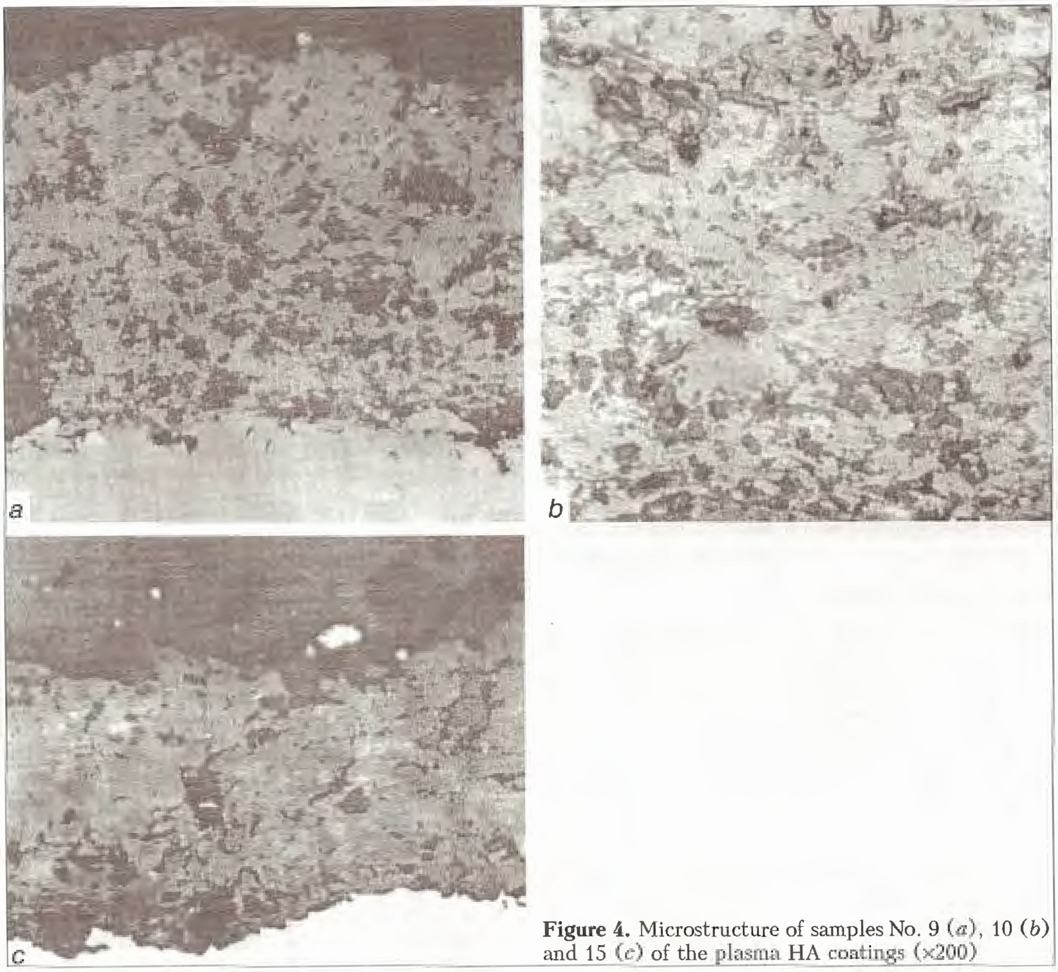

Figure 4. Microstructure of samples No. 9 (*a*), 10 (*b*) and 15 (*c*) of the plasma HA coatings (×200)

The effect of the plasma spraying parameters on structure and properties of the HA coatings was discussed by many investigators [3 – 6, 9, 10]. The most detailed analysis was conducted by Yang, Wang, Chang and Wu [4], who paid attention to the effect of a composition of the working gas on phase composition of the bioceramic coatings produced by spraying HA. They suggest that the heat content of the plasma jet is a key factor. However, it is associated only with a possibility of heating a HA particle to a melting point and higher. The limiting factor is a heat flow to the surface of the particle, which is determined by a temperature and thermal conductivity of the plasma jet. Addition of hydrogen and helium to argon leads to an increase in thermal conductivity of the plasma and enhancement of heating of the particles. This results in an increase in the value of the Biot criterion for ceramic materials (for oxides sprayed by the argon plasma $Bi = 0.04 - 0.10$ and for the hydrogen plasma $Bi = 1.2 - 3.5$). It means that difference in temperatures on the surface and in the centre of the particles increases. In this case the probability exists of substantial overheating of the upper layer of a particle, which leads to dissociation of HA. As to overcooling of particles on the substrate,

Table 3. Microplasma spraying parameters and results of investigation of structure of the coatings

Sample No.	*Size of powder particles, μm*	*Microplasma spraying parameters*			*Phase composition*
		I, A	*U, V*	*h, mm*	
9	40 – 63	50	43	90	HA, α-TCP, β-TCP, amorphous
10	40 – 63	40	42	90	HA, α-TCP, amorphous
15	100 – 125	50	44	70	Same

which can lead to amorphization of structure, temperature of the particle is just one of many factors. Velocity of the particle, which determines thickness of lamellae, and a number of other factors are of a higher importance [16].

Based on the above analysis, one should note the following peculiarities of microplasma spraying, which can affect composition of the coating produced by spraying of the HA powder:

- working gas is pure argon;
- powder particles are introduced to the plasma jet ahead of the anode spot (microplasmatron has an externally mounted anode);
- velocity of the oxide particles is 20 – 25 m/s (instead of 100 – 150 m/s with traditional plasmatrons);
- ratio of the plasmatron power to the working gas (argon) flow rate is 5 – 20 (instead of 0.5 – 1.0 with traditional plasmatrons).

It means that heating of the particles occurs under conditions of the plasma jet with a low thermal conductivity (argon), high temperatures of the plasma jet and a longer time during which the particles dwell in the heating zone. In this connection, it can be suggested that particles in their cross section have a smaller temperature difference, their upper layer has a lower degree of overheating and, as a result, this part of the particle material (HA) has a lower degree of dissociation. A lower velocity of the particles leads to a lower probability of amorphization of the material.

Therefore, the use of microplasma spraying offers the possibility of controlling a composition of the bioceramic coating produced by spraying HA and achieving the optimal ratio of its components in terms of bioactivity.

CONCLUSIONS

1. Microplasma spraying occurs under conditions of a laminar plasma jet and is characterized by a small size of the spraying spot (1 – 5 mm), low power of the plasmatron (1.0 – 2.5 kW) and low noise level (30 – 50 dB).

2. In microplasma spraying of HA the spraying spot has an elliptical shape with a ratio of axes equal to 1.25 – 1.70. The profile of the sprayed hills is described by the Gaussian function. For coatings with thickness of 0.8 mm the k factor is 0.5 – 0.6. In the case of the spraying spot about 3 mm in size, losses of the HA powder in application of coatings to small objects, e.g. dental endoprostheses, are 5 – 15 %, which is caused by a geometrical factor.

3. Structure of the microplasma bioceramic coatings consists of HA, α- and β-tricalcium phosphate and an amorphous phase. The ratio of components depends upon the process parameters, size of the particles, amperage and spraying distance.

4. Peculiarities of microplasma spraying of bioceramic coatings based on HA are associated with use of pure argon as the working gas, low velocity of the particles and a high ratio of the plasmatron power to the working gas flow rate, which reduces the probability of dissociation of HA and formation of the amorphous phase in the sprayed coating.

REFERENCES

1. de Groot, K., Geesink, R., Klein, C. *et al.* (1987) Plasma sprayed coatings of hydroxyapatite. *J. of Biomedical Materials Res.*, **21**, 1375 – 1381.
2. Kay, J.F. (1993) Plasma sprayed hydroxyapatite coatings for enhanced biocompatibility. *Materials Technology*, **8**, 26 – 29.
3. Cheang, P., Khor, K.A. (1995) Bioceramic powder and coatings by thermal spray techniques. In: *Proc. of Int. Thermal Spray Conf.*, Kobe.
4. Yang, C.Y., Wang, B.C., Chang, E. *et al.* (1995) The influence of plasma spraying parameters on the characteristics of hydroxyapatite coatings: a qualitative study. *J. of Materials Sci.: Materials in Medicine*, **6**, 249 – 257.
5. McPherson, R., Gane, N., Bastow, T.J. (1995) Structural characterisation of plasma-sprayed hydroxyapatite coatings. *Ibid.*, 327 – 334.
6. Khor, K.A., Cheang, P., Wang, Y. (1997) The thermal spray processing of HA powders and coatings. *JOM*, **2**, 51 – 57.
7. Khor, K.A., Cheang, P., Wang, Y. (1998) Plasma spraying of combustion flame spheroidized hydroxyapatite (HA) powder. *J. of Thermal Spray Technology*, **7**, 254 – 260.
8. Wang, Y., Khor, K.A., Cheang, P. (1998) Thermal spraying of functionally graded calcium phosphate coatings for biomedical implants. *Ibid.*, **7**, 50 – 57.
9. Brown, S.R., Turner, I.G. (1998) Acoustic emission analysis of thermal sprayed hydroxyapatite coatings examined under four point bend loading. *Surface Eng.*, **14**, 309 – 313.
10. Heimann, R.B., Vu, T.A. (1997) Low-pressure plasma sprayed (LPPS) bioceramic coatings with improved adhesion strength and resorption resistance. *J. of Thermal Spray Technology*, **6**, 145 – 149.
11. Bouyer, E., Gitzhofer, F., Boulos, M.I. (1997) The suspension plasma spraying of bioceramics by induction plasma. *JOM*, **2**, 58 – 62.
12. Wolke, J.G., de Groot, K., Kraak, T.G. *et al.* (1991) The characterization of hydroxyapatite coatings sprayed with VPS, APS and DJ systems. In: *Proc. of Nat. Thermal Spray Conf.*, Pittsburgh.
13. Yushchenko, K., Borisov, Yu., Pereverzev, Yu. *et al.* (1995) Microplasma spraying. In: *Proc of the Int. Thermal Spray Conf.*, Kobe.
14. Yushchenko, K., Borisov, Yu., Pereverzev, Yu. *et al.* (1998) Microplasma spraying. In: *Proc. of the Int. Thermal Spray Conf.*, Nice.
15. Borisov, Yu.S., Pereverzev, Yu.N., Vojnarovich, S.G. *et al.* (1999) Deposition of narrow-strip coatings by the microplasma spraying method. *Avtomaticheskaya Svarka*, **6**, 53 – 55.
16. Borisov, Yu., Korzhyk, V. (1989) Amorphous thermal spray coatings: theory and experimental data. In: *Proc. of the Int. Thermal Spray Conf.*, London.

PRODUCING OF COMBINED COMPONENTS WITH PERMANENT JOINTS USING PLASMA ARC REMELTING OF CHARGE

Yu.V. LATASH[1], **V.N. KOLEDA**[1], **G.F. TORKHOV**[1], **A.V. LIKHOBABA**[1], **V.P. SERGEEV**[2] and **G.F. GORBACHEV**[2]
[1]The E.O. Paton Electric Welding Institute, NASU, Kyiv, Ukraine
[2]Research Laboratory of Basalt Fibers, I.N. Frantsevich Institute for Materials Science Problems, Kyiv, NASU, Ukraine

ABSTRACT

Technology of producing combined components with permanent joints for the feeders of a basalt casting is developed. This technology makes it possible to use the wrought high-chromium alloys with higher operating characteristics. Plasma arc remelting of charge using a cold hearth is used for producing slab billets with a simultaneous melting-in of technological parts into it. The absence of welds and high quality of the remelted metal can increase the serviceability of the components.

Key words: *combined components, feeders, plasma arc remelting, heat-resistant alloy, permanent joints*

Combined components consisting of dissimilar metals and alloys are used often in structures, as in many cases they can decrease the consumption of expensive materials, simplify technology of manufacture and improve the operating characteristics of the products.

At present, welding, surfacing and casting are used mainly for producing the combined or bimetal components with permanent joints [1 – 5]. However, these methods do not always produce components of the required quality due to presence of welds and transition layers, whose properties are differed usually from the parent metal, and also due to the formation of pores, cracks, slag inclusions, shrinkage cavities, etc.

At the E.O. Paton Electric Welding Institute the technology has been developed for producing billets for combined components using the method of a successive plasma-arc cold hearth remelting of charge with a simultaneous melting-in of technological parts into it. This technology can be used for manufacture of products made from bimetal and similar materials, including those of an intricate shape. This technology makes it possible to use the metallic waste both as charge materials and also as technological inserts. In addition, the assortment of metals and alloys used can be widened significantly, especially when they are hard-to-deform or possess a poor weldability. Melting of billets of radiators from the waste of aluminium plates and also bimetal billets of cutting and agricultural tools, teeth of excavators, etc. may serve as examples of using this technology.

One of the most challenging trends of application of this technology is the manufacture of combined heat-resistant feeders of a basalt casting. Strict requirements are specified to these products both as to the working characteristics of used heat-resistant alloys, and also as to the defects. The feeders are operating in the range of 1250 – 1350 °C temperatures at a simultaneous contact with an air and liquid basalt that requires the use of alloys with a higher heat resistance. Moreover, the preheating of products is performed by 3000 – 3500 A current, therefore, the presence of even negligible defects can lead to their fracture.

All-cast or welded feeders, used at present, do not always provide the required quality due to difficulties in their manufacture, formation of casting or welding defects and limited assortment of the heat-resistant alloys.

To manufacture feeders by using plasma arc remelting, a copper water-cooled mould was designed and manufactured, which was mounted on a mobile carriage of existing installation OB-1957 (developed at the PWI). The installation consists of a melting chamber, inside of which a mobile carriage and groups of plasmatrons over it are located. The A-1458 type transformer in a set with A-1557 type rectifying unit were used to supply the plasmatrons PD-110.

Figure 1 gives a schematic diagram of the equipment and process of producing a feeder which represents a flat working plate (later, the grooves are made in it) with brazed-in fastening plates and current collectors. First, the current collectors *2* and fastening plates *3*, made from 10Kh18N9T (AISI 304) stainless steel, are placed to a copper

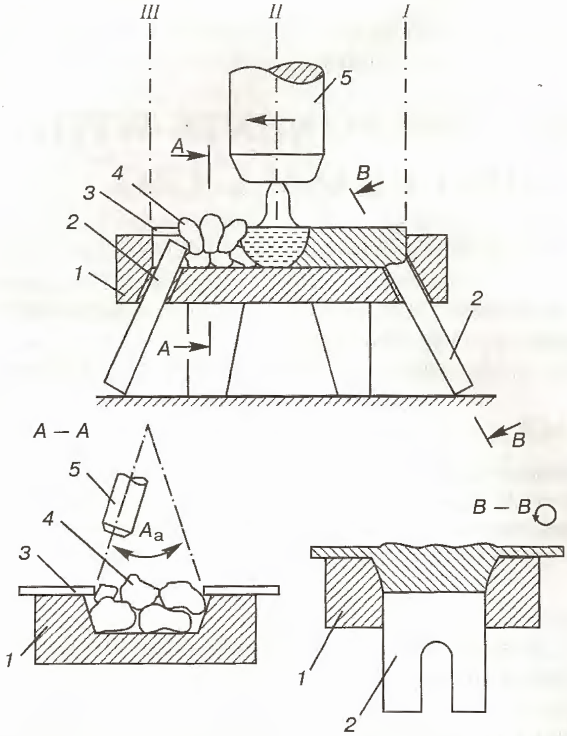

Figure 1. Schematic diagram of producing combined feeder using the method of plasma arc remelting (see designations in text)

mould *1* and then a layer of heat-resistant charge *4* is poured. Then, the carriage with the mould is mounted under a plasmatron *5*, the evacuated chamber is filled with argon and the charge is melted by transverse oscillations of the plasmatron arc. Amplitude A_a is selected in such a way that to provide a necessary width of the feeder working plate.

At the beginning of the process in one of extreme positions of the plasmatron, for example, *I* (Figure 1), a molten pool over the entire width of the charge layer is set and subjected to holding during

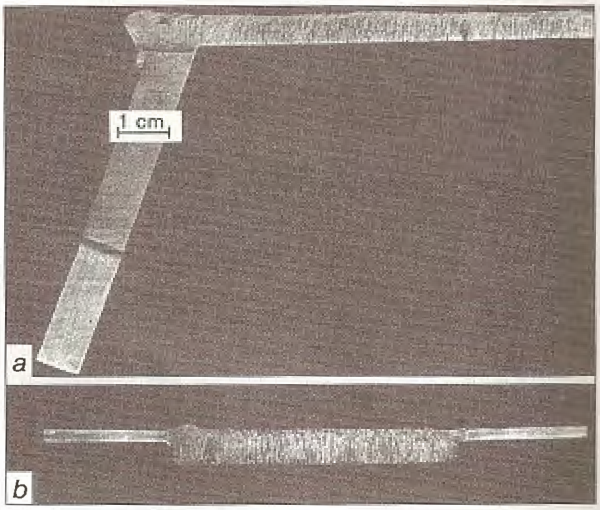

Figure 2. Macrosections of heat-resistant plate with melted-in current collector (*a*) and fastening plates (*b*)

several minutes, then it is moved to the opposite edge (*III*) until a complete melting of the charge. In addition, a partial melting of fastening plates and current collectors projecting from under the mould occurs. After solidification, all these parts are melted-in monolithically to the heat-resistant metal billet, as is shown in Figure 1, view *B–B*.

From the side of a copper mould the billet has a smooth surface and does not almost need additional treatment. Its top part is subjected to gouging up to a preset thickness to provide a uniform section of the heat-resistant plate over the entire length. The resulting feeder (Figure 2) has a high serviceability due to absence of defects in the form of lack of penetration, slag inclusions, pores, cracks, etc.

The described method of producing feeders does not require additional deformation of the melted billets, as it can control the orientation of crystals of alloys and their size depending on the chemical composition of the metal and technological factors of melting. This widens significantly the assortment of used alloys (most heat-resistant alloys are difficult-to-deform). Here, as compared with cast feeders, an expensive material is saved, as the current collectors and fasteners are made of a cheaper metal, but more suitable for this purpose.

Within the scope of investigations a work on optimizing the chemical composition of the heat-resistant alloy was carried out. The preliminary investigations of standard heat-resistant steels and alloys recommended for heat-resistant feeders [6 – 9] showed that Fe–Cr alloy with up to 35 % Cr possesses higher characteristics both as to the scale resistance and also to the resistance in the zone of contact with a liquid basalt.

The mentioned alloy was selected as a basis for the further investigation of effect of content of active alloying elements in the alloy on the angle of wetting of samples with a liquid basalt that characterizes the high creep resistance of the feeders.

Samples of heat-resistant alloys with 35 % Cr and additional alloying with Al, Zn, Ti and Si within 1 – 5 % were melted in a copper water-cooled mould with hollows using the above-mentioned installation OB-1957. The charge of a preset composition was poured into the hollows and melted by the plasma arc. Before melting the chamber was evacuated and filled with a shielding gas. The melting was performed at the following conditions: arc current I_a = 500 A; arc voltage U_a = = 40 V; speed of carriage movement at plasma arc location over the hollow v = 7 mm/min, at movement from hollow to hollow v = 40 mm/min. The samples after mechanical treatment were tested at

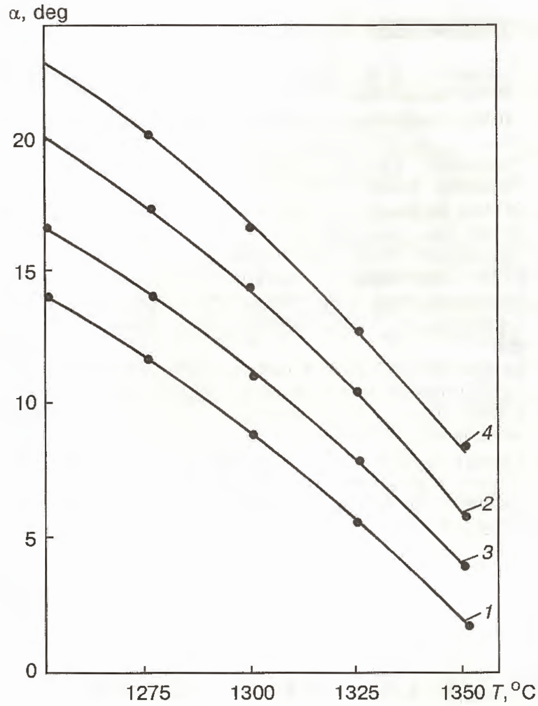

Figure 3. Dependence of angle of wetting of Fe–Cr alloys (Fe — base, Cr — 35 %) with a basalt on the content of the following elements, wt.%: Si — 3 (*1*); Al — 5 (*2*); Si and Al by 1 (*3*) and by 3 (*4*)

the I.N. Frantsevich Institute for Materials Science Problems.

To measure the angle of wetting of the heat-resistant alloy with a liquid basalt, a basalt tablet was placed on a clean surface of the sample and then the sample was heated in a laboratory furnace up to 1250 – 1350 °C temperature. Each 25 °C the wetting angle of the samples, soaked at test temperature for 30 min, was measured. As is seen from Figure 3, with an increase in test temperature the decrease in the angle of wetting of the alloy surface with a liquid basalt was observed in all the samples.

The investigations showed that the content of aluminium and silicon has a main effect on the angle of wetting of samples with a liquid basalt. Moreover, the aluminium has a greater influence on this parameter than silicon. In addition, the optimum composition of the heat-resistant alloy was obtained at a combined alloying with these elements. It contains, wt.%: Cr — 35 – 37; Al — 3 – 5; Si — 3 – 4.

To perform full-scale tests, a batch of combined heat-resistant feeders of a basalt casting was produced. A heat-resistant alloy of the above-given Fe-based optimum composition served a material of their working zone. Current collectors and fastening plates, which were melted-in into the billet, were made from stainless steel of 10Kh18N9T grade. During melting, the optimum conditions,

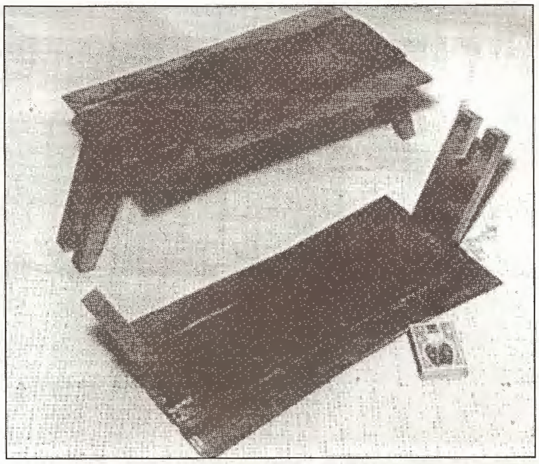

Figure 4. Appearance of feeder billet with melted-in current collector and fastening plates

selected earlier, were used to produce the quality billet with permanent joints: I_a = 800 – 850 A, U_a = 40 – 45 V, v = 7.0 – 7.5 mm/min, the arc oscillation amplitude was A_a = 40 mm.

To select the optimum design, the geometric sizes of the components of the feeders in billets were varied. The defects in permanent joints were not observed. After mechanical treatment the samples were transferred to the Research Laboratory of Basalt Fibres for the joint full-scale tests.

The full-scale tests of the produced feeders were performed in gas furnace for the basalt melting. A jet of a liquid basalt, coming from a feeder, was expanded with a compressed air to produce fine staple basalt fibres [8]. Electrical heating was made from transformer TVK-75. Here, the operating temperature of the feeder was 1250 – 1350 °C, and the time of setting this temperature for a feeder was 1 h. During heating the temperature of feeders and basalt jet, time before fracture, place of fracture and also behaviour of the basalt jet were recorded.

On the basis of tests the following geometric parameters of the feeders were selected (Figure 4):

working zone, mm:
- length 300
- width 55
- thickness 10

thickness of current conductors, mm:
- not less than 17

The life of these feeders in the range of 1250 – 1350 °C is about 20 days, while that of welded and cast feeders does not exceed 15 days.

The described technology of manufacture of heat-resistant feeders can be used also for producing other combined products with permanent joints, especially in case of application of non-wrought alloys with a poor weldability.

CONCLUSIONS

1. Technology of producing combined components with permanent joints using the method of a successive plasma arc cold hearth remelting of charge with a simultaneous melting-in of technological parts into the billet produced has been developed.

2. As a result of investigation of the effect of chemical composition of the heat-resistant alloys on an angle of wetting of their surfaces with a liquid basalt an optimum composition of the former was selected, including, wt.%: Cr — 35 – 37; Al — 3 – 5; Si — 3 – 4 and Fe — base.

3. Full-scale tests of a batch of combined feeders manufactured using the developed technology showed that their life is about 20 days, while that of welded and cast feeders does not exceed 15 days.

REFERENCES

1. Sentyakov, B.A., Timofeev, L.V., Shankhroziev, F.F. (1995) *Basalt fiber*. Izhevsk.
2. (1985) *Surfacing. Experience and efficiency of application*. Ed. by P.V. Gladky. Kyiv: PWI.
3. Chalabaev, Kh.Ch., Melikov, V.V. (1984) *Wide-layer surfacing*. Tashkent: Uzbekistan.
4. (1986) *Surfacing in manufacture of components of machines and equipment*. Ed. by P.V. Gladky. Kyiv: PWI.
5. Gorpenyuk, N.A., Gorpenyuk, B.N., Gorpenyuk, V.N. (1991) Surfacing of cutting tools with tungsten-free high-speed steel. *Svarochnoye Proizvodstvo*, **3**, 28 – 29.
6. Gudreman, E. (1964) *Special steels*. Moscow: Metallurgia.
7. Goldshtein, M.M., Grachev, S.V., Veksler, Yu.G. (1985) *Special steels*. Moscow: Metallurgia.
8. (1989) *Basalt fibrous materials*. Ed. by G.M. Matveev. Moscow: VNIIESM.
9. Gavrilyuk, V.P. (1975) Investigation and development of cast high-chromium alloys for operation in tin melt. *Author's abstract of thesis for degree of Cand. of Sci. (Eng)*. Kyiv: IMF AN UkrSSR.

PLASMA ARC TORCH WITH AN OXIDE CATHODE

V.I. LAKOMSKY
The E.O. Paton Electric Welding Institute, NASU, Kyiv, Ukraine

ABSTRACT

The application of a powder oxide cathode instead of a rod tungsten cathode in metallurgical plasmatrons (arctrons) is considered. This simplifies design significantly and increases the efficiency factor of the heating process. The arc discharge of the arctron is characterized by a well-formed plasma «flame» of the cylindrical shape and rising volt-ampere characteristic.

Key words: *electrical arc, arc plasmatrons, plasmatron nozzle, oxide cathode, arctron, design*

The present state-of-the-art of the plasma technology allows accomplishment of more than dozens of technological operations using the plasmatrons. First of all those operations should be noted, which refer to the metal processing, namely melting, welding, preparatory and machine-building cutting, heating and melting of surface, surfacing, etc. In all these cases the transferred arc-type plasmatrons are used, or plasmatrons with a remote-control arc, where the workpiece to be treated is a positive electrode of the electrical arc, if it concerns the DC plasmatrons. This makes it possible to increase the heat efficiency factor of the arc device.

Plasmatrons, which are usually used for the accomplishment of the above-mentioned operations represent themselves a classical design of a rod type. Here, a rod electrode, manufactured as a rule from alloyed tungsten and a water-cooled nozzle are arranged coaxially. A column of the electric arc is constricted with the help of the latter to increase the temperature of the plasma gas and a shaping of the gas plasma flow. To have a reliable operation of the nozzle, it should be cooled intensively by a running water. However, it «carries out» of up to 25 % of the plasmatron power [1], that decreases the heat efficiency factor of this device as a converter of the electrical energy into heat energy.

The losses are high for cooling a nozzle in plasmatrons for the metal cutting. There were attempts to make the nozzle diameter as small as possible to increase the productivity of the plasma cutting and to improve the cutting surface quality. But, as is shown in [2] such procedure on increasing the temperature of the gas plasma cannot be limitless. The plasmatron nozzle diameter d_n is associated functionally with electrical current of the arc I_a. Value 140 can be recognized as maximum (limited) ratio of I_a / d_n (in amperes per millimeter). Its exceeding leads to the nozzle burning-out.

In general, the nozzle, the same as a cathode, can be considered as worn-out parts of the plasmatron that, unfortunately, leads to the increase in the service expenses for the fulfilment of the technological operations.

Unlike the plasmatrons for cutting of metals, the nozzle in metallurgical plasma generators and also in fuel-arc torches [3] constricts not a column of the electric arc in principle, but a flow of the plasma gas inside of which an arc discharge is burning. In the above-mentioned gas-heating devices the geometric axes of the arc column and cylindrically-shaped flow of the plasma gas are coincided to stabilize the burning of the arc discharge, to heat effectively the plasma gas and to decrease the heat flow which enters the nozzle from hot gases.

In metallurgical plasmatrons the nozzle diameter, as a rule, exceeds that of the rod cathode and the hot end of the latter is introduced usually into the nozzle channel. At the 6 – 10 mm diameter of the tungsten electrode the nozzle diameter is 8 – 12 mm, and the cathode deepening to the nozzle channel is several millimeters. Sometimes, the cathode hot end is led out to the nozzle edge. Naturally, in these cases the lower heat is consumed in the nozzle of the metallurgical plasmatron than in plasma cutting of metals in spite of higher values of the electric arc current. In this connection the service life of the nozzle of the metallurgical plasmatron is increased and the linear rate of the gas plasma flow is decreased. Its «flame» has a less dynamic action on the metal melt, does not deform it, thus spreading smoothly over the metal pool mirror.

So, in the rod-type plasmatrons, not depending on their purpose, the nozzle plays a role of the device for shaping the gas plasma flow coming from the nozzle. Moreover, this aim is attained by the action of both the cold wall of the nozzle and also the cold gas flow on the arc column.

As was proved [4], this effect can also be attained not using the nozzle, but a powder oxide cathode which was developed as long ago as 1987. This cathode represents a copper water-cooled holder, whose blind hole has a pressed-in active powdered insert. This insert consists of powders of metals (zirconium or hafnium), chemical compounds or alloys with elements of II A subgroup of the periodic system of elements and technological additions. The blind hole diameter and, respectively, the diameter of the active insert (d_i) is rather high, i.e. from 3 to 5 mm.

The first switching-on of the arc with a powder cathode should be made in oxygen-containing gas atmosphere. Here, the active insert is oxidized. An oxide emission film is formed at its surface which serves further as a liquid emitter of the cathode electron current. Further, the oxide cathode can be used in burning of the electric arc both in air and also in any inert gas.

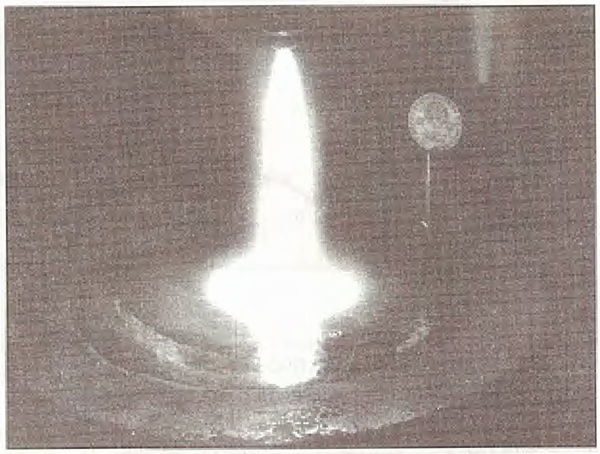

Figure 1. Electroarc discharge with a powder oxide cathode at I_a = 500 A, d_i = 5 mm, l_a = 140 mm; *in the right* the USSR metal rouble of 31 mm diameter is given for comparison

Figure 1 shows an appearance of the electric-arc discharge in air between the oxide powder cathode and a copper anode having a form of a mirror of copper, melted by the same discharge in a large water-cooled crucible. The discharge shape, which is not typical of a freely burning arc, attracts attention. In spite of a large interelectrode gap (140 mm) it is cylindrical, the same as in the plasmatron with a low degree of the arc constriction. Only near the cathode the arc column is constricted slightly, while near the anode it is widened. It was noted [5] that the diameter of the arc column depends on the diameter of the active insert, i.e. with the increase in the latter it increases. From a rough estimation their ratio, depending on arc current, is equal to 2 – 3.

The high self-stabilizing of the arc discharge observed is surprising. To provide the arc length $l_a \geq 150$ mm, neither nozzle, stabilizing gas flow, nor external longitudinal magnetic field are required. It was noted that the effect of self-stabilizing of long arcs is clearly expressed coming from I_a = 300 – 325 A. Evidently, this is due to a pinch-effect. Moreover, the arc burning is noiseless that confirms the high stability of processes in its near-cathode and near-anode regions.

The burning of the arc discharge with a powder oxide cathode at a vertical location of the cathode over a horizontal anode occurs under the conditions of intensive flows of hot gases from the cathode to the anode, so-called cathode blow, whose linear rate can reach 10^2 m/s [6], and opposite rising convective, comparatively slower flows of the cold gas moving at the periphery of the arc column. The latter are heated, coming in contact first with a surface of the hot anode and then with flows of the cathode blow along the flow direction.

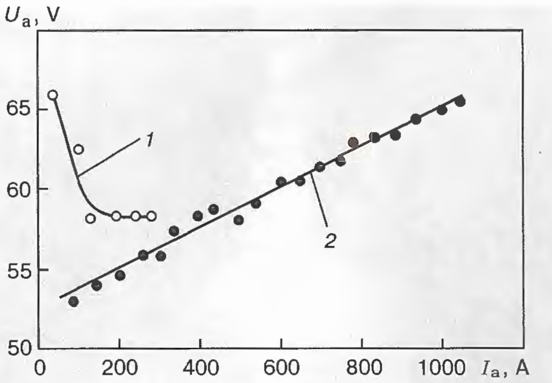

Figure 2. Static VAC of freely burning arcs with an oxide cathode (air): *1* — compact zirconium cathode, l_a = 40 mm, d_i = 3 mm [1]; *2* — powdered cathode, l_a = 50 mm, d_i = 5 mm

The above-described arc is characterized by a low gradient of the electrical voltage in the column. When burning in air it does not exceed 7 V/cm that is by a half of order or order lower than that in the arc column of the rod electrodes with coatings. There is no doubts, that this phenomenon is explained by a presence of easily-ionizing alkali-earth elements in the arc column, which enter the arc atmosphere from an emission film.

The most important feature of the arc with a powder oxide cathode is its rising volt-ampere characteristic (VAC). Under the conditions of arc burning in air the derivative of voltage by current is $1.25 \cdot 10^{-2}$ V/A. As is known, none of the burning arcs with non-consumable electrodes possesses the rising VAC. The same arc with an oxide cathode, but with an insert from a compact zirconium, has a falling characteristic, as a tungsten arc in argon (Figure 2). The arc with a powder oxide cathode has the same VAC at low arc currents (to 100 A) [5].

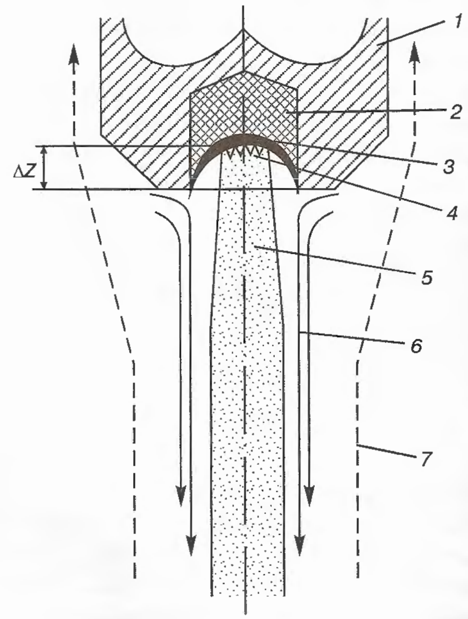

Figure 3. Scheme of oxide powder cathode: *1* — copper water-cooled holder; *2* — active insert; *3* — liquid emission film; *4* — cathode spot; *5* — arc column; *6* — jets of falling cathode blowing; *7* — jets of rising convective flow of air

Figure 2, which presents VAC of the arc with a compact zirconium and powder oxide cathode can confirm a low gradient of the electrical voltage in the arc column with a powder oxide cathode. This is also testified by a comparison of voltages at two arcs using similar current, for example, 200 A. At the first arc of 40 mm length the voltage is 58 V, while at the second arc of 50 mm length it is 55 V.

The powder oxide cathodes are peculiar by their heat efficiency factor which depends on their service life. At the beginning of the new cathode operation, when the deepening of the cathode spot ΔZ (Figure 3) is equal to zero, the efficiency factor is highest and reaches 95 %, while at the end of the service life when the deepening increases to 4.5 mm it is decreased to 85 %.

A small amount of energy of the arc discharge is scattered at the emission film of the powder oxide cathode. Extrapolation of the diagram of dependence of the power scattered at the cathode on deepening (Figure 4) to value $\Delta Z = 0$ shows that voltaic equivalent at the cathode is only 2 V.

The depth of pressing-in of the powdered active insert is 5 mm, and its mass at diameter d_i = 5 mm is 0.5 g. The service life of the cathode is determined as a quotient of division of this mass into a rate of the cathode corrosion. The latter is $2 \cdot 10^{-8}$ g/C for air conditions at 650 A current under the stationary conditions. Such low rate of corrosion is observed only in unalloyed tungsten cathode in argon. At lower current and in argon it will be even lower for the oxide cathode.

The long-time experience of use of oxide cathodes during welding of metal with carbon materials in the air showed that under these conditions the erosion rate is increased. Evidently, this occurs due to evolution of the carbon vapours of the highly-heated anode to the arc atmosphere,

The distribution of a heat flow from the plasma flow and arc column in the heated metal-anode is

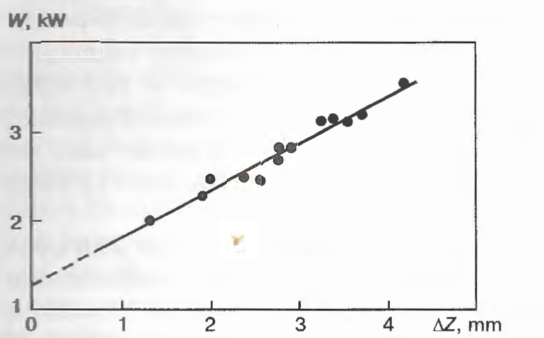

Figure 4. Dependence of arc power dissipating on a powder oxide cathode on cathode spot deepening (I_a = 650 A, U_a = = 40 V, air)

Technical characteristics of dimensional series of arctrons

Characteristics of arctrons	*D-1*	*D-2*	*D-3*	*D-4*
Operating current, A	20 – 120	120 – 350	250 – 600	250 – 750
Pressure of cooling water, MPa	0.2	0.3	0.3	0.3
Consumption of cooling water, m^3/h	0.05	0.30	0.60	0.60
Consumption of argon (if necessary), m^3/h	0.2 – 0.3	0.6 – 0.8	0.6 – 0.8	–
Service life of cathode, h	8 – 10	4 – 8	4 – 6	4 – 6

also unusual. In the powder oxide cathode the diameter of the cathode spot is rather large. i.e. 1.3 – 1.8 mm at d_i = 4 mm and I_a = 450 – 750 A, and, respectively, 1.8 – 2.5 mm at d_i = 5 mm and I_a = = 450 – 850 A. As the coefficient of concentration of the electron flow to the anode is low (from $8.4\cdot10^{-3}$ to $16\cdot10^{-3}$ mm^{-2}), then the diameter of the anode spot reaches high values, i.e. 27 – 39 mm. This makes the above-described arc suitable, as compared with other arc heat sources, for surfacing works and surface heating of the metal components. If also to add that during the heat transfer from the arc with powder oxide cathode 75 % of heat is transferred to the anode by a convective heat transfer, then it will become clear how the arc considered can be a «soft» heat source. Such a high share of convective transfer to the anode is observed only in metallurgical plasmatrons, but they require the argon supply for operation, while in our case it is sufficient to fill the chamber once with a gas and the arc heater with a powder oxide cathode will provide the conditions of heating which are similar to those of the metallurgical plasmatron.

The arc with a powder oxide cathode is also differed from other arc heat sources by a maximum density of the heat flow to the anode observed in the center of the heating spot. It is usually 22 – 24 W/mm^2 and does not exceed 40 W/mm^2 at most intensive conditions of the arc operation. It means that during metal heating by such arc the molten metal in the center of the heat spot is not overheated greatly and does not cause the selective evaporation of low-boiling alloying elements of alloys and corresponding changing in the chemical composition. By the level of density of the heat flow to the anode the arc with a powder oxide cathode is between the tungsten arc in argon and acetylene-oxygen flame.

The powder oxide cathodes became the basis for the designing the machine and manual arc torches. The latest found the widest spread and

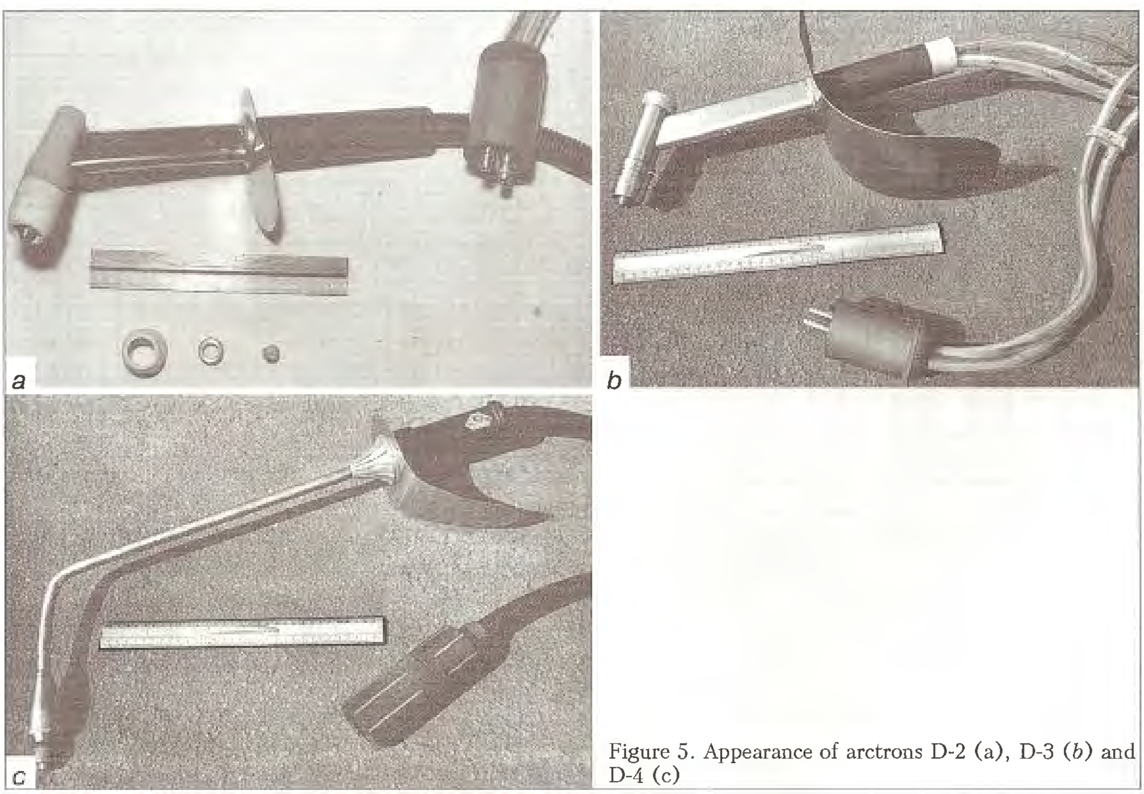

Figure 5. Appearance of arctrons D-2 (a), D-3 (*b*) and D-4 (c)

were named arctrons. A dimensional series of these torches was developed (Table).

The arctron D-1 is recommended for welding thin-sheet structures from low-alloyed and stainless steels, cladding of wear-resistant alloys in repair of expensive cutting tools. Due to a negligible dilution of the wear-resistant alloy with a parent metal, the required properties can be produced even in the first layer.

The arctron D-2 (Figure 5, *a*) is designed for surfacing and welding jobs, but its highest effect is pronounced in argon-arc treatment of the boundaries of the welds of butt and fillet joints. It can be used instead of argon-arc torches with a tungsten electrodes. The application of this arctron makes it possible to obtain the smooth transition from weld to the parent metal without manipulation of a torch. The productivity of the welder's labour is increased, as there is no need for him to spend time for the tungsten electrode sharpening.

The arctron D-3 (Figure 5, *b*) is used for melting out of a cavitation-damaged metal of hydroturbine blades during their repair instead of using the air-arc cutter with a carbon electrode. Moreover, it is possible to avoid the carburization of the metal treated, to eliminate the next cleaning of the cutting zone with manual grinders and to improve the sanitary-hygienic conditions of labour at the work site. This arctron is also used for compacting the scrap of noble metals, thus reducing drastically the technological cycle of producing the high-quality ingot and decreasing the unreturnable losses of the noble metals.

The arctron-4 (Figure 5, *c*) is the universal arc heater of current-conducting materials. It is used for a preliminary or auxiliary heating in copper welding, in surface heat treatment and separating cutting of metal components. This arctron found its widest spread for welding of different carbon materials with metals in air to produce welded multiamperage contacts in units of the non-ferrous electrometallurgy that made them well-known in such countries, as Australia, Great Britain, Italy, the USA and Israel.

All the types of the arctrons are supplied from serially-produced rectifiers with a falling or steeply falling characteristics.

REFERENCES

1. Esibyan, E.M. (1971) *Plasma arc equipment*. Kyiv: Tekhnika.
2. Bykhovsky, D.G. (1972) *Plasma cutting*. Leningrad: Mashinostroyeniye.
3. Karp, I.N. (1977) Development and investigation of fuel-arc torches. In: *Fuel-plasma torches*. Kyiv: Naukova Dumka.
4. Paton, B.E., Lakomsky, V.I., Kovalevsky, E.V. (1988) Electroarc heat source with cathodes of the new type. *Avtomaticheskaya Svarka*, **2**, 43 – 46.
5. Lakomsky, V.I. (1997) *Oxide cathodes of electric arc*. Zaporozhje: Internal.
6. Volchenko, V.N., Yampolsky, V.M., Vinokurov, V.A. *et al*. (1982) *Theory of welding processes*. Moscow: Vysshaya Shkola.

MODIFICATION OF PVR-402UKhL4 INDUSTRIAL PLASMATRON FOR SPRAYING OF WEAR-RESISTANT COATINGS IN A GAS-AIR PLASMA

A.V. KALASHNIKOV[1] and **V.N. KORZH**[2]
[1]State Technical University, Poltava, Ukraine
[2]National Technical University «KPI», Kyiv, Ukraine

ABSTRACT

The feasibility of updating the series-produced air-plasma cutting plasmatrons for their application in plasma spraying of powdered materials is shown. Method of optimizing of geometric sizes of a channel of nozzle and anode to achieve optimum values of the material utilization factor is given.

Key words: *plasmatron, gas-air plasma, thermal spraying*

Plasmatrons are the main elements of equipment for the plasma spraying and cutting. Special plasmatrons for spraying have been developed and widely spread. For coating deposition, the series-produced plasmatrons for air-oxygen cutting can also be used after a certain modification.

To spray coatings of refractory powdered materials the series-produced PVR-402UKhL4 plasmatron was subjected to modification. This plasmatron is used in the APR-402 type installation for a mechanized air-plasma cutting of ferrous materials, aluminium and its alloys of up to 130 mm thickness, and also copper and its alloys of up to 100 mm thickness.

Devices of the above-mentioned type have a water cooling with 0.007 dm^3/s water consumption, 400 A rated operating current, 100 % duty cycle, 380/180 V open-circuit voltage, 200/120 V operating voltage, 1.2 – 2.8 dm^3/s air consumption at 0.13 – 0.60 MPa pressure [1].

Modification of the plasmatron was aimed at its adaptation for deposition of the wear-resistant coating on cylinder surface by spraying the powder of aluminium oxide Al_2O_3 with 80 – 120 μm size of particles.

The principle of the plasmatron modification was reduced to the design of a nozzle and preserving the service life of the cathode during action of plasma and combustion products of propane-butane mixture on it. For this purpose, a standard electrode-nozzle set of the ESP-01 type, completed additionally with a water-cooled anode of copper M1, was used.

The experience of service of the plasmatrons completed with the EP-01 type cathode for the air-plasma cutting which is included into the ESP-01 set [1 – 3] shows that during operation in the gas-air mixtures at 0.10 – 0.15 MPa pressure the life of a hot cathode with a hafnium or zirconium insert without using special measures is decreased on average by 20 – 30 % as compared with that during its operation in air atmosphere. To protect a hot cathode from damage, caused by products of combustion of hydrocarbon gases, a nozzle from a standard ESP-01 set was used as a metal interelectrode insert. Here, the supply of air at 0.25 MPa pressure and consumption G_{air} = 1 m^3/h (between

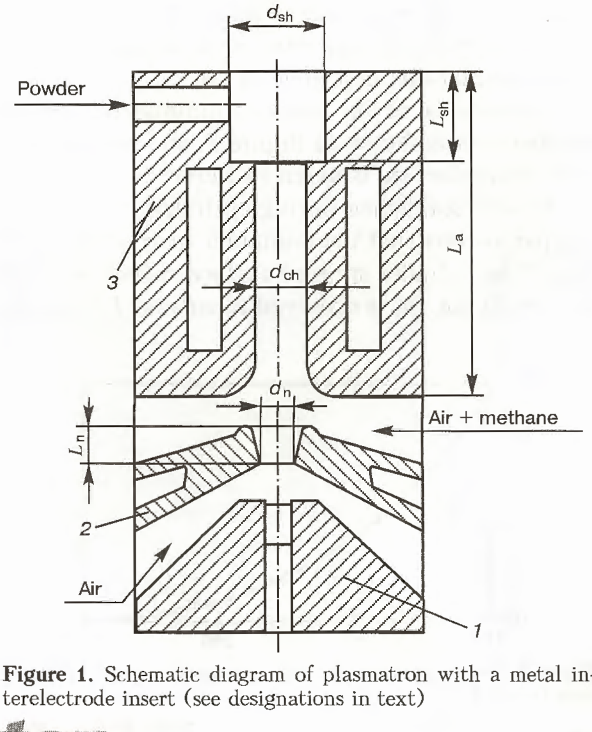

Figure 1. Schematic diagram of plasmatron with a metal interelectrode insert (see designations in text)

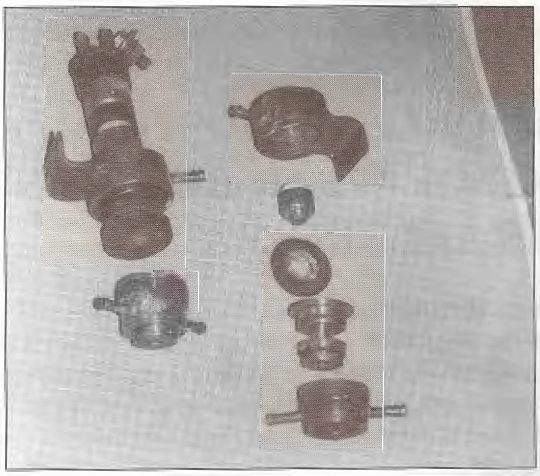

Figure 2. Appearance of the designed plasmatron and its components

a hot cathode and insert) and a gas-air mixture with consumption $G_g = 1.8$ m^3/h, and also excess of air $a = 0.9$ (between anode and insert) made it possible to preserve the thermal resistance of the cathode at an earlier level.

Figure 1 gives a diagram of the updated plasmatron. It consists of a cathode *1* (EP-01 type), interelectrode insert *2* (nozzle from ESP-01 set) and water-cooled anode *3*.

In designing of the nozzle-anode, the recommendations [2 – 8] were used taking into account the main parameters of the plasmatron operation conditions. Geometric sizes of the nozzle-anode channel were selected for its possible operation under subsonic and supersonic conditions. This is attained by a ratio of a nozzle length L_n and its diameter d_n [6, 8], equal to unity. The ratio of the rest geometric sizes was selected in accordance with recommendations described in [5].

Appearance of the updated plasmatron and its components is shown in Figure 2, and its volt-ampere characteristic is given in Figure 3.

It was established during optimizing the spraying parameters that the minimum wear of the coating of the cylinder sprayed surface, which is equal to $U = 28$ mg/h, is observed at current $I = 250$ A,

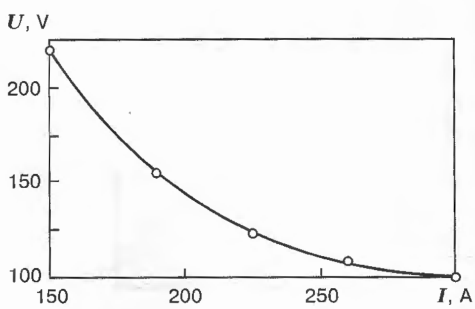

Figure 3. Volt-ampere characteristic of updated gas-air plasmatron ($a = 0.9$)

Levels of factors varying

Diameter of channel d_{ch}, mm (x_1)	*Diameter of shoulder d_{sh}, mm (x_2)*	*Depth of shoulder, L_{sh}, mm (x_3)*
6.00	8.00	7.00
8.00	10.00	10.00
6.58	8.23	8.23
5.42	7.77	5.77
4.00	6.00	4.00

consumption of plasma gas $G_g = 1.8$ m^3/h and powder $G_p = 0.8$ kg/h, distance of spraying $L_d = 85$ mm.

Shape and characteristics of the plasma jet as well as a shape of the flow of heated particles of the material sprayed depend greatly on the geometric sizes of the nozzle-anode channel and influence such technological characteristic as a metal utilization factor (MUF). In this connection, MUF is taken as a parameter of optimizing (function of response *Y*) for further optimizing the geometric parameters of the nozzle-anode channel.

To schedule the experiment a central orthogonal plan of the second order was used [9].

Number of experiments in the schedule was determined as $N = 2^{k-p} + 2k + 1$, where *k, p* are the number of factors and generators of the schedule. At $k = 3$ and $p = 0$ we obtain $N = 15$. Minimum number of repetitions γ is 3, and a total number of experiments is 45.

The following parameters were taken as factors of varying: L_{sh} is the depth of shoulder, d_{sh} is the shoulder diameter, d_{ch} is the diameter of the anode channel.

The varying levels of factors are given in Table.

Results of investigations according to the schedule of experiment were processed in the computer using applied and specially-developed programs. The coefficients of regression were determined and the model of the process in the form of a second-degree polynomial was obtained:

$$Y = 64.81 + 0.1x_1 - 0.0102x_2 - 0.327x_3 + \\ + 0.616x_1^2 + 0.101x_2^2 + 0.289x_3^2 + 0.216x_1x_2 + \\ + 0.343x_1x_3 - 2.26x_2x_3.$$

Validation of the model by the Fisher's criterion showed that for the model it is lower than critical value: $F = 14.93/6.287 = 2.375 < F_{cr} = 2.53$.

After removal of unimportant coefficients, the polynomial of optimizing has a final form

$$Y = 64.52 + 0.616x_1^2 - 2.26x_2x_3.$$

After transition from coded values a calculation formula in a real system of coordinates was obtained:

$$Y = 64.52 + 0.616\left(\frac{d_{ch} - \frac{8+4}{2}}{\frac{8-4}{2}}\right)^2 -$$

$$- 2.26\left(\frac{d_{sh} - \frac{10+6}{2}}{\frac{10-6}{2}}\right)\left(\frac{L_{sh} - \frac{10+4}{2}}{\frac{10-4}{2}}\right).$$

After simplifications, the final mathematical model for determination of MUF, %, for the updated plasmatron has a form

$$\text{MUF} = 49.25 - 0.15d_{ch}^2 + 1.85d_{ch} - 0.38d_{sh}L_{sh} +$$

$$+ 2.64d_{sh} + 3.01L_{sh}.$$

The obtained relationship was analyzed in computer for a maximum MUF value depending on geometric sizes of the plasmatron anode (Figure 1). It was established that the optimum diameter of the channel is d_{ch} = 6.0 mm at the diameter of shoulder d_{sh} = 7.92 mm and its depth L_{sh} = 7.0 mm. Moreover, 75 % MUF is provided for the above-mentioned spraying parameters.

CONCLUSIONS

1. Coatings of powdered materials can be sprayed using series-produced plasmatrons of the PVR-402UKhL4 type for plasma cutting after their modification which consists of the design of the anode nozzle.

2. The offered calculation procedure makes it possible to optimize the geometric sizes of the nozzle-anode channel to attain the acceptable values of MUF.

REFERENCES

1. Shirshov, I.G., Kotikov, V.N. (1987) *Plasma cutting*. Leningrad: Mashinostroyeniye.
2. Petrov, S.V., Karp, I.N. (1993) *Plasma gas-air spraying*. Kyiv: Naukova Dumka.
3. Zhukov, M.F. (1977) *Experimental investigations of plasmatrons*. Novosibirsk: Nauka.
4. Dutov, G.Yu., Dzyuba, V.L., Karp, I.N. (1933) *Plasmatrons with stabilized arcs*. Kyiv: Naukova Dumka.
5. Karasev, M.V., Chernykh, Yu.K. (1991) Multicriterial optimizing of parameters of air-plasma plasmatrons for coating spraying. *Svarochnoye Proizvodstvo*, **6**, 39 – 41.
6. Esibyan, E.M. (1971) *Plasma arc equipment*. Kyiv: Tekhnika.
7. Ingham, N.S., Fabel, A.G. (1975) Comparison of plasma flame spray gases. *Welding J.*, **2**, 101 – 105.
8. Petrov, S.V., Karp, I.N., Gorbatov, I.N. (1992) Plasma spraying of powdered materials in combustion products. *Svarochnoye Proizvodstvo*, **2**, 2 – 5.
9. (1977) *Experiment scheduling in investigation of technological processes*. Ed. by E.K. Letsky. Moscow: Mir.

«PLASMATRON» COMPANY IS 10 YEARS OLD

The Research-and-Production small-business state-owned Company «Plasmatron» founded by the E.O. Paton Electric Welding Institute on the base of its R&D and design division, a traditional developer of equipment for air-plasma cutting (APC), is an independent self-supporting entity incorporated into the Scientific-and-Technical Complex «The E.O. Paton Electric Welding Institute».

In January 2001 «Plasmatron» will celebrate its tenth anniversary, carrying on the renowned traditions of its predecessor. The primary object the Company, being small in number, which it has set itself since the very first days of its existence, is development and implementation of new ideas developed from R&D in the field of APC. During the elapsed period the Company has developed a new generation of the APC machines (Duplex-1, Duplex-2, Kyiv-5 and Kyiv-8U) and arranged in its premises their fabrication within the scopes that meet demand of the national market for such machines.

Production facilities of the Company include several modest-sized workshops: for machining, welding and electrical assembly, where engineers (electrical, production and design) work in close collaboration with operators (turners, fitters and assembly electricians).

Thinking about its future, this year the Company has increased its staff by hiring a group of young specialists — graduates of the National Technical University of Ukraine «Kyiv Polytechnical Institute». The young specialists are trained following the program of engineering and scientific specialization in the field of plasma technology.

Normal functioning of the Company under current conditions is made possible owing to its flexible organizational structure, where specialists involved in assembly, setting up and testing of the machines can spend part of their working hours for research and development.

In view of a relatively low buying capacity of the national customers, the Company has developed such activities as repair and upgrading of the existing fleet of the APC machines, delivery of spares for them (plasmatrons and replacement parts — cathodes, nozzles) and rendering technology services on metal cutting, etc.

Along with organization of the technology design and production activities, the «Plasmatron» managers are responsible for supply of materials and machinery for production purposes and marketing of finished products. The present territorial isolation results in an extra load on the managers — public services and utilities (electric and heat supply, repair of premises, security, etc.).

Owing to its production business, this mini-integrated enterprise is in a position to continue R&D in its sphere of activity, based on the principle of complete self-repayment. In our opinion, this form of organization in the field of applied research is, if not the best, but absolutely justifiable under the present-day conditions. Practice has proved substantial benefits of such a mini-integrated enterprise: it is capable of mastering manufacture of new products within the shortest possible terms (1.5 – 2.0 months) and expeditiously making amendments in flow diagrams and designs of products to meet Customer's requirements.

In its striving for entering the foreign market, the Company continues working hard to ensure further increase in the technical level of its products, their reliability, quality and exterior design.

«Plasmatron» maintains scientific relations with the departments of the PWI engaged in similar research fields and identifies the most important areas for its scientific activity at technical meetings with Prof. B.E. Paton, Director of the Institute.

Despite a low level of wages and salaries of the staff and shortage of a working capital for development, improvement of public services and utilities at working areas, the advanced scientific-and-technical orientation of «Plasmatron» raises assurance in its future.

Developments of the Company are shown in cover page 2.

Dr. E.M. Esibyan
Board Chairman
and Research Manager

PORTABLE MEGNETOCOPYING HINGE-TYPE MACHINE «CONTUR-500» FOR PLASMA CUTTING OF SHEET ROLLED METAL

F.G. CHULYUKOV, Yu.P. MODIN, V.I. DRYGANT, Yu.N. VORONKOV and **A.P. MALCHENKO**
OJSC ANITIM, Barnaul, Russia

ABSTRACT

The hinge-type machine for plasma cutting of the sheet rolled stock using a magnetocopying method of forming the contour of the component being cut is described. This machine is equipped with a device for a working gap tracing that provides its stabilization with an accuracy of ± 0.2 mm at cutting speeds up to 2500 mm/min. A kit of tools and components is also developed for the modification of the series-produced machines of the «Ogonyok» type for a thermal cutting.

Key words: *plasma cutting, magnetocopying machine, sheet rolled stock, technical characteristics*

The manufacture of the machine «Contur-500» in a mobile performance for plasma cutting of sheet rolled stock of small geometric sizes was developed and mastered. The machine is manufactured on ball-bearing supports to have a feasibility of moving along the sheet being laid-out and fixation in the zone of the layout. Its transfer during sheet changing is performed by a hoisting device or manually. The plasma cutting machine on the wheeled supports is moved within the range of the cable length.

The demand for this type of machines was evident long ago. Their manufacture was organized abroad by such known companies as «Koike Sanso Kogyo» (Japan), ESAB (Sweden), etc. These machines found wide spread in shipbuilding, power machine-building, and also in fabrication of different metal structures.

These machines are of a special importance for enterprises where there are no specially-equipped shops or sections of the preparatory manufacturing.

The delivery set includes a hinge-type machine proper, a unit of control and stabilizing and a plasma cutting unit. In addition, there is a remote control panel with a 6 m cable. The hinge-type machine is manufactured by the known scheme with a magnetocopying head which provides a contour of the component by an equidistant tracing around a path with a rotating magnetic finger. The magnetic flux, unlike the machine of the «Ogonyok» type, is generated with the help of a disc-type circular constant magnet. To intensify the engagement of the finger with a magnet the magnetic discs are arranged along the edge of the working contour. Transition from the internal working contour to the external contour is performed at a lowered magnetic finger. The templates are fastened at a special traverse with the help of movable supports. Traverse is mounted on a rack and fixed to it by clamps. The rack is also fixed to a base by clamps.

To widen the functional capabilities of the equipment and to improve the quality of cutting the machine is completed with a so-called automatic device for cutting-in and stabilization of the «plasmatron–workpiece» working gap. Stabilization is made according to the diagram with a variable-capacitance transducer. The mechanism of stabilization provides a vertical travel of plasmatron for 40 mm. Error in tracing of the set working gap is ± 0.2 mm at 2500 mm/min cutting speed. In addition, the mechanism provides so-called a high-altitude ignition, i.e. breakdown of the sheet with an operating arc at a some lifting equal to a 2 – 3-fold working gap that provides a direct cutting-in at a thickness of more than 20 mm without splashing and damage of the plasmatron with metal splashes. The cycle of cutting-in consists of a plasmatron setting into initial position in height of the arc switching on, hanging over the sheet, setting for a working gap and starting the movement along the contour. The cycle parameters are set by the operator from the control panel and realized automatically in accordance with an algorithm of control. The minimum thickness of the sheet is regulated by its load-carrying capacity as to the rigidity and equal to 2 – 3 mm.

The machine (Figure 1) is completed with a plasma cutting machine of the «Plasma-K152» type (OJSC ANITIM). It has all necessary (for control) external signals of exchange that makes it possible

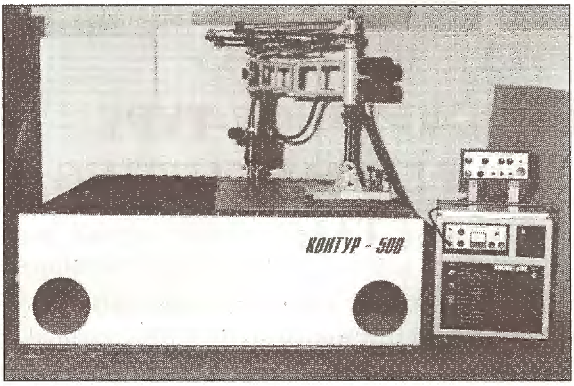

Figure 1. General view of machine «Contur-500»

to use it in combination with programmed gantry-type machines. Range of the operating current is from 40 to 120 A with a smooth adjustment. The machine is completed with air-cooled plasma cutters of an European manufacture. Delivery set can also include a manual cutter, that makes it possible to organize the station of the manual layout.

Technical characteristics

Largest sizes of parts being cut out, mm:	
linear	900×290
circular	500
Thickness of sheet used, mm	3 – 25
Error in cutting, mm	± 0.5
Speed of cutter movement, mm/min	100 – 2500
Mass, kg:	
without plasma power source	120
with plasma power source	240

The machine is easily transformed into a stationary device for the layout of the rolled stock according to preliminary cut-out maps. In addition, it can be included into a composition of the integrated object-installation, production line and complexes. It is possible to update the old machines of «Ogonyok» type by mounting a special set, which will include special components and units from the machine «Contur-500», a module of the automatic device of cutting-in and stabilization (Figure 2), a control unit and a plasma cutting equipment. After mounting this set of units the machine will be capable to lay-out the sheet rolled stock of thickness from 2 to 25 mm at working speeds from 100 to 2500 mm/min at a stabilized working gap along the contour of the component being cut out.

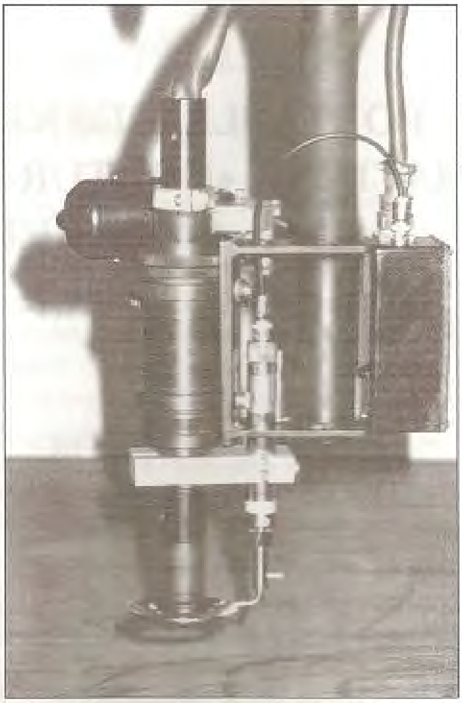

Figure 2. Mechanism for a welding gap stabilization

MODERN RUSSIAN LOW-POWER EQUIPMENT FOR AIR-PLASMA CUTTING

R.G. LITVIN
JSC «Spetselektromash», St.-Petersburg, Russia

ABSTRACT

Peculiarities of low-power equipment for air-plasma cutting, imported to Russia at the first half of the 1990s, are considered. Specialized equipment for the air-plasma cutting designed and manufactured now at the JSC «Spetselektromash» is described.

Key words: *air-plasma cutting, low-power equipment, characteristics, cutting automation, plasmatron*

Technology of the air-plasma cutting has significant advantages as compared with a widely-used oxygen cutting. First of all, it is higher cutting rate (especially at metal thickness of up to 20 – 30 mm) and feasibility to perform cutting of ferrous and non-ferrous metals and also alloys using the same equipment without its resetting. In addition, during the air-plasma cutting the thin metal is not subjected to distortion and the cleanness of a cut makes it possible to perform welding of prefabrications without mechanical treatment. The cutting of non-ferrous metals and high-alloyed steels, which cannot be cut by the oxygen cutting, is most effective.

The changed economy in the states of the former USSR, a rapid process of decentralizing, which divided the metal working fabrication into smaller entities required creation of relatively small-sized and cheap plasma cutting machines which could treat metal prefabrications (plates and sheets) of thickness from 1.0 – 1.5 up to 20 – 40 mm and be simple in service and repair.

The creation of equipment, which meets these requirements, was delayed to a great extent by the absence of series-produced plasmatrons capable to operate at a compressed atmospheric air and 50 – 150 A operating current, and, what is most important, to be characterized by a compactness and quality. At high temperature and rate of plasma flow, even small mismatches in sizes of the plasmatron components, their roughness and misalignment lead either to an increased consumption of changeable elements or to an increase in time of preparatory operations, thus reducing the cutting efficiency and increasing the cost.

Due to some objective circumstances a new class of equipment has appeared, i.e. low-power air-plasma cutting machines. Until the middle of the 1990s almost all similar machines were imported, in particular, Air Plasma 40-90 («Ozas», Poland), Superplasma 90/3, 120/3 («Telwin», Italy), Plasma Prof 92, 122 («Cebora», Italy).

At present the imported low-power plasma machines begin to be replaced by the equipment, designed and series-produced both at well-known factories («Selma», Simferopol; «Electric», St.-Petersburg) and also at the new enterprises («Tekhnotron», Cheboksary; «Spetselektromash», St.-Petersburg). These three-phase units, as a rule, are characterized by a small mass (up to 130 – 140 kg) and dimensions (comparable with dimensions of the TDM-401 type transformer). Plasmatrons of foreign manufacture (German or Italian) are used as a working organ.

The application of modern plasma torches at small output currents (about 30 – 140 A) made it possible to cut the ferrous steel of up to 50 mm thickness (stainless steel — up to 40 mm, and aluminium — up to 30 mm, respectively) at a high speed and quality.

In principle, these machines are designed by a classical scheme and consist of five basic subassemblies: electrical power part, control system, pneumatic equipment, oscillator and plasmatron.

The electrical power part consists of a three-phase transformer (whose windings have significant fields of scattering), connected to a three-phase rectifier, which is assembled by a bridge connection. The primary and secondary windings are most often have a star connection. Sometimes, they have a delta connection (for example, units of Superplasma 60/3, 90/3, 120/3 type of Italian company «Telwin»). The external characteristic of the power source is steeply falling.

Under the no-load conditions the voltage at the rectifier terminals is 200 – 300 V. The voltage in the operating point is determined to a greater extent by inner geometric parameters of the working

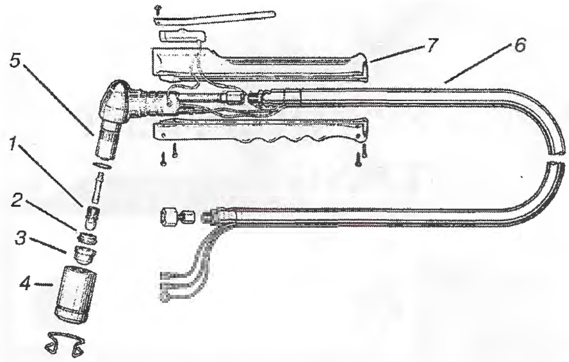

Figure 1

chamber of the plasmatron and depends on the arc length. This voltage is 125 – 150 V for the plasmatrons of type A.90, A.140 («Trafimet», Italy), HP 150 («Telwin», Italy), R90, R120 («Cebora», Italy), Smoothcut 140 («Hobart», USA).

To ensure the required quality of cut and rate, convenient for a cutting operator, the updated machines of low-power air-plasma cutting have several current conditions (2 – 3, as a rule) which provide a step adjustment (rarely, a smooth electronic adjustment).

The control system provides an interaction of all the elements of the air-plasma cutting machine according to a preset cycle (very similar to a cycle of operation of the control system of the argon-arc welding machine), and also the indication of the conditions.

The oscillator is a special device required for a contactless ignition of a pilot arc and consists, as a rule, of two parts, namely a generator and a high-frequency transformer.

A compressed atmospheric air, supplied to the machine, takes part in the process of a plasma forming, and also cools the elements of the plasmatron working chamber. The air-plasma cutting machines contain a necessary system of pneumatic devices for preparation and control of the compressed air, including usually a flow meter, oil and moisture separator, regulator, pressure relay, pneumatic distributors and reducing valve. To provide the high-quality compressed air at its sufficiently high consumption (120 – 220 l/min at 0.4 – 0.6 MPa) is one of the main tasks (if not most important) during service of the low-power plasma-cutting machines, because the life of cathodes and nozzles, stability of arc ignition, rate and cut quality depend directly on it. The supplied air should be pure, without moisture and oil. Its feeding should be uniform without pulsations. For the air purification the filters (oil and moisture separators) and coolers with steam traps are used, while for smoothing pulsations the receivers (for 100 – 150 l usually) mounted near the station and regulators, are used.

During development, manufacture and purchasing of the air-plasma cutting machine a selection of the type of the plasmatron taking into account the design peculiarities of technology of manufacture and reliability of its changeable elements is of a special importance. The latter defines the expenses for service of the air-plasma cutting station.

All the plasmatrons of the foreign production which are used in the low-power units are provided with an air cooling.

The main elements of the plasmatron (Figure 1) are as follows: cathode *1* with a hafnium insert, a ceramic diffusor *2* (providing an air flow twist), nozzle *3* with a sized hole (1.0 – 1.9 mm diameter), insulating packing *4*, head part *5* and cable-flexible pack *6* with a handle *7* of an ergonomic shape.

For cheap portable machines of up to 60 A operating current there are plasmatrons in which one of electrodes (cathode or nozzle) is mobile, thus giving a feasibility to excite the arc by a contact. Here, the power source does not include an oscillator.

JSC «Spetselektromash» designs and manufactures different welding low-power machines (up to 250 A), including also two models of the air-plasma cutting machines of the UPR-007 and UPR-907M types.

The UPR-007 type unit represents a cheap portable single-phase machine of a simple and reliable design, which is intended for a manual air-plasma cutting of small thicknesses. Having about 27 kg mass, this machine can perform cutting of low-carbon steel of up to 7 mm, aluminium — up to 5 mm. The use of the PSB 32S plasmatron («Binzel», Germany) in the machine eliminated the use of an oscillator and increased significantly the reliability of all the machine. The duty cycle is 25 % at a 5-minute cycle, that is quite sufficient for the fulfillment of works in repair of bodies at the autoservice workshops, mounting of ventilation skips or manufacture of metal doors.

The UPR-907M type machine (Figure 2) was designed taking into account the requirements specified to the industrial equipment and intended for cutting of small and medium thicknesses used in machine-building and fabrication of metal structures (low-carbon steel — up to 35 mm, aluminium — up to 25 mm). Three-phase power source has 115 kg mass and pivoted wheel supports for convenient movement. To perform cutting in the manual condition the machine is completed with the plasmatron A.90 («Trafimet», Italy), and in case of use of the gas cutting machines an automatic plasmatron R90 («Cebora», Italy) and a remote control panel are delivered. These plasmatrons provide the high-efficiency (10 mm low-carbon steel is cut at 140 cm/min rate) and quality cutting (cut width is not more than 2 – 3 mm).

The presence of a three-step current regulator of cutting, oscillator and condition of a «soft» ignition of a pilot arc makes it possible not only to select an optimum rate of cutting of different thicknesses, but also to reduce the wear of cathodes and nozzles.

Both models of the machines are equipped with equipment of a compressed air preparation, a convenient light indication of the conditions and a system of blockings, which prevent accidental coming out of order.

To make the operator's labour most effective, it is necessary to manufacture a special layout table equipped with a local illumination and a lower vent of a sufficient capacity. The layout table which presents itself a frame of a rectangular shape is made of a steel section angle. The upper table plane is open. It has fasteners for mounting of transverse changeable knives at a 100 – 150 mm pitch. Changeable knives are made from steel (or aluminium) strip of 5 – 10 mm thickness, the upper edge of the changeable knives is chamfered.

If it is necessary to cut parts of a simple shape and the requirements to the quality are not too high, then a stack cutting can be used. The metal sheets are assembled into a packet and tied with cramps. The total thickness should not be more than 75 % of the cut metal limiting thickness, indicated in the machine certificate.

At a large volume of similar prefabrications, it is rational to mechanize the cutting process. The mechanized cutting, as compared with the manual cutting, eliminates the operation of marking-out, decreases tolerances and, moreover, the higher efficiency, and the mostly important, the uniform rate of cutting is provided, thus having a positive effect on the quality of prefabrications.

It is possible to automate the process of the air-plasma cutting more easily with the help of hinge-type machines for the mechanized gas cutting (ASSh-2, «Ogonyok», etc.). These machines are designed for cutting prefabrications of relatively small dimensions. They occupy a minimum working area. They are simple in operation and do not require large expenses for service. A system of a contoured control is based on a magnetic guide block manufactured from 6 – 8 mm steel sheet in the scale 1:1.

Figure 2

The modification of machines is reduced to dismantling of gas sleeves and negligible changing in a holder of torches in such a way that to replace an oxygen-acetylene torch by a plasmatron of the so-called automatic (or pencil) type. The machine is switched on by an operator from the remote control panel, the rate of movement can be controlled smoothly.

In general, the rate of the plasmatron movement influences greatly on the cut quality. At the proper rate the cut is smooth, narrow (width is not more than a doubled diameter of the nozzle) and without «flay marks»; cut edges are without roundings; edge surfaces are smooth or with small grooves directed almost vertical. The flash is removed easily from the lower edge of the cut by nipping pliers or a hammer. This quality can be provided for cutting metal up to the thickness equal to 75 – 85 % of the limiting value.